Temporal coding and auditory processing in the prothoracic ganglion of crickets.

Gary Marsat

Biology Department,
McGill University, Montreal.

August 2006,

A thesis submitted to McGill University in partial fulfillment of the requirements of the degree of Doctor of Philosophy.

Your file Votre référence
ISBN: 978-0-494-32214-7
Our file Notre référence
ISBN: 978-0-494-32214-7

Table of contents

List of Figures

Chapter 5:

Summary

We used the auditory system of crickets as a model system to examine the importance of temporal coding in sensory processing. The bilaterally paired Ascending Neurons 1 and 2 (AN1 and AN2) of crickets receive inputs from the auditory receptors on one side and carry the information to the brain. We used stimuli with either conspecific-like or predator-like (i.e. bats) carrier frequency to quantify the accuracy with which the interneurons code the information contained within the amplitude modulation (AM) envelope of the stimulus. AN1, which is tuned to the dominant carrier frequency of cricket songs, selectively codes the limited range of amplitude-modulation frequencies that occur in these signals. AN2, which is most sensitive to ultrasound, serves as a "bat-detector" and codes a broader range of AM frequencies, as occur in bat calls.

A striking characteristic in AN2's responses to ultrasound is the presence of bursts of high-frequency spiking separated by relatively sparse spikes. We examined the relative importance of isolated spikes and bursts in the processing of ultrasound. We showed that bursts reliably signal the occurrence of salient amplitude increases. Furthermore, we showed that burst, but not isolated spikes, reliably predict behavioural responses. We suggest AN2 encodes behaviourally important information with bursts.

The Omega Neuron 1 (ON1) responds to conspecific signals and to the ultrasonic echolocation sounds. ON1's temporal coding properties vary with carrier frequency, allowing it to encode both of these behaviourally important signals. Furthermore, the temporal coding properties of ON1 in response to cricket-like sound and bat-like sound match those of AN1 and AN2 respectively.

ON1 is a source of contralateral inhibition to AN1 and AN2, enhancing binaural contrast and facilitating sound localization. We used dichotic stimulation to examine the importance of the temporal structure of

contralateral inhibition for enhancing binaural contrast. Contralateral inhibition degrades the accuracy with which amplitude modulation is encoded by AN1 and AN2, but only if the temporal pattern of inhibitory input matches that of excitation. Our results show that the CF-specific coding properties of ON1 allow this single neuron to enhance localization cues most effectively for both cricket-like and bat-like acoustic signals.

Résumé

Nous avons utilisé le système auditif du grillon comme système model afin d'examiner l'importance du codage temporelle dans le traitement de l'information sensorielle. Les neurones ascendants 1 et 2 (AN1 et AN2) des grillons existent en paires bilatérales. AN1 et AN2 sont stimulés par les récepteurs provenant d'une seule oreille et conduisent cette information jusqu'au cerveau. Nous utilisons des stimuli dont les fréquences porteuses sont similaires à celles des chants de grillons ou des sons de chauve-souris et déterminons la précision d'encodage des modulations d'amplitudes du stimulus. AN1, qui est sensible aux frequences de grillons, est aussi sélectif pour les patrons de modulations d'amplitudes caractérisants les chants de grillons. AN2 fait fonction de "détecteur de chauve-souris" et encode un plus large spectre de fréquences temporelles, reflètant la diversité de structure des sons de chauve-souris.

Un aspect frappant de la réponse de AN2 est la présence de rafales de potentiels d'action separées par des décharges isolées. Nous montrons que les rafales détectent de façon fiable les pointes d'amplitude les plus saillantes et que seulle ces rafales évoquent une reponse comportementale.

La neurone omega 1 (ON1) répond aux chants de leurs congénères mais aussi aux ultrasons des chauve-souris. La manière avec

laquelle ON1 code les modulations temporelles varie selon la fréquence porteuse du stimulus de façon à ce qu'elle puisse coder adéquatement ces deux types de signaux. De plus, les caractéristiques des réponses de ON1 aux fréquences de grillon et aux ultrasons sont similaires à celles de AN1 et AN2 respectivement.

ON1 est une source d'inhibition contralatérale pour AN1 et AN2 qui augmente la différence bilatérale dans la réponse des ANs, falicitant ainsi la localisation du son. Nous utilisons des stimuli dichotiques pour évaluer l'importance de la structure temporelle de l'inhibition dans le traitement de l'information. L'inhibition contralatérale dégrade la précision avec laquelle les modulations d'amplitude sont codées, mais seulement si le patron de l'inhibition correspond à celui de l'excitation. Nos résultats montrent que les caractéristiques de codage bimodales de ON1 permettent d'améliorer l'acuité de localisation spécifiquement pour les sons ressemblants à des chants de grillons ou des cris de chauve-souris.

Contribution of authors

Chapter 2 was published in the Journal of neurophysiology under the title "Differential Temporal Coding of Rhythmically Diverse Acoustic Signals by a Single Interneuron". A large part of the experimental and analytical design was an original idea of G. Pollack. I performed the execution and analysis of the experiments except for figure 2.6 for which the experiments on the auditory receptors were performed by G. Pollack. I prepared the figures and the initial draft of the manuscript whereas the final wording was done in collaboration with G. Pollack.

Chapter 3 was published in the Journal of Neuroscience under the title: "Effect of the Temporal Pattern of Contralateral Inhibition on Sound Localization Cues". The experiments and analysis were designed and performed by me. I prepared the figures and the initial draft of the manuscript but the final wording was done in collaboration with G. Pollack.

Chapter 4 was submitted to The Journal of Neuroscience under the title: "A behavioural role for feature detection by sensory bursts". The experiments and analysis were designed and performed by me. I prepared the figures and the initial draft of the manuscript, the final wording was done in collaboration with G. Pollack.

Chapter 5 will be submitted to the Journal of Neurophysiology under the title: "Efficient inhibition of bursts in the auditory system of crickets". The experiments and analysis were designed and performed by me. I prepared the figures and the initial draft of the manuscript, the final wording was done in collaboration with G. Pollack.

Acknowledgement

I would like to thank my supervisor, Dr. Gerald Pollack, for his patient mentoring and his contagious enthusiasm for science. I am in debt for the countless hours he spent teaching me experimental, analytical or writing skills. I am also grateful to my supervisory committee members, Dr. Chase and Dr. Krahe and Dr. Drapeau, for their insightful comments, their cheerful encouragements and for the many reference letters they wrote for me.

I would like to acknowledge the sources of funding that supported my work: NSERC and CIHR grants received by my supervisor, and the McGill Graduate Student Fellowship that I received in 2004.

My years as graduate student would never have been so successful and enjoyable without the friendly and stimulating environment I found in the biology department, in particular in Dr Pollack's lab: I think of Annie-Helene S. that helped me get started in the cricket world; Nicole T., Kim N., Pat G. and Pat S. with whom I had many fruitful discussions, and the other former and current members of the lab.

Lastly, I am grateful to my family and friends for their everlasting support and faith in me. In particular, I would like to thank Annie L. for walking that long road with me and for so much more.

Chapter 1: Introduction

Introduction

Sensory coding

Sensory systems must encode the behaviourally relevant signals occurring in the environment. Sensory coding can be examined from many points of view: ethological, evolutionary, computational, cellular, and many others. The goal of this section is to introduce a few concepts particularly relevant to this thesis and thus I focuses on the encoding of behaviourally relevant information of sensory signals, in particular in the auditory system.

Signal recognition

Sensory signals

Sensory signals are modulated over time. Auditory signals contain modulations in amplitude and in frequency. Visual scenes change as we move, thereby stimulating visual receptors with changing patterns of light intensity. Tactile, olfactory and electrosensory signals are also modulated in amplitude over time. In auditory signals, as for other modalities, the temporal modulation in amplitude carries much of the meaning of the signal. Communication sounds of most species have characteristic rhythmic modulations (Pollack 2001) in amplitude that are required for the recognition of the signal. Human speech for example can be recognized based largely on the amplitude modulation of less than 50 Hz that it contains (Shannon et al 1995). A conspicuous aspect of human speech is the presence of short consonants followed by longer vowels. The time between the onset of a consonant and the onset of the vowel, the VOT (Voice Onset Time), has been the focus of many studies on speech recognition. Millisecond differences in the length of the VOT underlie the perceptual categorization of consonants: voiced syllables, such as /da/, have short VOTs whereas unvoiced syllables, /pa/ for example, have longer VOTs (Lisker and Abramson, 1964, Schirmer, 2004).

The importance of the temporal pattern of a sensory signal for its recognition has been demonstrated for several modalities and a variety of organism. Songs of birds, frogs and insects have stereotypical, specie-specific, temporal structures. These songs are most often directed toward conspecifics and may signal sexual readiness, territoriality or aggression (Kroodsma and Bryers, 1991, Gerhardt, 1994; Pollack, 2000). The structure of these calls allows the receiver to identify the emitter of the communication signals (e.g. species, sex, individual) but also carries information about the message being sent (e.g. mate attraction, aggression...). Electric fish also use small modulations in the amplitude of the electric fields to communicate with conspecifics. In *Apteronotus* for example, chirps of different length are used in the context of aggressive encounters than during courtship interactions (Engler and Zupanc, 2001).

The temporal pattern of sensory stimuli is exploited not only to decipher communication signals but also in the analysis of inter-specific and environmental signals. Electric fish localize prey (such as *Daphnia*) based on small and local modulations in the fish's electric field (Nelson and Maciver, 1999). Flight control and navigation in bees relies in part on modulations of the optic flow on each side of the animal (Srinivasan et al., 1996). Bat echolocation provides a sophisticated example of temporal analysis of non-communication signals (although echolocation is sometimes called autocommunication). Bats can detect insects, and even recognize different types of insects, based on the structure of the echoes of the ultrasound pulses of its sonar (Schnitzler 1987). Delays in the echoes of as little as 10 ns have to be analyzed by the bat's nervous system in order to draw a detailed spatial map of its environment (Simmons, 1989).

Signal coding and recognition.

Recognition is often accomplished by neural circuits in which neurons are highly selective for specific aspects of sensory signals. These neurons can

be characterized as "feature detectors". Recognition of faces in the visual system of primates can provide an extreme illustration of feature detectors. The so-called "grandmother cell" hypothesis postulates that the activity of a single neurons are associated with the percept of recognizing a face (Barlow, 1995). Although this hypothesis, taken literally, raises some issues that require more subtlety in its formulation, single cell recording in humans show selective responses to specific faces (Quian Quiroga et al., 2005). Neurons that respond to specific patterns of stimulation are also thought to underlie auditory recognition. For example, in the anuran midbrain, Edwards et al (2002) showed that some neurons are dedicated to counting sound pulses with the right period and respond only to signals with species-specific temporal pattern. In the forebrain of songbirds, neurons respond to complex spectro-temporal features of their songs such as frequency sweeps or multi-peaked frequency stacks (Sen et al, 2001).

In humans, speech recognition occurs in highly specialized cortical circuits of the Wernicke area (for review see Damasio and Geschwind, 1984). Lesions to this area lead to incapacity to understand speech although the sound itself is perceived. On the other hand, recognition relies on detailed description of the sound structure provided by afferents from the auditory cortex. The minute differences in VOT length that I describe above are well encoded in the primary auditory cortex (Eggermont, 1995; Steinschneider et al, 2003) thereby allowing phoneme categorization and recognition.

The human auditory cortex presents an asymmetry in its ability to process rapid temporal pattern. The dominant hemisphere (usually the left) is more involved in temporal processing whereas the right hemisphere is more sensitive to spectral features of the sound (Zatorre and Belin 2001). This reflects the specialisation of the dominant hemisphere in processing speech and the importance of temporal processing in speech recognition. Deficits in temporal processing have been correlated with

auditory neuropathy (Zeng et al, 1999). Accuracy in temporal processing in the midbrain degrades with age and leads to difficulties in speech comprehension in noisy backgrounds (Frisna and Frisna, 1997). Studies on dyslexic individuals show that accurate temporal coding is necessary for speech recognition tasks. McAnally and Stein (1996) examined the precision in representation of the stimulus time course and their experiment suggests that the deficit in rapid temporal coding observed in dyslexic adults can be traced back to the brainstem and is not limited to one modality. This deficit also leads to a difficulty in sound segregation (Helenius et al, 1999, also see the section on the interdependence of temporal and spatial processing for a related discussion). Research on dyslexia illustrates well how accurate temporal coding at lower levels of the sensory system is essential for adequate processing at higher levels.

Coding specificity for natural signals

Sensory systems are faced with the task of extracting behaviourally relevant signals out of very complex and diverse sensory environments. Based on psychological observations Barlow (1961) formulated, more than 40 years ago, three principles that he believed guided the operation of sensory systems.

The first one says that sensory pathways must encode aspects of the sensory environment most important for behaviour (the so-called "password" hypothesis). The second hypothesis states that sensory relays must transform the signal according to the requirements of other parts of the nervous system. The last hypothesis stresses that sensory systems should encode most accurately information-rich aspects of the sensory environment and neglect redundant portions of the signal (Barlow 1961). This "efficient coding theory" thus claims that the goal of sensory coding is to encode the maximal amount of information about behaviourally relevant stimuli. To quantify coding accuracy, neurophysiologist traditionally used artificial stimuli with simple and fixed patterns -such as sinusoidal or

pulsed stimuli modulated at specific rates- or actual communication signals, and subsequently measured the response strength and timing accuracy. Another approach is to use information theoretic and signal processing tools, which often rely on the use of white noise stimuli to quantify the input-output function of the neurons. Such tools have provided convincing confirmations of Barlow's theory. Studies in several organisms and sensory systems have shown that the coding properties of sensory neurons are often optimized for stimuli with the characteristics of behaviourally relevant signals: in the visual system (vertebrates: Baddeley et al.,1998; Vinje and Gallant, 2002; Simmoncelli and Olshause, 2001; Dan et al 1996; invertebrates: Laughlin, 1981; Brenner et al., 2000), in the auditory system (vertebrates :Lewicki, 2002; Swartz and Simoncelli, 2001; Reike et al., 1995 ; Attias and Schreiner 1998 ; Nagarajan, 2002; Woolley et al., 2006; Nelken, 2004; invertebrates: Machens et al; 2001, 2005); and in the electrosensory system of fish (Chacron et al., 2005). For example, Machens and colleagues (2001, 2005) used series of iterative reconstructions to define the stimulus characteristics that elicited the best coding accuracy in locust auditory receptors. Their finding suggest that instead of maximizing the average information gained about natural stimuli, the receptors appear to maximize the information gained about specific, less often occurring aspects of natural stimuli. Thus, sensory systems may seek to match their coding properties to behaviourally relevant features of natural stimuli, rather than according to the average statistics of these stimuli.

Auditory processing in vertebrates

Neuroscience has greatly benefited from the study of simple model organism, but to quote Dr. Wilder Penfield: "The problem of neurology is to understand man himself". I outline the transformations implemented by sub-cortical areas of the vertebrate auditory system (in particular higher vertebrates) in order to lay out some principles and raise some issues

central to the understanding of auditory processing and to subsequently allow comparison with crickets.

Carrier frequency analysis and information sorting in the cochlear nucleus

In vertebrate auditory systems, sound vibrations are first picked up by hair cells in the cochlea. These hair cells respond only to narrow ranges of carrier frequency (Fettiplace and Fuchs, 1999). Thus, at the level of receptors, sound signals are separated in different channels based on the carrier frequencies they contain. Hearing in reptiles and birds is usually limited to lower frequencies (less than ~ 10 kHz), but due to their middle ear, mammals are able to hear higher frequencies (up to 20 kHz in humans , 60 kHz in cats, 120 kHz in bats; Oertel 1999). In the auditory nerve, neurons phase lock to the carrier for low frequencies (less than ~ 4 kHz). In response to higher frequencies, the neurons' response structure will represent mainly the modulation in amplitude of the sound (Rhode and Greenberg, 1994). Auditory receptors can be categorized based on their threshold (Frisna et al 1996). The fact that receptors have different thresholds allows the population of receptor to encode a wider range of sound amplitude. Adaptation in the receptors also participates in widening the dynamic range of amplitude coding (Dean et al., 2005)

The convergence of receptors in the cochlear nucleus (CN) provides an input with a wide dynamic range and enhanced synchronization. The CN is organized tonotopically with respect to carrier frequency (Spirou et al., 1993). The CN is composed of several types of cells and their outputs project to different nuclei. Bushy cells and globular bushy cells provide the bilateral inputs to the superior olivary complex (SOC) necessary for the analysis of sound localization cues: interaural intensity and time differences (IID and ITD respectively; Moore, 1987). Stellate and octopus cells are part of a monaural pathway projecting to the VNLL (ventral nucleus of the lateral lemniscus), and are thought to provide

information useful for sound recognition. Thus, neural circuits of the CN separate the information contained in the stimulus into different channels, carrying cues for sound localization (IID or ITD sensitivity) or sound recognition.

Spatial processing and the superior olivary complex

The SOC is the first stage of binaural comparisons. The lateral and medial superior olives differ in the structure of their input. Neurons of the MSO receive bilateral excitatory input from the CN, organized in delay lines, whereas LSO neurons receive excitatory inputs ipsilaterally and inhibitory inputs contralaterally (Thomson and Schofield, 2000). These two kinds of bilateral interaction underlie the processing of interaural time and intensity differences (for further details see the section on localization). The MSO processes interaural time difference whereas neurons of the LSO are mainly sensitive to interaural intensity differences (Moore, 1987).

Although the SOC seems specialized for processing bilateral cues necessary for sound localization its functions might not be restricted to this. One line of evidence supporting that statement comes from studies on IID sensitivity in pigs. Pigs have large interaural distances, good high frequency hearing and a large LSO, which should allow them to process IID. Nevertheless, they seem incapable of using IID cues for sound localization (Heffner and Heffner, 1989). Also, the SOC contains cells innervated monaurally (Kuwada and Batra, 1999). In the light of these facts, it was suggested that the SOC's function is not limited to processing localization cues but might also participate in sound recognition.

Coding of sound structure in some SOC neurons differs from the coding properties typically found in previous levels in that their mean firing rate varies as a function of the AM frequency of the stimulus. This difference in coding property reflects a trend in auditory systems: peripheral neurons encode the structure of the sound by copying the modulation pattern in their firing rate (i.e. temporal code) whereas more

central neurons will vary their mean firing rate as a function of the stimulus' temporal pattern but do not reproduce the modulation pattern (i.e. rate code; Frisina, 2001).

Sensory integration and the inferior colliculus.

The influence of amplitude modulation (AM) frequency of the stimulus on the neurons' response properties is even more conspicuous in the inferior colliculus (IC). Indeed, it was found that the IC of cats is organized tonotopically with respect to the carrier frequency in one dimension and to AM frequency in the other (Langner and Schreiner, 1988). Single unit recordings showed that AM encoding is more selective than lower in the auditory pathway (Møller and Rees, 1986). IC neurons show maximal response for AM rates below 90 Hz; however their sensitivity to interaural time differences of the amplitude envelope extends up to 350 Hz (Batra et al 1989). This suggests that the temporal information available for recognition in higher centers is limited to low AM rates but that a wider range of temporal patterns is involved in the elaboration of localization cues.

The IC receives ascending projections from several areas in the midbrain (e.g. SOC, VNLL) but also descending projections from the cortex. It is the main source of auditory input to the thalamus and the cortex (Olivier and Huerta, 1992). It is therefore thought to play an integrative role, combining several aspect of the sensory environment into a spatial map.

Sound localization and temporal coding

Auditory signals contain information about the identity and the message of the sender but also about its location. I describe in this section how the auditory system extracts this spatial information. I also show how the

interplay between spatial and temporal coding underlies perceptual abilities in noisy situations.

Sound localization and the role of precise spike timing.

Ears usually come in pairs for a good reason: binaural hearing underlies spatial processing. A sound signal presented from directly in front of a subject will reach the two ears at the same time and with the same intensity. When the stimulus is located on one side, the signal will reach the ipsilateral ear earlier and with more energy. The distance between the two ears, and also the amount of acoustical shading produced by the head determines the conspicuousness of the binaural differences. Interaural time differences (ITD) can be used as a localization cue insofar as the neural responses can time-lock to the stimulus. For low carrier frequencies (<4 kHz), auditory receptors phase-lock with the stimulus waveform, whereas for higher frequencies, receptors phase lock to the amplitude modulations of the stimulus (Oertel, 1999). Therefore binaural differences in timing can be resolved based on phase difference of the carrier for low-frequency. For high frequencies, timing differences can only be determined based on the amplitude envelope. Un-modulated, high frequency stimuli can nevertheless be localized based on interaural intensity differences (IID) of the sound.

The first site of binaural convergence is the SOC. Physiological studies reveal that neurons of the LSO are commonly sensitive to IID and MSO neurons are most sensitive to ITD (Moore, 1987).

In the MSO, phased-locked input arrives from the cochlear nucleus from both sides of the body. Binaural inputs converge onto neurons that respond selectively to inputs arriving at the same time from the left and right ear. The axons of contralateral inputs systematically vary in length from one MSO cell to the next. Spikes traveling along the longer axons will arrive at the MSO neurons with a delay relative the ipsilateral input. On the other hand, spikes carried by shorter axons will arrive before the ipsilateral

input. Coincidence detectors connected to inputs with varying length will thus receive simultaneous excitation for sounds with various ITD thereby mapping sound location by the activation of specific MSO neurons. This delay-line is a central concept in the Jeffress (1948) model of sound localization. Fifty years after Jeffress proposed this model, the essence of it was verified in several organisms such as the barn owl (Joris et al., 1998) although some concerns about the validity of that model in mammals have been raised (Beckius et al 1999, Mcalpine and Grothe, 2003). In particular, inhibitory inputs to the MSO, which were not included in the Jeffress model, also play a role in ITD processing. Inhibitory inputs might rescale the sensitivity to ITD to a behaviourally relevant range or act as a gain control mechanism (see Grothe 2003 for review).

Most LSO neurons receive excitatory inputs from the ipsilateral ear and inhibitory inputs from the contralateral one. They code IID by subtracting the activity of the inhibitory input from the excitatory one. The degree of inhibition is determined by the intensity difference of the sound but also varies for different cells, allowing the population to code for a wide range of sound direction (Pollak et al., 2002). Intensity differences also lead to difference in the latency of the response. This time-intensity trade-off has probable functional consequences on binaural processing in the LSO (Grothe and Park, 1995). Indeed, the timing and the duration of the inhibitory input to the LSO has been shown to have a great influence on the response of the post synaptic cells and IID sensitivity (Park et al., 1996; Park, 1998; Oswald et al., 1999; Irvine et al., 2001).

Thus temporally precise neural interactions are necessary for the processing of both ITD and IID. This precise timing constraint is best illustrated by ITD processing in barn owls: owls can resolve sound location with an accuracy of a few degrees, for which interaural time difference is as short as 5 μs (Moiseff and Konishi, 1981). Because precise timing of the neural response relative to the stimulus is required for sound localization, the temporal coding properties of the neurons along the

auditory pathway are relevant not only to sound recognition but also to sound localization.

Interdependence of spatial and temporal processing

In natural settings, animals are often exposed to more than one acoustic signal at the same time. Sounds coming from a variety of animals and background noise may deteriorate the signal to noise ratio of the sound being attended to. It is thus necessary for the nervous system to extract and segregate the signal originating from one source from the rest of the acoustic environment to allow accurate recognition of the signal. Psychoacoustic experiments on humans and other vertebrates show that the nervous system does solve this "cocktail party" problem. The cocktail party effect was first described by Cherry (1953) and refers to the fact that human listeners are able to attend to one conversation in a room were many other conversations are going on. In such a situation, the nervous system must bind together the sound elements originating from one sound source in order to extract distinct perceptual objects.

Resolution of this cocktail party problem relies on binaural processing capacities. Human subjects using only one ear (the other one being blocked) performed much worse at attending and understanding speech embedded in noise (Hawley et al., 1999) than during binaural listening. Speech comprehension improves when the different sound sources are widely separated in space (Roman et al., 2003). Also, segregation of two concurrent sounds is facilitated if the signals have uncorrelated spectro-temporal characteristics. These psychoacoustical effects clearly underline the interdependence of spatial and temporal processing in difficult, noisy, conditions. However, little is known about the neural basis of this perceptual ability (for review see Feng and Ratnam, 2000).

A model of auditory processing developed by Cherry (1961) in order to account for these psychoacoustic phenomena relied on running

binaural cross-correlation. Other models have proposed a mechanism based on equalization-cancellation theory (Durlach, 1963), where contralateral inhibition cancels the response to the signal on one side but not to the noise (Breebaart et al. 2001). These two models could reflect the EE and EI processes of the auditory pathway (see the section on localization).

Neurophysiological experiments have focused on two specific aspects of the problem: spatial release from masking and the precedence effect. In IC neurons of cats for example, detection of a signal is improved if a source of background noise (the masker) is spatially separated from the signal, paralleling the psychoacoustic data (Litovsky et al, 2001). The precedence effect refers to the fact that if two signals are presented in rapid succession, one to each ear, only the first signal will be perceived. It would be particularly useful to suppress perception of the echoes elicited by an attended signal. Single neuron recording in the IC of cats identified neural correlates of this effect: depending on the time lag between the two sounds, the neurons often showed response to the first signal even though the second signal, when presented by itself, was encoded by the neuron (for review see Litovsky et al 1999).

The precedence effect has also been examined in insect auditory systems. Crickets will respond only to the first of two pulses presented from each side with delays from 4 to 75 ms (Wyttenbach and Hoy, 1993), but a neural correlate could not be identified in the first relay center (the prothoracic ganglion), thus the authors suggested it arises from brain circuits. Male bushcrickets sing in synchrony and female choice is most often directed toward the male that established temporal leadership. The phenomenon is similar to the precedence effect in that attention is oriented towards the leading of two signals. Contralateral inhibition in the prothoracic ganglion, the first site of binaural interaction, is thought to be responsible for this phenomenon (Römer et al., 2002).

Although we do not have a clear picture of the interaction between spatial and temporal processing, the evidence described here clearly indicate that one does not occur independently of the other and that this interdependence is most useful in difficult listening conditions.

Auditory processing in crickets

The auditory system of crickets shares similar challenges and solutions with ours: behaviourally relevant signals must be recognized and localized and the nervous system specializes to perform these tasks. In crickets, the behaviourally important signals are simple and the sensory cues are well understood. The auditory system is composed of relatively few neurons (compared to vertebrates), simplifying the study of neural circuits at the cellular level. Furthermore, auditory behaviour can often be linked to the response of a few central neurons. Therefore, the cricket is a good model organism to study auditory processing. I describe in this section the most relevant aspects of auditory processing in crickets.

Auditory environment of crickets and behaviour

Sound perception and production in crickets co-evolved as a communication tool (Stumpner and von Helversen, 2001). Male crickets produce songs to communicate with conspecifics. These songs are produced in the context of mate attraction and courtship or during aggressive encounters (for review see Hoy 1998). Crickets are also sensitive to ultrasound, which allows detection of hunting bats. The use of hearing for detecting insectivorous bats, in crickets, is thought to have evolved after conspecific communication: the hearing range was most probably widened to encompass the ultrasound of echolocating bats (Hoy 1992, Yager 1999).

Behavioural responses to conspecifics and predators (i.e. bats) are distinct behaviours. Flying or walking female crickets will orient towards a

conspecific calling male whereas when stimulated with ultrasound, the cricket will try to steer away from the sound source (Moiseff et al., 1978, Nolen and Hoy, 1986). These behaviours also differ in latency: ultrasound avoidance is a reflex-like response with a short latency (30-40 ms) and attraction to calling song occurs after several hundred ms of signal evaluation. Furthermore, ultrasound avoidance is robust during flight (Nolen and Hoy, 1984) but weak and infrequent when the cricket is walking (Pollack et al., 1984).

Females recognize conspecific males based on the carrier frequency and the temporal pattern of their song. In *Teleogryllus oceanicus*, the calling song has a dominant carrier frequency of around 4.5 kHz and harmonics at much lower intensity (20-40 dB lower, Balakrishnan and Pollack, 1996). These songs contain amplitude modulation rates between 1 and 35 Hz. The calling song is a repetition of a stereotypical phrase (see Fig. 1.1). During the chirp part of the phrase, pulses are emitted at around 16 pulses/s. The chirps are followed by trills which are pulse doublets (intra-doublet frequency: ~25-30 Hz) emitted at around 8 Hz. Behavioural experiments using sound pulses presented at different rates showed that females are attracted selectively to the pulse rate of chirps (~16 Hz). AM rates that deviate from this pattern, even the other AM rates contained in the song (i.e. 8 Hz, 25 Hz), elicit, at best, weak responses (Pollack and ElFeghaly, 1993). Behavioural responses to artificial songs are less selective for the carrier frequency of the signal than for its temporal pattern. Stimuli with the appropriate temporal pattern (pulses presented at 16 Hz) but with unnatural carrier frequency also elicit positive phonotaxis as long as the carrier frequency is within the audible range and not ultrasonic (i.e. 4-16 kHz; Moiseff et al., 1978).

Ultrasound avoidance is widespread among nocturnally flying insects. (Hoy 1994). Experiments on tethered crickets show that their ultrasound avoidance behaviour is not selective for specific patterns of modulation (Pollack and ElFeghaly, 1993). Echolocating bats produce

sound pulses of varying length (1 to >20 ms) and at various repetition rates (1 to 200 Hz) depending on the species of bat and the task they perform. Typically, bats will increase the repetition rate and decrease the length of their sound pulses when they require better temporal resolution in their auditory representation of space. For example, while searching for insects in open spaces, the bats emit pulses at low rates (a few Hertz) but increase the rate as they approach an insect for capture. In the terminal phases of the bat-insect pursuit, pulses are often only 3-5 ms apart (for review see Schnitzler and Kalko, 2001). Considering the variability in echolocation call structure, the relative insensitivity of ultrasound avoidance for ultrasound pulse rate is an advantage. The experiments that assessed the temporal pattern dependence of ultrasound avoidance indicate that this behaviour is unselective for temporal pattern of brief sounds, but this conclusion might be limited by the experimental conditions in which the crickets were tested. Indeed it is known, for example, that the behavioural response to prolonged stimulation habituates quickly (May and Hoy, 1991) in a rate dependent manner. Moreover, in most experiments, the sound source was immobile, whereas during a bat-insect pursuit the sound source is constantly moving relative to the cricket. This changing geometry of the sound introduces additional spatial and amplitude modulations that might influence auditory processing. The bat's signal could also be degraded by ambient noise and echoes. The stimulus patterns used thus far are probably a poor representation of the range of acoustic conditions encountered in nature, and might mimic only the simplest bat-crickets interactions. This field of research is in need of a better description of the dynamics of bat-cricket interactions and of the pattern of stimulation that the cricket has to process in real situations.

Auditory receptors and carrier frequency segregation

The ears are located on the tibia of the fore legs. The auditory information is carried from the ear to the prothoracic ganglion by the auditory receptors, where the information is then relayed to other ganglia such as the brain. The population of about 60-70 auditory receptors is composed of distinct types of cells based on their anatomy and carrier frequency sensitivity. Two morphologically different types of receptors were identified by Imazumi and Pollack (1999, 2001, 2005): medially terminating receptors (MT) and bifurcating neurons (BC). BC neurons are sensitive to the carrier frequency of conspecific songs (4-5 kHz) and have relatively high thresholds (>65 dB SPL). Receptors anatomically defined as MT are sensitive to one of three ranges of carrier frequency. The MT receptors most sensitive to communication sounds (4-5 kHz) have lower threshold than BC types of receptors (<55 dB SPL). The other MT receptors are most sensitive to ultrasound (>18 kHz) or to mid-range frequencies (9-12 kHz), many of which are also sensitive to ultrasound. The proportion of low-frequency sensitive receptor neurons is large: 73% of receptors examined by Imazumi and Pollack (2001) were most sensitive to low frequency (45% of which are MT type), compared with 12% and 15% for mid-frequency and ultrasound receptors respectively.

The MT receptors provide inputs to several interneurons of the prothoracic ganglion such as the ascending neurons and the omega neurons (see next section). BC receptors terminate in a more lateral and posterior region of the prothorax than MT receptors and seem to make few, if any, direct contact with the aforementioned interneurons. Imazumi and Pollack (1999, 2001, 2005) suggested than BC type receptors might be part of a descending pathway of sound processing.

Wyttenbach et al (1996) showed, through behavioural tests, that crickets have a categorical perception of frequency. Specifically they used an habituation-dishabituation paradigm to show that stimuli with varying carrier frequency were categorized either as attractive or repulsive and that a sharp transition between the two categories occurred around 16

kHz. Categorical perception has been identified in a number of systems (Ehret 1987). In humans for instance phonemes with varying VOT length will be perceived categorically.

Prothoracic interneurons and their role in auditory processing

Circuitry and sensitivity of prothoracic neurons

The auditory information is relayed from the receptors to the brain by bilaterally paired, identified interneurons (see Fig. 1.2). Two particularly important and well studied neuron pairs are the ascending neurons 1 and 2 (AN1 and AN2). They receive mostly monaural excitatory inputs from receptors (Hardt and Watson, 1994). AN1 is sharply tuned to the carrier frequency of calling song and AN2 is most sensitive to ultrasound. Another prothoracic neuron, the omega neuron 1 (ON1) has a "w-shaped" tuning curve with enhanced sensitivities in both frequency ranges (Atkins and Pollack, 1986). ON1 receives input from the receptors on one side and provides contralateral inhibition to the interneurons on the other side of the ganglion (AN1, AN2 and ON1; Selverston et al, 1985; see Fig. 1.2). Intracellular recordings of ON1 show that the structure of the input from the receptors differs for low and high frequency sounds. EPSPs in response to low frequency sound pulses are smooth in shape whereas for high frequency sounds, the response consists of series of large discrete synaptic potentials (Pollack, 1994). This difference is thought to arise from the differences in receptor-to-interneuron circuitry. It was suggested that while there are 3-4 time more low frequency receptors than ultrasound receptors, the former have a smaller post-synaptic impact than the latter.

Role of prothoracic interneurons in behaviour

The role of AN2 in ultrasound avoidance has been examined by Nolen and Hoy (1984) who performed simultaneous recordings of AN2 and of the flight steering muscles. They showed that if AN2 is hyperpolarized, the motor response to ultrasound pulses is suppressed, and that stimulating

AN2 at high firing rates (>180 Hz) was sufficient to elicit a response. Their experiment indicates that AN2 functions as a command neuron for ultrasound avoidance.

In a similar experiment, Schildberger and Hörner (1988) hyperpolarized AN1 or AN2 while the cricket performed positive phonotaxis towards conspecific calls. Hyperpolarizing AN1 on one side caused the cricket to turn toward the other side independently of the location of the sound source. Hyperpolarization of AN2 caused only small errors in the direction of locomotion and the effect was visible only for intense stimuli. Furthermore, hyperpolarizing AN2 could not cause the direction of walking to reverse.

In mature adults ON1 doesn't project to the brain (Atkins and Pollack, 1986), thus its role in behaviour must be exerted through its contralateral inhibition of the ANs. ON1's inhibition enhances the bilateral contrast in the response of the ANs thereby enhancing localization cues. Indeed, hyperpolarizing ON1 while the cricket tracks a conspecific song introduces systematic orientation errors (Schildberger and Hörner 1988; see also Atkins et al 1984).

Signal recognition and localization

Temporal coding and signal recognition

Ultrasound avoidance in crickets is not very selective for specific sound temporal patterns. Avoidance responses occur rapidly after stimulus onset (30-40 ms; Nolen and Hoy, 1984) suggesting that few synapses separate sensory input from motor output. Ultrasound sensitive brain neurons have been classified in two categories by Brodfuehrer and Hoy (1990): local brain neurons (LBN) and descending brain interneurons (DBIN). These brain neurons have arborisations in an area that also receives projections from AN2, although their latencies suggest that only one type of LBN cell is directly connected to AN2. This type of neuron, which arborises on both sides of the brain, is excited by ipsilateral sound pulses and inhibited by

contralateral ones. The other brain neurons are either excited or inhibited by ultrasound. The exact role of ultrasound sensitive brain neurons in the elaboration of ultrasound responses is not known.

Attraction to conspecific calling song is strongly selective for pulse repetition rate but AN1 encodes a broad range of pulse rates and thus cannot account for behavioural selectivity. Schildberger (1984) has identified several brain neurons whose selectivity for temporal pattern could account for the behavioural selectivity. Morphological characterization of these neurons indicates that AN1 and AN2 connect to brain neuron class 1 (BNC1) which in turn connect to BNC2. The difference in latency of the response of AN1 (16-38 ms), BNC1 (22-42 ms) and BNC2 (38-79 ms) corroborates the proposed connectivity. Temporal coding in the brain neurons is generally sharper than in the ANs. Many BNC1 neurons have high-pass or low-pass temporal selectivity and BNC2 neurons have a narrow, band-pass selectivity that corresponds to the attractive rate of the calling song. Band-pass selectivity in BNC2 is thought to arise from combining low- and high-pass inputs from BNC1 neurons. BNC2 neurons, and to a certain extent BNC1, do poorly at copying the sound structure in the structure of their spike train, despite their strong selectivity for temporal pattern. This change in coding properties, from faithful copying of a wide range of pattern to tonic temporally selective responses can also be found in the vertebrate auditory system where temporal coding at the periphery is replaced by rate coding higher up in the system.

The coding properties of these neurons suggest that song recognition is achieved by means of temporally matched filters. Despite this evidence, several other mechanisms for song recognition can be conceived (see Hennig et al., 2004, for review). A first hypothesis is that brain circuits estimate the spectrum of the temporal envelope. This mechanism would require the signal to contain the appropriate AM rates but not necessarily with the right phase relationship. Based on that

concept, Pollack and Hoy (1979) examined the attractiveness of shuffled artificial calling songs (in which pulse periods were retained but not pulse order). They found that these shuffled songs were nearly as attractive as normal, un-shuffled songs. This experiment could indicate that *T oceanicus* (the species that was examined) might perform signal recognition through spectral analysis. However, the sibling species *T commodus* differs in its requirement for temporally structured songs as they required pulses with the right period to be organized in a specific sequence (Hennig and Weber, 1997). Thus, doubts arise on whether such closely related species could have widely different recognition mechanisms. Another mechanism for song recognition would rely on circuits performing cross- or auto-correlation. The song pattern would be compared to an internal template (cross-correlation) or to a delayed copy of the pattern (auto-correlation). No physiological evidence for this kind of mechanism has been found in crickets, although Hennig (2003) suggested that such a mechanism could easily explain the different requirements for recognition in *T oceanicus* and *T commodus*. Recognition could also be achieved by neurons with intrinsic oscillation at species-specific rate as appears to be the case in some katydids (Bush and Schul, 2006). The favoured hypothesis, and the one that fits best the physiological data about brain neurons, relies on neurons selective for specific aspect of the signal: pulse period, pulse duration or duty cycle for example.

Recognition and sound localization: serial or parallel

Another issue related to the song recognition mechanism concerns the interdependence of temporal (recognition) and spatial (localization) processing. In grasshoppers localization and recognition are thought to occur in parallel, in other words they occur independently (von Helversen and von Helversen, 1995). Several lines of evidence suggest that in crickets, these processes happen serially or at least that they are interrelated. If temporal and spatial processing happened in parallel,

localization cues would be encoded independently of the recognition cues. If a sound with the right temporal pattern activates recognition, localization cues will not be drawn specifically from this signal but from the overall auditory environment. Stable et al (1989) tested these hypotheses by playing a conspecific song from directly on top of the cricket, thus providing no directional cues. In addition, they played a tone from one side of the cricket. The ANs on the side of the tone had higher firing rates, and thus if localization and recognition happened in parallel the cricket would orient toward that side since this higher activity would indicate that the sound comes from that side. However, the cricket oriented towards the other side where the ANs' response best reflected the temporal pattern of the song. This suggests that the cricket turns toward the side where the song pattern is most clearly represented. Furthermore, Pollack (1986) showed that crickets are able to segregate two simultaneously played songs and orient toward the most attractive. This result further strengthens the hypothesis according to which temporal and spatial aspects of sound signals are both used to allow segregation of multiple sound sources.

When a cricket is presented with a song played alternatively from the left and right, the cricket will alternate its locomotion path accordingly (Pollack and Hoy, 1981). Similarly Hedwig and Poulet (2004) used precise measurement of locomotion to show that crickets reacted to each sound pulse with reactive steering movement. Their experiment suggests that there is a short-latency pathway, probably through neurons descending from the prothoracic ganglion to the motor output, which influences phonotaxis directly. They propose that this descending input is modulated by information descending from the brain, thereby accounting for the ability to segregate several songs. Together these results indicate that temporal and spatial processing must be interrelated to explain the segregation ability of cricket, but the precise mechanism by which this is accomplished is still unclear.

Localization cues and ON1's inhibition

In crickets the interaural distance is small, yielding only small differences between the sounds reaching each ear (i.e. an intensity difference of 2 dB). This difference is mechanically increased by the coupling of the two ears (Michelsen and Löhe, 1995). As a result, the maximum effective intensity difference of a 4.5 kHz sound between the two ears is 10-15 dB. This difference in sound intensity is encoded in the auditory neurons by a lower firing rate on the sound-contralateral side and a longer latency of the response. The relative importance of differences in timing and intensity of the response as cues for sound localization is unclear. Pollack (2003) examined this issue by comparing neural and behavioural recordings. His experiment indicates that the main localization cue used to process communication sounds is the bilateral difference in response strength.

The omega neuron 1 provides contralateral inhibition to the ascending neurons as well as to its contralateral homologue. This reciprocal inhibition greatly enhances the directional selectivity of ON1. The role of ON1 in sound localization has been most thoroughly examined for communication sounds. Horseman and Huber (1994) quantified the contrast gain introduced by ON1. The contralateral inhibition enhances the bilateral spike count difference in the AN1 pair by 2-3 fold.

The timing of the contralateral inhibitory input could be important to enhance bilateral contrast (e.g. Rheinlaender and Mörchen, 1979). ON1's response latency is longer in response to low frequency compared to ultrasound. Faulkes and Pollack (2000) examined the importance of the timing of inhibition on the activity of the ANs. Altering the timing of the contralateral inhibition affects the timing and spike count of the ANs responses. Disruption of the temporal pattern of AN1's response should have an impact on sound localization since it relies, not only on bilateral differences in response strength, but also on differences in song pattern encoding (Stable et al, 1989). This is particularly true in situations where the cricket must attend to one of multiple signals. Behavioral tests show

that crickets are able to segregate different sound sources, such as two singing males (Pollack 1988; see previous section). Recordings of ON1 in a similar stimulus configuration (two cricket songs presented from each side of the cricket) reveal that the neuron encodes only the loudest of the two songs (i.e. the ipsilateral song), even though the other was accurately encoded when presented alone. This would allow ON1 to enhance localization cues specifically for one signal thereby implementing a sort of selective attention.

Thesis objectives

I explained in this chapter that binaural comparisons are important for processing auditory information, in particular the spatial aspect of the sound. In vertebrates, binaural processing relies on temporally very precise neural interactions, thus on neurons capable of accurate temporal coding. Furthermore, under noisy conditions, signal recognition depends on sound segregation, and thus sound localization.

The prothoracic ganglion of crickets is the first stage of binaural comparison along the auditory pathway. The contralateral inhibition provided by ON1 is present for low frequency, communication-like, sounds but also for ultrasonic, bat-like, stimuli. It was suggested that, due to its coding properties, ON1 might implement a mechanism for spatial segregation. Auditory processing in the prothoracic ganglion offers a good opportunity to examine the role of temporal coding in spatial processing for a number of reasons: 1) processing relies on identified, easily accessible interneurons; 2) circuitry is relatively well known; 3) localization and recognition cues are well characterized; 4) the roles of major interneurons are known.

In this thesis I will clarify how ON1's temporal coding properties participate in shaping the auditory information. Specifically, I quantify the coding properties of ON1 in chapter 2 and show that they vary with carrier

frequency. I show in chapter 3 that these carrier-frequency specific properties are important to adequately shape the temporal and spatial information travelling in the ascending neurons. I clarify in chapter 4 the nature of the neural code for ultrasound stimuli and demonstrate that behaviourally relevant information is carried by bursts of spikes in AN2. Finally I verify in chapter 5, that ON1's inhibition efficiently enhances the bilateral contrast during these bursts. The results reveal that ON1's coding properties enable the enhancement of localization cues selectively for behaviourally relevant signals.

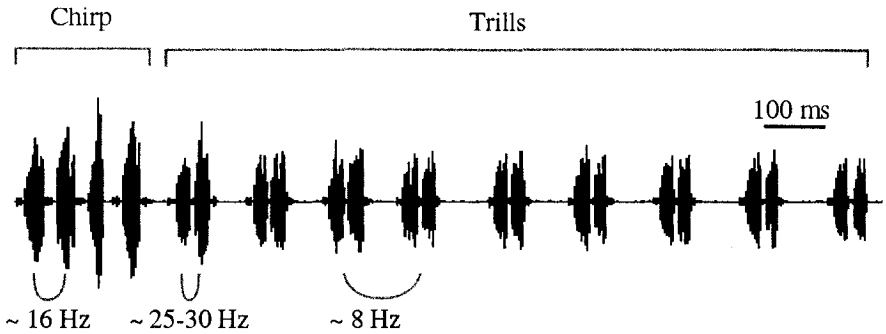

Figure 1.1: Temporal structure of a phrase of the calling song of *Teleogryllus oceanicus*. We indicate typical pulse repetition rate of the different components of the song below the trace.

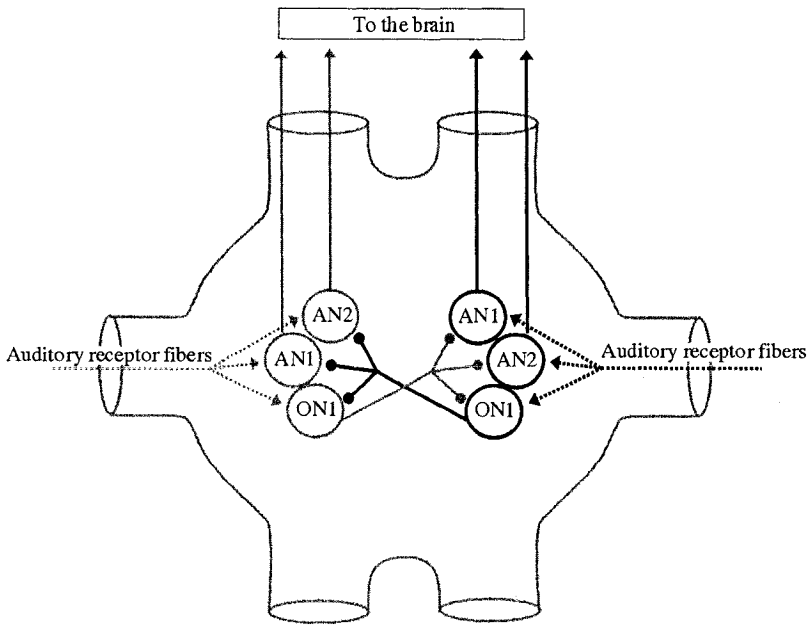

Figure 1.2: Schematic drawing of circuitry in the prothoracic ganglion. Auditory receptors provide monaural input the bilaterally paired ascending neurons (AN1 and AN2) and to the omega neuron 1 (ON1). The ascending neurons project to the brain. ON1 provides contralateral inhibition to the ascending neurons as well as to its contralateral homologue.

Chapter 2:

Differential temporal coding of rhythmically diverse acoustic signals by a single interneuron

Marsat G, Pollack GS.

Journal of Neurophysiology (2004); 92: 939-948;

Abstract

The Omega Neuron 1 (ON1) of the cricket *Teleogryllus oceanicus* responds to conspecific signals (4.5 kHz) and to the ultrasonic echolocation sounds used by hunting, insectivorous bats. These signals differ in temporal structure as well as in carrier frequency. We show that ON1's temporal coding properties vary with carrier frequency, allowing it to encode both of these behaviourally important signals. Information-transfer functions show that coding of 4.5 kHz is limited to the range of amplitude-modulation components that occur in cricket songs (<32 Hz), whereas coding of 30 kHz stimuli extends to the higher pulse rates that occur in bat sounds (~100 Hz). Nonlinear coding contributes to the information content of ON1's spike train, particularly for 30 kHz stimuli with high intensities and large modulation depths. Phase locking to sinusoidal amplitude envelopes also extends to higher AM frequencies for ultrasound stimuli. ON1s frequency-specific behaviour cannot be ascribed to differences in the shapes of information-transfer functions of low- and high-frequency-tuned receptor neurons, both of which are tuned more broadly to AM frequencies than ON1. Coding properties are nearly unaffected by contralateral deafferentation. ON1's role in auditory processing is to increase binaural contrast through contralateral inhibition. We hypothesize that its frequency-specific temporal coding properties optimize binaural contrast for sounds with both the spectral and temporal features of behaviourally relevant signals.

Introduction

Sensory information is often conveyed by the temporal structures of signals. This is particularly evident for acoustic signals. Speech, bird song, and communication sounds of many other species are characterized by stereotypic rhythms of modulation of frequency and/or amplitude.

Behavioural tests have shown that these temporal features carry much of the signal's information (e.g. Shannon et al. 1995; Ghazanfar et al. 2001).

Crickets communicate using songs composed of rhythmical sequences of sound pulses. Both the carrier frequency of songs and their temporal structures are important cues for signal recognition. Sounds with spectral and temporal properties similar to those of cricket song elicit orientation and locomotion towards the sound source (reviewed in Pollack 1998). Crickets also hear the echolocation calls of hunting, insectivorous bats; such sounds elicit evasive responses (Nolen and Hoy 1986).

Cricket songs and bat calls differ both in spectrum and in temporal pattern. Songs of the cricket species studied here, *Teleogryllus oceanicus*, have a dominant carrier frequency of ca. 4.5 kHz, with higher harmonics that are lower in intensity by at least 20 dB. The sound pulses that comprise the songs are 20-35 ms in duration, and occur at rates from ca. 7 to 32 pulses/second (Balakrishnan and Pollack 1996). Bat calls are ultrasonic (> 20 kHz) and consist of series' of brief sound pulses (typically 1-20 ms) occurring at rates up to 200 pulses/second (Wimsalt 1970).

The auditory system of *T. oceanicus* is specialized to detect sound frequencies similar to those that occur in cricket songs and bat calls. This is apparent at both the receptor-neuron and interneuron levels, where individual neurons respond most strongly to either cricket-like or bat-like frequencies (Atkins and Pollack 1987; Imaizumi and Pollack 1999). The identified interneuron ON1 is unusual in that it is dually tuned, with enhanced sensitivity to both ranges of sound frequency (Atkins and Pollack 1986). Each ON1 receives excitatory input mainly from the receptors of one ear and inhibits neurons that receive input from the opposite ear, thus enhancing binaural contrast and, presumably, facilitating sound localization (Selverston et al. 1985; Horsemann and Huber 1994; Faulkes and Pollack 2000).

Work in several systems has shown that the temporal coding properties of neurons are matched to the structures of behaviourally

important signals (Rieke et al. 1995; Theunissen et al. 2000; Machens et al. 2001; Nagarajan et al. 2002). ON1 is unusual among auditory neurons in that this single neuron processes two different classes of signal, cricket songs and bat calls, that differ in carrier frequency, temporal structure, and behavioural consequence. ON1 is specialized for the differing carrier frequencies of these signals. Here, we show that it is also specialized to encode their differing temporal structures.

Materials and Methods

Electrophysiology.

Teleogryllus oceanicus were reared in the laboratory. Virgin females were used for experiments at age 10-21 days after the final molt. They were mounted on a support ventral-side uppermost, with the front legs (the site of the ears) held flexed against the pronotum in a position similar to that adopted during flight. The prothoracic ganglion was exposed by ventral dissection, supported on a metal platform, and bathed in physiological saline (Strausfeld et al 1983). ON1 was recorded extracellularly from its soma-contralateral processes in the prothoracic ganglion using blunt glass microelectrodes filled with 1M NaCl (resistance, 5-10 Mohm). ON1 can be identified unambiguously in this recording configuration by its increased sensitivity to electrode-contralateral sound (threshold lower by 10-20 dB; see Pollack (1986) for further details), as well as by its greater sensitivity, and longer latency, to 4.5 kHz stimuli than to ultrasound (Faulkes and Pollack 2000). Receptor neurons were recorded intracellularly at the entrance of the leg nerve to the prothoracic ganglion. Threshold for recorded neurons at 4.5 kHz and/or 30 kHz was defined as the minimum sound level (accuracy of ±1 dB for ON1, ±2.5 dB for receptors) that consistently evoked >1 spike per 30 ms sound pulse. Recordings were digitized (16 bits, sampling rate 10 kHz; Digidata 1320A, Axon Instruments) and analyzed off-line.

Sound stimuli.

Stimuli were either 30 ms sound pulses (including 5 ms linear onset and offset ramps) presented at 2 pulses/s, 15 s tones (4.5kHz or 30 kHz) the amplitude of which was modulated sinusoidally (100% modulation depth, amplitude-modulation (AM) rates 1-140Hz; Sinusoidal Amplitude Modulation: SAM), or 15-30 s tones that were modulated in amplitude by multiplication with a low-pass-filtered Gaussian signal (<200Hz) with standard deviation of 3 dB except where otherwise noted (Random Amplitude Modulation: RAM). Stimuli were produced by National Instruments AD/DA boards with 12 bits of resolution, at a sampling rate of either 100 or 200 kHz. Sounds were broadcast from loudspeakers situated perpendicular to the cricket's longitudinal axis, ipsilateral to the ear driving the recorded neuron. For ON1, 30 kHz and 4.5 kHz stimuli were presented in alternation; low- and high-frequency receptor neurons were stimulated with 4.5 kHz or 30 kHz stimuli, respectively. Stimuli were followed by silent recovery periods of 45 s (15 s stimuli) or 90s (30 s stimuli). Sound level was calibrated using Brüel and Kjaer instruments (4135 microphone, 2610 sound-level meter).

Data analysis

Information-transfer functions. Temporal coding properties of neurons can be described in terms of the information contained within their spike trains about changes in a stimulus. We used two approaches to compute information-transfer functions. We derived the maximum information content of the spike train from the variation between responses to repeated presentations of an identical RAM stimulus, yielding an upper-bound estimate of information transfer (although, in our experiments, this corresponds to the actual information-transfer rate; see below). We also constructed estimates of the stimulus based on an optimal linear filter relating the neuron's spike train to preceding stimulation (reverse

reconstruction), and derived a lower bound on information transfer from the difference between the actual and estimated stimulus.

We used two methods to compute the upper bound on information transfer. **1**. We described the neuron's response to each trial, $r_i(t)$, as firing rate in successive 0.5 ms-wide bins, (i.e. firing rate per bin either 0 or 2000 Hz). These arrays were averaged across trials, yielding $\bar{r}(t)$. $\bar{r}(t)$ represents the component of the response that is determined by variations in stimulus amplitude. Deviations from $\bar{r}(t)$ on individual trials were assumed to be due to additive noise, $n_i(t)$, and were calculated as $r_i(t) - \bar{r}(t)$. Signal-to-noise ratio as a function of AM frequency, *SNR*(*f*) was calculated as $P\bar{R}(f)/\overline{PN_i}(f)$, where $P\bar{R}(f)$ and $\overline{PN_i}(f)$ are, respectively, the power spectrum of $\bar{r}(t)$ and the mean of the power spectra of $n_i(t)$ (Haag and Borst 1997). Information transfer was calculated as $I(f) = \log_2(1+SNR(f))$ (Borst and Theunissen 1999). This method was applied to 5 ON1s, with the RAM stimulus repeated 30 times. **2**. Spike timing was compared between pairs of responses by calculating response-to-response coherence (Roddey et al. 2000). Each individual response, expressed as firing rate, ($r(t)$), was separated into overlapping, Hanning-windowed, 300 ms segments and converted to the frequency domain ($R(f)$) using the fast Fourier transform. The coherence of a pair of responses *i* and *j* was calculated as:

$$Coh = \sqrt{\langle R_i(f) * R_j(f) \rangle \langle R_j(f) * R_i(f) \rangle / \langle R_i(f) * R_i(f) \rangle \langle R_j(f) * R_j(f) \rangle},$$

where '*' indicates complex conjugation, and $\langle\ \rangle$ indicates averaging across the 300 ms response segments. For each neuron, coherence was calculated for all pair wise combinations of responses to the same stimulus and averaged across response pairs, yielding $\overline{Coh}$. Information was calculated as $I(f) = -\log_2(1-\overline{Coh})$ (Borst and Theunissen 1999).

The two methods of calculating upper-bound information-transfer functions were compared for five ON1 neurons, and the results were indistinguishable. Here, we present results from the second method. Receptor neurons can be recorded for only a few minutes (Imaizumi and Pollack 1999), and we were able to repeat RAM stimuli only 2-3 times. The first method cannot be applied with such small sample sizes, but these are sufficient data for the second method (Roddey et al 2000); thus, only the second method was used for receptors.

If signal power and noise power both have Gaussian probability distributions, the upper bound on information transfer equals the actual information transfer rate (Borst and Theunissen 1999). For the subset of ON1s that were tested with 30 stimulus repetitions, we confirmed that these requirements were met by comparing the distributions of signal (in this case, $\overline{R(f)}$) and noise ($N_i(f)$, for all i) with Gaussian distributions having the same mean and standard deviation (Kolmogorov-Smirnov test; range of p values, 0.11 – 0.6).

Lower-bound information transfer functions, reflecting linearly coded information, were derived from reconstructions of the stimulus envelope based on an optimum linear filter describing the relationship between the stimulus and ON1's firing rate (Theunissen et al. 1996; Clague et al. 1997). Arrays representing firing rate, $r(t)$ and the stimulus envelope, $s(t)$, were expressed as variations around their respective means, yielding $r'(t)$ and $s'(t)$.These arrays were segmented and Fourier-transformed as described above, yielding $R'(f)$ and $S'(f)$. The frequency-domain representation of the linear reverse filter for response i was calculated as: $H_i(f) = \langle R_i'(f) * S_i'(f) \rangle / \langle R_i'(f) R_i'(f) * \rangle$. $H_i(f)$ was converted to the time domain, $h_i(t)$, using the inverse Fourier transform. The result of these operations is equivalent to the cross-correlation of $r'_i(t)$ and $s'_i(t)$, divided by the autocorrelation of $r'_i(t)$ (Press et al, 1992.). $h_i(t)$ was convolved with $r_i(t)$ to reconstruct the neuron's estimate of the stimulus, $est_i(t)$. Noise, $n_i(t)$, was computed as $s_i(t)$ - $est_i(t)$. Signal-to-noise ratio,

$SNR_i(f)$, was computed as the power spectrum of $est_i(t)$ divided by that of $n_i(t)$, $SNR_i(f)$ was averaged for all i and information transfer was calculated from $SNR(f)$ as above.

Firing rate adapts markedly during the first few seconds of the response, yet an assumption behind our calculations is that the response statistics are stationary over time (Rieke et al. 1997). To restrict our analysis to the stable, i.e. adapted, portion of the response, the first five seconds were excluded.

We summarize information-transfer functions by the maximum rate of information transfer, the AM rate at which information transfer is maximum, and the half-width, defined as the (possibly non-contiguous) range of AM frequencies at which information rate is greater than half the maximum.

Synchronization coefficient. Synchronization coefficient was calculated for responses to SAM stimuli as $\sqrt{(\sum x_i)^2 + (\sum y_i)^2}/n$, where x_i and y_i are, respectively, the cosine and sine of the phase of the sinusoidal AM envelope at which the i^{th} spike occurs, and n is the number of spikes included in the analysis (Goldberg and Brown 1969). Synchronization coefficient ranges from 0 to 1, and reflects both the extent of spike clustering during each cycle of AM, and the consistency of response phase from cycle to cycle.

Calculations were performed using programs written for Scilab (www.scilab.org). Statistical tests were performed using Statistica 5.5 (Statsoft, Tulsa, OK).

Results.

Dependence of temporal coding on carrier frequency

ON1 shows enhanced sensitivity to both cricket-like (4.5 kHz) and ultrasonic (>20 kHz) frequencies, but threshold is lower for the former frequency range (4.5 kHz: 53.6 ± 3.5 dB SPL; 30 kHz: 65.8 ± 4.6, n=15; cf. Atkins and Pollack 1986). To compare coding in these two ranges, we

presented stimuli at equivalent intensities relative to threshold (20 dB above threshold unless otherwise stated, denoted as +20 dB).

Fig. 2.1A shows excerpts of the responses of a single ON1 to repeated presentations of RAM stimuli with the identical modulation envelope, but with carrier frequency of either 4.5 kHz or 30 kHz. The spiking patterns differ for the two stimuli. This is most obvious in the second half of the response segments shown, where ON1's spike train more precisely reflects features of the stimulus envelope for the 30 kHz stimulus.

We characterized ON1's coding of the stimulus envelope by comparing responses to repeated presentation of the identical RAM stimulus (see Methods). The result of this analysis, the information-transfer function, quantifies, as a function of the frequency of amplitude modulation (AM), the information content of the neuron's spike train pertaining to changes in stimulus amplitude. These functions vary with carrier frequency (Fig. 2.1B). For 4.5 kHz stimuli, the rate of information transfer drops markedly for AM frequencies > 25 Hz; at AM frequencies > 50 Hz, little or no information about the AM envelope is coded in the neuron's spike train. For 30 kHz stimuli, information rate drops more gradually, approaching 0 only at AM rates above 100 Hz. This is reflected by the half-width of the curve, which is greater for 30 kHz (4.5 kHz: 31.9 ± 1.3 Hz; 30 kHz: 69.7 ± 2.9 Hz; mean ± s.e.; paired t-test, $p<10^{-5}$). Information transfer reaches higher peak rate for 4.5 kHz (1.9 ± 0.1 bits/s) than for 30 kHz (1.1 ± 0.1; $p<10^{-6}$), but the frequency at which the peak occurs is similar for the two carrier frequencies (4.5kHz: 12.2 ± 1.6 Hz; 30 kHz: 18.2 ± 4.1; $p>0.1$).

Effects on coding of stimulus intensity and modulation depth.

The curves shown in Fig. 2.1B were derived from responses to stimuli presented at equivalent sound levels relative to threshold (+20 dB), with envelope standard deviation of 3 dB. Under these conditions, mean firing

rate is lower for 30 kHz stimuli (24.4 ± 1.8 spikes/s vs. 46.2 ± 2.3 spikes/s, paired t-test, $p < 10^{-5}$). However, this does not account for the difference in shape of the information transfer functions, which is apparent over a range of stimulus intensities and firing rates (Fig. 2.2A, B). For example, firing rates are similar for responses to 4.5 kHz, 20 dB above threshold (Fig. 2.2A, 46.2 ± 2.3 spikes/s) and 30 kHz, 30 dB above threshold (Fig. 2.2B, 43.7 ± 3.3 spikes/s; p = 0.5), yet half-width is still greater for 30 kHz (81.7 ± 2.9 Hz, vs. 31.9 ± 1.3 Hz for 4.5 kHz; $p < 10^{-9}$). Mean firing rates are also similar for the two carrier frequencies even at the same mean stimulus intensity (+20 dB) when modulation depth is greater (see below), and again the information-transfer curves maintain their frequency-specific shapes (Fig. 2.2C, D).

For 4.5 kHz stimuli, information-transfer curves change only slightly, though significantly, with changes in stimulus intensity (Fig. 2.2A). Peak information rate varies slightly (though not monotonically) with intensity (ANOVA: p=0.04), frequency at which the peak occurs increases (ANOVA: $p<10^{-7}$), and half-width increases (ANOVA: $p<10^{-4}$). For 30 kHz, peak information rate increases markedly with increasing intensity (ANOVA: $p<10^{-10}$), but other features of the curves are unchanged (ANOVA: frequency at which information rate is maximal, p=0.6; half-width, p=0.6).

Coding is strongly affected by changing the depth of modulation, i.e., the standard deviation of the stimulus envelope, even though overall (rms) sound level is constant (+20dB; Fig. 2.2C,D). For both carrier frequencies, the peak information-transfer rate increases with modulation depth (ANOVA: $p<10^{-5}$ for 4.5 kHz, $p<10^{-4}$ for 30 kHz), but other parameters of the information-transfer curves are unchanged. For 4.5 kHz, mean firing rate does not change significantly with modulation depth (range: 41.3 ± 3.2 to 42.5 ± 2.8 spikes/s ANOVA: p=0.98), although it does increase for 30 kHz stimuli (Fig. 2.2D, inset; ANOVA: p=0.03). For envelope standard deviation of 7 dB, mean firing rate is similar for the two carrier frequencies (paired t-test, p=0.27) although, as stated earlier, the

information-transfer curves clearly differ in shape (half-widths: 37.3 ± 1.9 Hz for 4.5 kHz; 108.7 ± 6.2 for 30 kHz, paired t-test, p=0.0008).

ON1's coding of information about changes in stimulus amplitude could, in principle, be accounted for by a linear relationship between amplitude and spike rate. Alternatively, this relationship might also include nonlinear components. Linear and nonlinear coding (if present) both contribute to the information-transfer functions in Figs. 2.1 and 2.2. We estimated how much information was transmitted with a linear code by reconstructing the stimulus envelope using a linear reverse filter (see Methods). Time-domain representations of the reverse filters (i.e., the filter impulse functions) are shown in Fig. 2.3A. The impulse function derived from responses to 30 kHz stimuli is narrower than that for 4.5 kHz, and latency between its peak and ON1's action potential is shorter by several ms (c.f. Faulkes and Pollack, 2000). The stimulus estimate derived from the response to 4.5 kHz reflects mainly slower changes in stimulus amplitude, whereas that derived from the 30 kHz response captures more rapid amplitude changes (Fig. 2.3B).

Linear estimates of information transfer are compared with the actual information-transfer rates in Fig. 2.3C. For the conditions illustrated, envelope standard deviation of 7 dB, stimulus intensity 30 dB above threshold, the linear estimate capture only a portion of the information in the spike train. Nevertheless, the information-transfer functions based on linear estimates retain their characteristic carrier-frequency-specific shapes (Half-width: 33.3 ± 1.1 vs. 86.7 ± 12.4 Hz; Frequency of maximum information: 15.3 ± 3.1 vs. 28.6 ± 0.8 Hz; Maximum information rate: 1.57 ± 0.06 vs. 0.75 ± 0.02 bits/s; 4.5 kHz vs. 30 kHz respectively; $p<0.001$ for all comparison)

As shown in Fig. 2.2, the information transfer rate increases with increasing stimulus intensity and envelope standard deviation. Total information transfer can be partitioned into linear and nonlinear components (Fig. 2.3D). For 4.5 kHz stimuli, both linear and nonlinear

components increase in parallel, but for 30 kHz stimuli the increase in information is due predominantly to a marked increase in the nonlinear component. For 30 kHz stimuli with high intensity and standard deviation, linear coding accounts for less than 20% of the overall information content of ON1's spiking response.

Responses to sinusoidally amplitude-modulated stimuli

For computational reasons, our analysis of information transfer excluded the initial few seconds of the response (see Methods), but behavioural responses (avoidance of ultrasound; attraction to cricket song) occur with short latency (avoidance: 25-70 ms, Nolen and Hoy 1986; attraction: 300-400 ms, Pollack 2003). Another way to assess temporal coding, which can be applied even to the early portion of a response, is to examine responses to sinusoidally amplitude-modulated (SAM) stimuli. For low AM frequencies, ON1's initial response captures the temporal structures of SAM stimuli with both 4.5 kHz and 30 kHz carrier frequencies; however for high AM frequencies, the spike train reflects the amplitude envelope only for the 30 kHz stimulus (Fig. 2.4).

We examined coding of SAM stimuli quantitatively by plotting the relationships between synchronization coefficient and AM frequency (synchronization-coefficient modulation transfer function: scMTF) and between firing rate and SAM frequency (firing-rate modulation transfer function: frMTF). To analyze synchronization during the initial portion of the response, we computed synchronization coefficients for responses to the first four cycles of AM. Initial synchronization is best at lower AM frequencies for both 4.5 kHz and 30 kHz stimuli (Fig. 2.5A). However, synchronization to high AM frequencies is better for ultrasound stimuli (ANOVA, $p<0.0001$; Tukey test, $p<0.05$ for AM rates 45, 65 and 100 Hz), resulting in a less sharply tuned scMTF (half-widths: 36.2 ± 11.4 for 4.5 kHz and 63.7 ± 30.5 for 30 kHz; $p=0.008$). We measured initial firing rate as the maximum instantaneous rate (i.e. inverse of the smallest interspike

interval) during the response to the first cycle of AM. This measure thus reflects sensitivity to the rate of change of amplitude, rather than to the repetition rate of AM cycles. For both carrier frequencies, instantaneous firing rate was low for low AM frequencies, and increased to an approximate plateau (Fig. 2.5B). For rates above 25 Hz, however, firing rate was higher for ultrasound stimuli, (ANOVA, $p<0.0001$; Tukey test, $p<0.05$ for all AM frequencies above 25 Hz).

We also examined coding of SAM stimuli after adaptation was established, by computing MTFs for the response during the last 10 s of a 15 s stimulus. As for the initial response, synchronization at high AM frequencies was greater for ultrasound stimuli (Fig. 2.5C; ANOVA, $p<0.0001$; Tukey test, $p<0.05$ for AM rates >25 Hz). However, the frMTF differed markedly from that at the onset of the response. Whereas instantaneous firing rate at response onset is greater for 30 kHz, during the adapted portion of the response, mean firing rate is lower for 30 kHz (ANOVA, $p<10^{-6}$; Fig. 2.5D). The frMTFs for the two carrier frequencies also differ in shape. Firing reaches a peak at higher SAM frequencies for 30 kHz carrier than for 4.5 kHz (median frequency: 45 Hz for 30 kHz, 18 Hz for 4.5 kHz, Wilcoxon test, $p=0.002$).

Coding properties of auditory receptor neurons

ON1's coding properties might simply mirror the coding properties of auditory receptor neurons. We examined this possibility by recording receptor responses to RAM stimuli. Based on frequency-sensitivity, receptors fall into three groups, which are most sensitive to the low frequencies that occur in cricket song (low-frequency receptors), to ultrasound, or to a mid-range of frequencies (Imaizumi and Pollack 1999). Most of the latter also respond strongly to ultrasound; here, we consider these last two groups together as high-frequency receptors. Low-frequency receptors comprise two distinct groups that differ in anatomy as well as in a number of physiological parameters, including threshold

(Imaizumi and Pollack 2001). Based on anatomy, low-frequency receptors are either MT types (midline-terminating) or BC types (bifurcating arbors). The former type has lower threshold. Receptors with threshold, at 4.5 kHz, ≤55 dB SPL were classed here as low-threshold (putative MT types), and those with thresholds ≥65 dB SPL as high-threshold (putative BC types). Six receptors of each threshold class were stained with Lucifer yellow; in all cases, their structures matched their putative anatomical designation. We also stained four high-frequency receptors; their structures also matched that described previously (Imaizumi and Pollack 2001) for mid-frequency and ultrasound receptors (which are anatomically indistinguishable).

ON1's frequency-specific coding properties differ from those of receptors. Information-transfer functions of receptors (Fig. 2.6) peak at higher AM frequencies and are broader than the corresponding functions for ON1 (i.e., low-frequency receptors vs. ON1's response to 4.5 kHz carrier; high-frequency receptors vs. ON1's response to 30 kHz carrier; see figure legend for statistics). Surprisingly, for the stimulus conditions we used (10-15 dB above threshold, envelope s.d. of 3 dB), only four of the ten low-threshold, low-frequency receptors that we recorded showed statistically significant coding of the stimulus envelope, as assayed by jackknife resampling (Efron, 1993); Fig. 2.6A includes only these four receptors. All of the high-threshold, low-frequency receptors significantly coded the stimulus envelope (Fig. 2.6B). Information-transfer rates of both groups of low-frequency receptors are lower than that of ON1. By contrast, information rates of high-frequency receptors (all of which coded significantly) are higher than that of ON1 (Fig. 2.6C).

As for ON1 (see Fig. 2.3D), coding by receptors includes both linear and nonlinear components (Fig. 2.6D). For 4.5 kHz stimuli of equivalent intensity and modulation depth (envelope standard deviation, 3 dB), the proportion of the total information transfer ascribed to nonlinear coding is similar for receptor neurons and ON1 (low-frequency, low-threshold

receptors vs. ON1, 10 dB above threshold: $p>0.3$; low-frequency, high-threshold receptors vs. ON1, 30 dB above threshold: $p>0.15$). For 30 kHz stimuli, however, nonlinear coding is more pronounced in ON1 than in receptors (high-frequency receptors vs. ON1, 10 dB above threshold: $p<0.02$).

Frequency-specific coding characteristics do not require contralateral inhibition

Wiese and Eilts (1985) suggested that ON1's temporal selectivity is determined by the dynamics of reciprocal inhibition between the left and right ON1s. We tested this hypothesis by comparing information-transfer functions before and after cutting the contralateral auditory nerve, thus removing input from the contralateral ear. Information-transfer curves were largely unaffected by unilateral deafening (Fig. 2.6A) although, for 4.5 kHz stimuli, there was a slight increase in peak information-transfer rate, and decrease in the frequency at which information is maximal (paired t-test; $p=0.03$ in both cases).

Responses to SAM stimuli were also similar before and after removing contralateral input. As expected, mean firing rate increased when contralateral inhibition was removed, but the shapes of the frMTFs were unchanged (Fig. 2.6B; no difference in SAM frequency of maximal firing rate: Wilcoxon test, $p>0.5$ for 4.5 kHz and $p>0.3$ for 30 kHz). Similarly, the shapes of the scMTFs were unaffected (Fig. 2.8; no difference in half-width, paired t-test, $p>0.5$ for both carriers).

Coding properties and natural stimuli

ON1's frequency-specific temporal coding properties are well suited to behavioural requirements. In Fig. 2.8A we compare ON1's information-transfer curve for cricket-like carrier with the temporal structure of the species' calling song. It is clear that ON1's coding properties are well matched to the song's structure. We also show behavioural selectivity for

stimuli consisting of sound pulses presented at different rates (Pollack and El-Feghaly 1993). These stimuli differ substantially from the RAM stimulus used to derive the information-transfer function, and so behavioural and neural curves are not directly comparable. Nevertheless, the behavioural curve is centered on only one peak in the song spectrum, whereas ON1's coding includes the entire song spectrum, Thus, ON1's coding properties do not appear to account for behavioural selectivity.

Fig. 2.8B shows ON1's information-transfer function for bat-like stimuli, along with the ranges of pulse rates found in the calls of several species of bat. ON1's enhanced coding of high AM frequencies encompasses much of the range of pulse rates in these bat sounds. In addition, bat pulses may be very brief (<2 ms, Jones and Corben 1993; Jones 1999) and thus rapidly modulated in amplitude. Such stimuli elicit strong, phase-locked responses in ON1 (see Fig 2.5A, B).

Discussion

Coding characteristics.

The temporal characteristics of ON1's response differ for cricket-like and bat-like sound frequencies. Information in ON1's spike train about stimuli with cricket-like carrier frequency is restricted to a narrow range of AM frequencies below ca. 30 Hz, similar to the range of temporal components of intraspecific communication signals. The drop off of information is more gradual for bat-like carrier frequencies, extending ON1's coding into the higher range of AM frequencies that occur in bat echolocation signals (Fig 2.8). ON1's differential coding of signals with cricket- and bat-like carriers is also apparent in its ability to synchronize to SAM stimuli, as well as in its firing rates to such stimuli. Thus, these two approaches to studying temporal coding lead to qualitatively similar conclusions.

A limitation of the information-theoretic approach is that it cannot be used to characterize coding during the initial, nonstationary portion of the response, even though it is during this period that behavioural responses

are initiated. Avoidance responses to ultrasound, in particular, are initiated after only a few spikes in AN2, occurring with high instantaneous rate (Nolen and Hoy 1984, 1986). We characterized coding by ON1 during this period using responses to SAM stimuli. Like AN2, ON1 responds strongly at the onset of ultrasound stimuli, with instantaneous firing rate approaching 500 spikes/s. Moreover, maximum instantaneous firing rate is highest for stimuli with rapid rates of amplitude modulation (Fig. 2.5B), a characteristic of bat sound pulses. Thus ON1s initial response to ultrasound is well suited to influence even the onset of ultrasound-elicited behavioural responses. Moreover, neither ultrasound-avoidance responses nor attraction to cricket songs are restricted to only the first few milliseconds after stimulus onset. Positive phonotaxis to cricket-song stimuli persists for minutes (e.g. Pollack and El-Feghaly 1993). Recent infrared movies of bat-insect encounters show that these may continue for several seconds as the bat follows its intended prey through successive evasive manoeuvres (Simmons 2003). Although ON1s responses to SAM stimuli change as it adapts, its temporal coding characteristics remain well matched to the structures of cricket songs and bat calls (Fig. 2.5 A, C).

Nabatiyan et al. (2003) also studied temporal selectivity of ON1 of another cricket species, *Gryllus bimaculatus*. Their stimuli were trains of sound pulses with cricket-like carrier frequency, presented at different pulse rates. They found that maximum instantaneous firing rate per pulse increased with increasing pulse period, reaching a plateau at the pulse period that occurs in the species' song. They present a model in which the number of spike-rate peaks per chirp varies in a band-pass manner with pulse period, mirroring the behavioural effectiveness of the stimuli. Because of differences in the design of stimuli, we cannot compare our results directly with theirs. However, the coding properties that we describe do not appear to account for behavioural selectivity to temporal pattern (Fig. 2.8A).

Schildberger (1984) described neurons in the brain that respond selectively to behaviourally effective sound-pulse rates. Anatomical evidence suggests that the source of input to these brain circuits is the ascending neurons, AN1 and AN2. If ON1 (which, in mature adults, is a local, prothoracic neuron; Atkins and Pollack 1986) affects brain recognition circuits, it must do so indirectly, through its inhibition of the ascending neurons.

ON1's coding properties include both linear and nonlinear components. The nonlinear component is most evident for responses to higher intensities and larger envelope standard deviations. The underlying cause may be high intensity in both cases; because rms intensity was held constant, peak stimulus intensity increased with envelope standard deviation (see Fig. 2.2C inset). The nonlinear contribution to coding was much more pronounced for 30 kHz stimuli. Other features of our data also point to nonlinear response properties for this carrier frequency. Mean firing rate increases at greater-than-linear rate with increasing intensity of 30 kHz RAM stimuli over the range of intensities 10-30 dB above threshold, whereas the increase for 4.5 kHz stimuli is approximately linear (see Fig. 2.2B inset). Moreover, when stimulus intensity was held constant, mean firing rate increased with envelope standard deviation (and thus peak stimulus intensity), but only for 30 kHz stimuli.

Increasingly nonlinear coding with increasing stimulus intensity has been described previously. In the visual system of flies, linear coding accurately describes the responses of motion-sensitive interneurons, provided that the changes in velocity of the stimulus are small. For larger changes in velocity, nonlinear coding accounts for a substantial fraction of the information. As for ON1, the shape of the function describing coding as a function of stimulus frequency is similar whether or not nonlinear coding is taken into account (Haag and Borst 1997). Nonlinear coding also increases with stimulus intensity in wind-sensitive sensory neurons of cricket cerci (Roddey et al. 2000). In this case, however, nonlinearity is

most prominent for stimulus frequencies that are poorly coded at low intensities. As a result, selective coding of particular frequencies is lost as intensity increases.

Enhanced coding of behaviourally relevant features of natural stimuli, as we have shown above for ON1, has been described previously. For example, in auditory receptors of bullfrogs and grasshoppers the rate of information transmission is highest for signals with temporal structures similar to those of conspecific communication signals (Rieke et al. 1995; Machens et al. 2001). Similarly, coding of amplitude modulation by electroreceptors of weakly electric fish improves as the bandwidth of the stimulus envelope is restricted to match the range of AM frequencies found in natural signals (Wessel et al. 1996). Recently, it has been shown that neurons in the brains of electric fish also exhibit different coding properties specific to signal geometries characteristic of signals from prey and conspecifics (Chacron et al. 2003). Like ON1, these neurons have different coding properties for different behaviourally relevant signals.

Possible mechanisms

Receptor neurons implement a first stage of temporal filtering, with broad selectivity to low AM rates (Fig. 2.6). Selectivity of ON1 for ultrasound stimuli is only slightly sharper than that of high-frequency receptors. For 4.5 kHz sound frequencies, this second stage of filtering is much sharper. The difference in the range of AM frequencies coded by ON1 for the two carrier frequencies cannot be explained by sharper filtering by low frequency receptors compared to ultrasound receptors.

Weise and Eilts (1985) proposed that temporal selectivity of ON1 might result from inhibitory interactions with its contralateral partner. In this case, the characteristics of contralateral inhibition would be expected to differ for low- and high carrier frequencies. Indeed, the timing of contralateral inhibition does differ for these two frequencies (Faulkes and Pollack 2000). However, we found nearly no difference in ON1's temporal

coding properties, either in information transfer functions or in the MTFs, when its contralateral partner was deafferented. In our experiments, stimuli were presented from an azimuth of 90° on the neuron's most sensitive side, a location that would only weakly stimulate the contralateral ON1 (Pollack 1986). We cannot rule out the possibility that, for stimuli arising closer to the midline, the resulting stronger contralateral inhibition might influence temporal coding. Nevertheless, the fundamental coding properties that we describe do not require contralateral inhibition.

Mechanisms contributing to temporal filtering in other systems include synaptic plasticity (Fortune and Rose 2000), passive filtering, active conductances (Fortune and Rose, 1997), and network structure (Grothe 1994; see Pollack 2001 for review). If passive filtering were to explain ON1's properties, receptor neurons tuned to low and to high sound frequencies would be expected to terminate at different regions within ON1s dendritic tree. One subset of low-frequency receptors (MT) and ultrasound receptors terminate in nearly the same region of auditory neuropil, overlapping with ON1's dense dendritic branches (Imaizumi 2000; Imaizumi and Pollack 2001). It seems unlikely that passive filtering would differ greatly for inputs from these two groups of receptor neurons. The other subset of low-frequency receptors (BC) terminate lateral and posterior of ON1's dense dendritic arbor, and probably make few if any direct connections with ON1 (Pollack and Imaizumi 1999; Imaizumi and Pollack 2001).

Nevertheless, the nature of input from low-frequency and ultrasound receptors to ON1 differs markedly. Ultrasound receptors elicit large, monosynaptic, unitary EPSPs (Faulkes and Pollack 2001), whereas discrete, unitary EPSPs are not seen for low-frequency stimuli; rather, a smooth, graded depolarization occurs (Pollack 1994). This might result from summation of small, monosynaptic EPSPs from many low-frequency receptors. Consistent with this, low-frequency receptors outnumber high-frequency receptors by a factor of 3-4 (Imaizumi and Pollack 1999, 2001).

Moreover, the information content of responses of single low-frequency receptors is less than that of ON1 (Fig. 2.6), suggesting that pooling of inputs from many receptors may be required to account for ON1's coding properties. By contrast, information content of single high-frequency receptors exceeds that of ON1, suggesting that pooling might not be required in this case.

Another possible explanation for the difference in EPSPs elicited by low and high frequencies is that low-frequency input to ON1 may be mainly polysynaptic (Faulkes and Pollack 2001). If the putative intervening neuron(s) were non-spiking, then a smooth, graded EPSP might be expected in ON1. In any case, low-frequency-elicited EPSPs in ON1 rise and decay more slowly than those evoked by ultrasound, and it is possible that this difference in EPSP shape contributes to ON1's temporal properties. Of course, if ON1's low-frequency input is primarily polysynaptic, then its filtering properties for low-frequency stimuli may be imposed by the intervening circuitry.

Behavioural significance

ON1 enhances binaural contrast through contralateral inhibition, thus facilitating sound localization (Atkins et al. 1984; Schildberger and Hörner 1988; Horseman and Huber 1994). Among ON1's contralateral targets are the ascending neurons AN1 and AN2, which carry information about cricket songs and bat calls, respectively, to the brain. The timing and strength of ON1's response to a temporally patterned stimulus will thus influence its inhibition of its targets (Faulkes and Pollack 2000).

We hypothesize that ON1's frequency-specific coding of temporal pattern affects the efficiency of contralateral inhibition so as to maximize bilateral differences among its targets specifically for stimuli with both the carrier frequencies and temporal structures of behaviourally relevant signals. This would enhance localization cues precisely for those stimuli that must be localized, while less relevant sounds would be perceived as

spatially more diffuse. Thus, the coding properties we describe might implement a type of spatially selective attention.

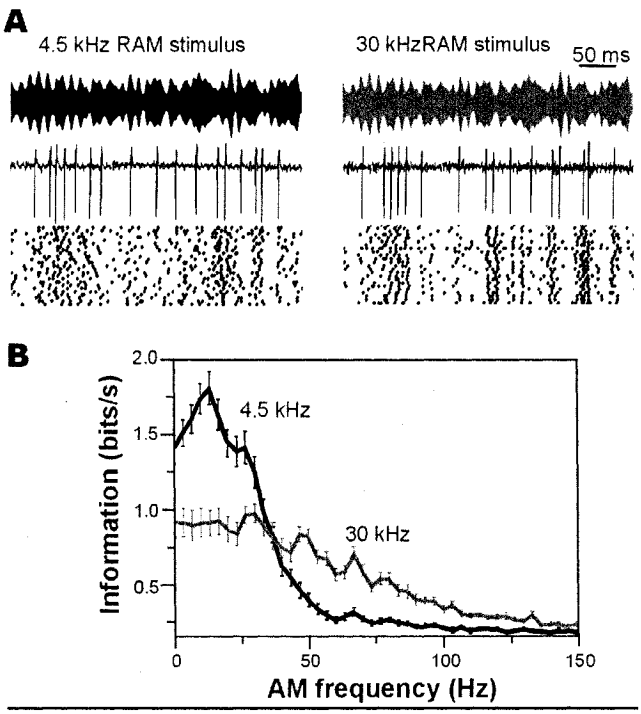

Figure 2.1: Coding of RAM stimuli by ON1. **A.** Responses of ON1 to repeated presentations of RAM stimuli with either cricket-like (4.5 kHz; left) or bat-like (30 kHz; right) carrier frequencies. Top: stimuli; middle: example spike trains; bottom: raster plots showing spike trains for 25 presentations of the stimulus. **B.** Mean (±s.e.) information transfer function of 15 ON1s for 4.5 kHz and 30 kHz carriers played at the same intensity (+20 dB) relative to threshold.

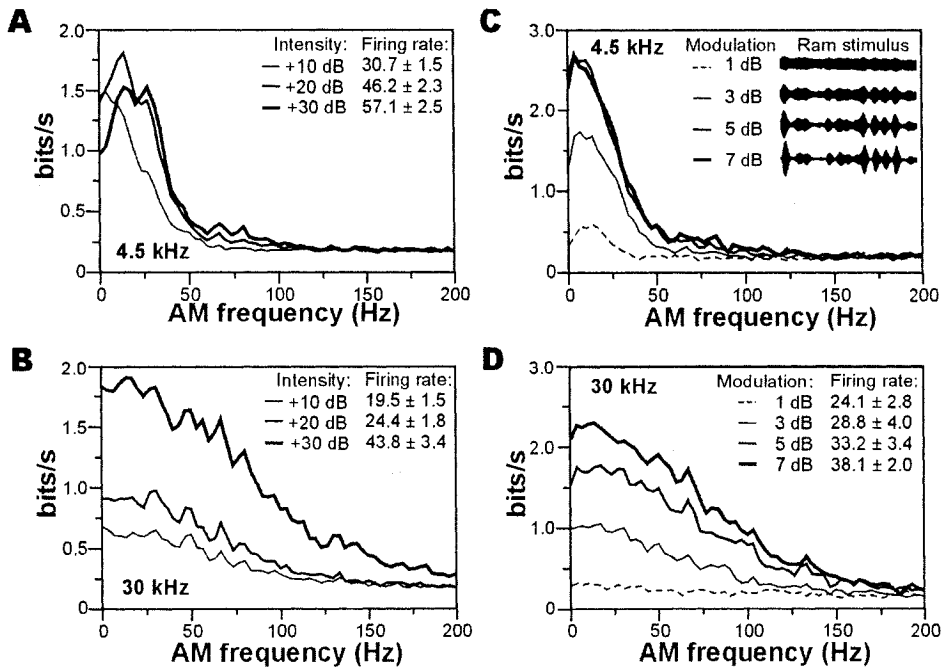

Figure 2.2: Effect of intensity and modulation depth on information transmission. **A,B.** Mean information transfer rate of ON1 (n=15) in responses to stimuli presented at various intensities (rms) above threshold (envelope standard deviation: 3 dB) with a carrier frequency of 4.5 kHz (A) or 30 kHz (B). **C,D.** Mean information transfer rate of ON1 (n=10) in responses to stimuli with the same intensity relative to threshold (+20 dB) but different modulation depths, with a carrier frequency of 4.5 kHz (C) or 30 kHz (D). Modulation depth is quantified as the standard deviation of the modulation envelope (see C, inset). The firing rates shown are mean ± s.e. Firing rate did not change in panel C (range: 41.3 ± 3.2 to 42.5 ± 2.8 spikes/s).

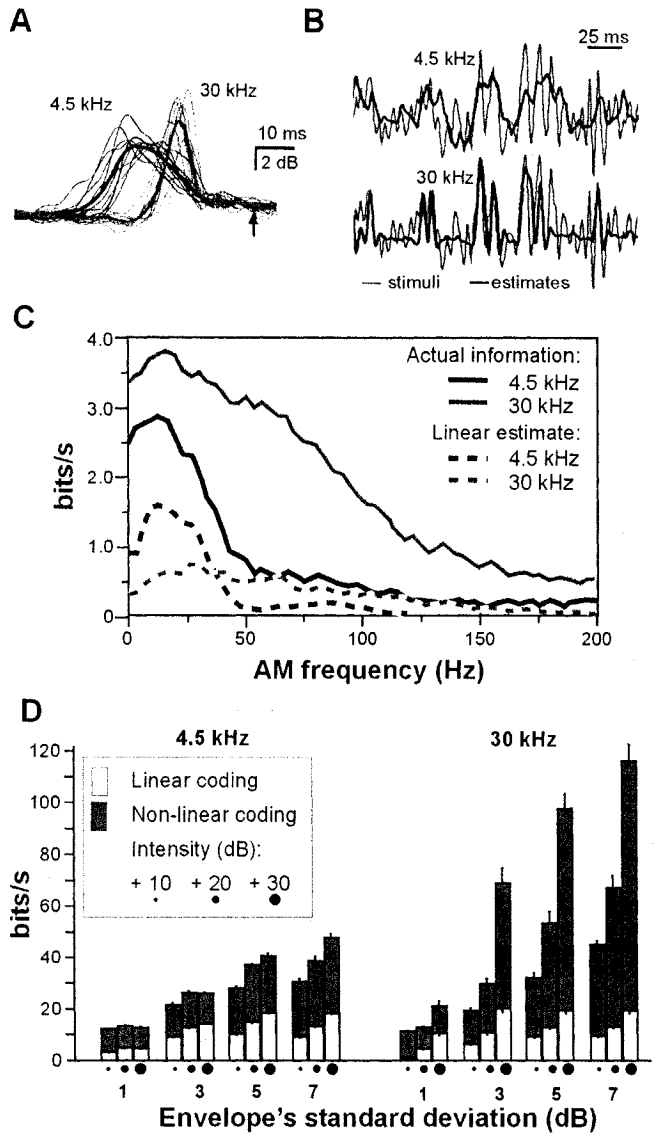

Figure 2.3: Nonlinearity of ON1's coding. **A.** Impulse responses of ON1's linear reverse filters for RAM stimuli with 4.5 kHz or 30 kHz carrier frequency (intensity +20 dB, envelope standard deviation: 3 dB). Thin lines represent individual neurons (n=10); thick lines are their means. The vertical arrow indicates the timing of ON1's spike. **B.** Estimates, for a representative ON1, of stimulus modulation envelopes determined by linear reverse reconstruction. **C.** Comparison of information-transfer curves representing actual information and information coded linearly. Curves are means of five neurons. Stimulus intensity (rms): 30 dB above

threshold; standard deviation of the modulation envelope: 7 dB. **D.** Total information rate (summed over all AM frequencies) for stimuli with different mean intensities, modulation depths (i.e. envelope standard deviations) and carrier frequencies. Information transmission that cannot be accounted for by linear coding (white) is attributed to nonlinear coding (grey). Data are means (± s.e.) of five neurons.

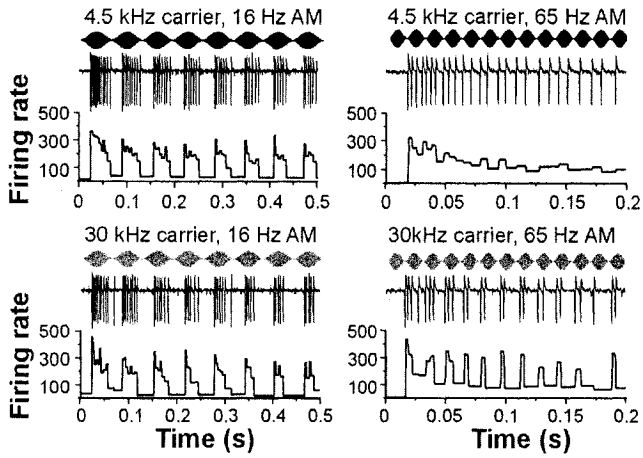

Figure 2.4: Responses to SAM stimuli vary with carrier frequency. Panels show SAM stimuli (top), ON1 spike trains (middle) and instantaneous firing rate, i.e., inverse of inter-spike interval (bottom) for low- and high SAM frequencies (left and right panels, respectively), for stimuli with 4.5 kHz and 30 kHz carriers (top and bottom panels), at rms intensity 20 dB above threshold.

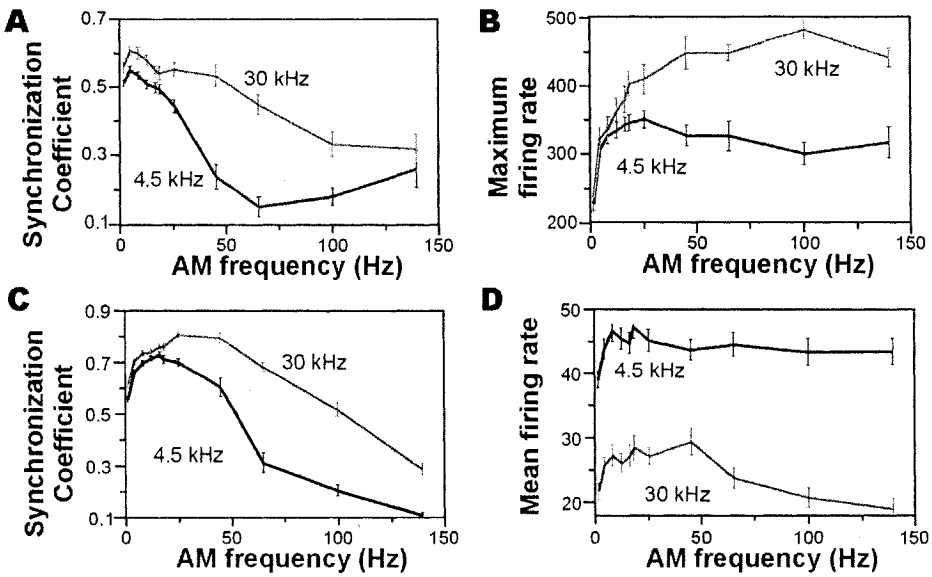

Figure 2.5: Modulation transfer functions. **A.** Mean (± s.e.) synchronization coefficient (SC) of responses of 17 ON1s as a function of SAM frequency, calculated for the first four cycles of stimulation. **B.** Maximum firing rate during the response to the first cycle. **C.** Synchronization coefficient during the adapted portion of the response, i.e. starting 5 s after sound onset. **D.** Mean firing rate of the adapted response.

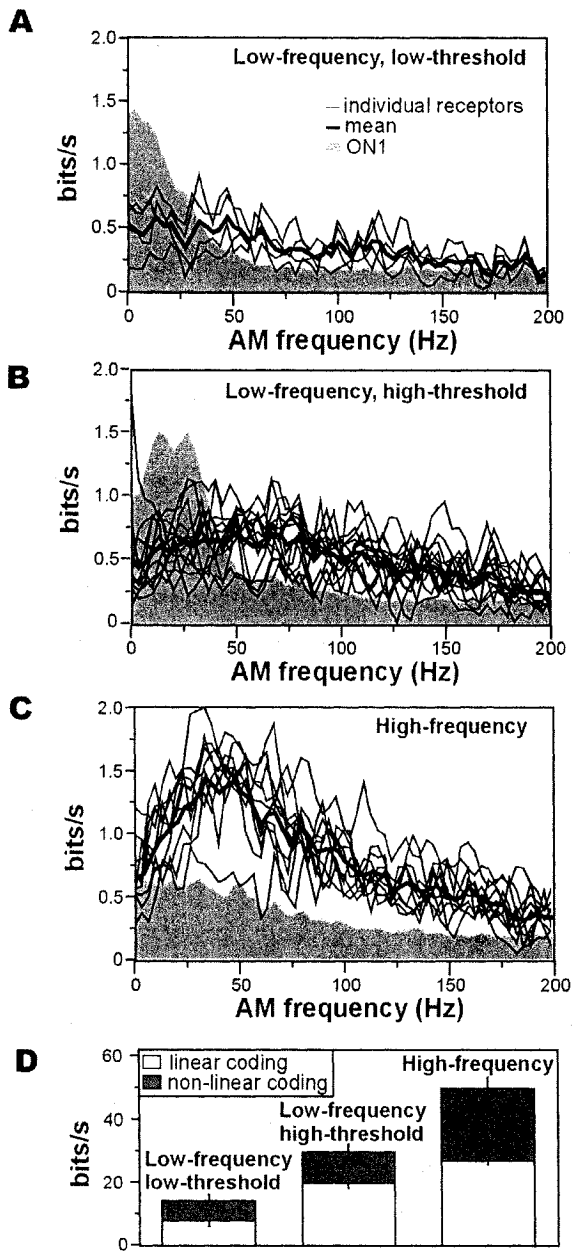

Figure 2.6. Information-transfer functions of receptor neurons. Stimuli were presented at 10-15 dB above threshold, with either 4.5 kHz (A, B) or 30 kHz (C) carrier frequency. **A.** Coding by low-frequency, low-threshold, receptor neurons. Only four of the 10 receptors that we recorded significantly coded the stimulus temporal pattern, as assayed by jackknife resampling (Efron 1993). Information-transfer functions for the non-coding

receptors are not shown. Mean stimulus intensity for the receptor neurons was 62.5 dB SPL. Coding of 4.5 kHz stimuli by ON1, at mean intensity of 63.6 dB SPL (10 dB above threshold) is also shown for comparison. Key applies to B and C as well. Frequency at which information transfer is maximum: ON1, 4.6 ± 0.8 Hz (mean ± s.e.); receptors that coded significantly, 42.5 ± 22.9 Hz; t-test, $p<0.004$. Half-widths: ON1, 24.5 ± 1.6 Hz; receptors that coded significantly, 86.9 ± 16.0 Hz; $p<10^{-5}$. Maximum information rate: ON1, 1.5 ± 0.1 bits/s; receptors that coded significantly, 0.7 ± 0.1 bits/s; $p<0.001$. **B.** As in A, except comparing low-frequency, high-threshold receptors (mean stimulus intensity: 79.6 dB SPL) and ON1, 4.5 kHz responses (mean intensity 83.6 dB SPL; 30 dB above threshold). All of the low-frequency, high-threshold receptors coded significantly. Frequency at which information transfer is maximum: ON1, 20.4 ± 1.9 Hz; receptors, 46.7 ± 5.6 Hz; $p=0.0003$. Half-widths: ON1, 34.7 ± 1.5Hz; receptors, 119.8 ± 9.2 Hz; $p<10^{-5}$. Maximum information rate: ON1, 1.6 ± 0.1 bits/s; receptors: 0.9 ± 0.1 bits/s; $p<0.009$. **C.** Coding by high-frequency receptors (mean stimulus intensity: 76.5 dB SPL) and ON1, 30 kHz responses, mean stimulus intensity 75.8 dB SPL (10 dB above threshold). All of the high-frequency receptors coded significantly. Frequency at which information transfer is maximum: ON1, 19.1 ± 3.5 Hz; receptors, 47.6 ± 5.0 Hz; $p=0.0002$; half-widths: ON1, 69.7 ± 6.1Hz; receptors, 91.1 ± 4.5 Hz, $p=0.001$. Maximum information rate: ON1, 0.8 ± 0.1 bits/s; receptors: 1.6 ± 0.1 bits/s; $p<0.0009$. **D.** Mean (± s.e.) total information rate of receptors. All low-threshold, low-frequency receptor neurons were included, rather than only those with significant coding, so as not to over-represent the total information carried by this receptor class. Information transmission that cannot be accounted for by linear coding (white) is attributed to nonlinear coding (grey).

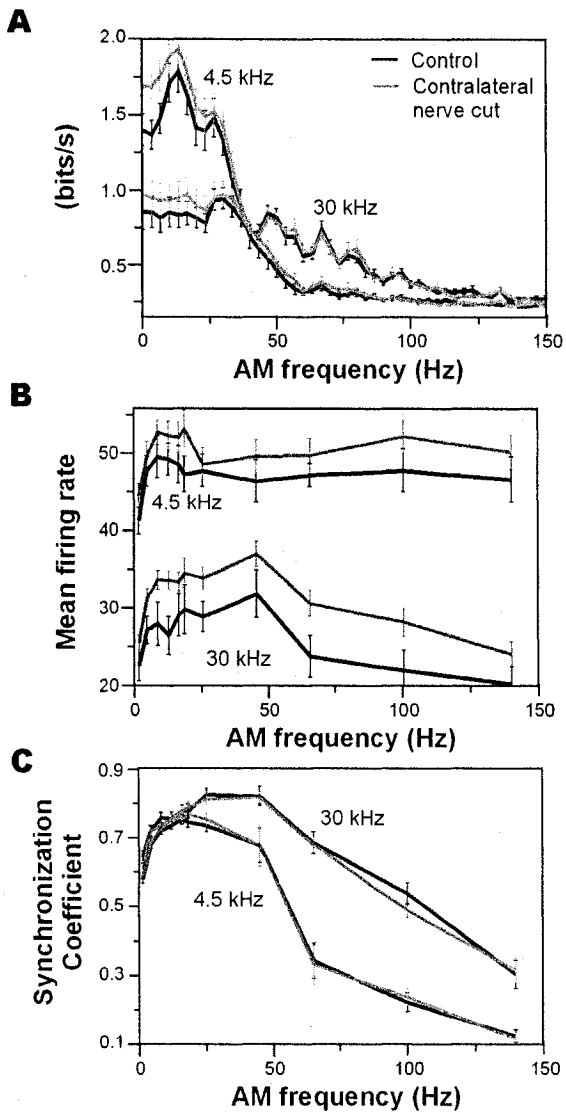

Figure 2.7. Effects of removal of contralateral input on temporal coding. Curves are means ± s.e. (n=10). **A.** Information transfer functions. **B.** Mean adapted firing rate as a function of AM frequency. **C.** Mean synchronization coefficient (during the adapted portion of the response) as a function of AM frequency.

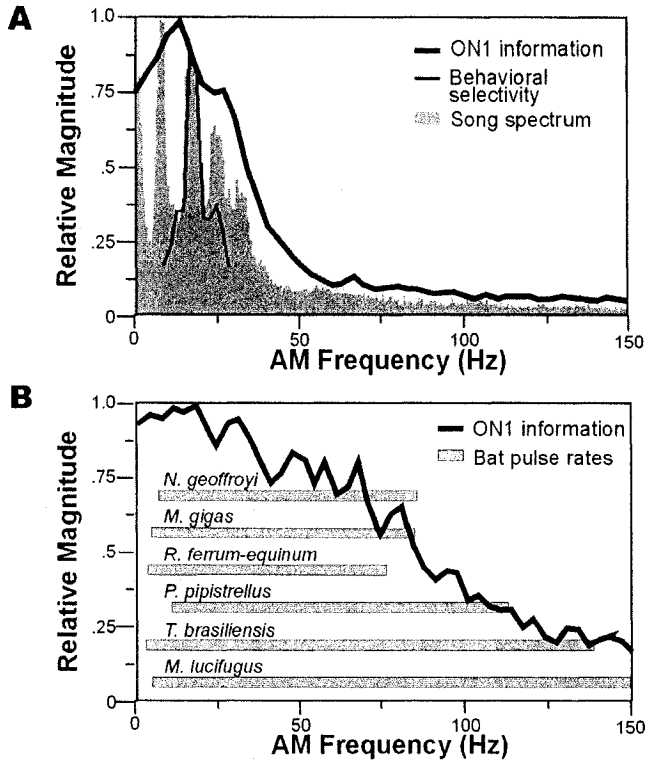

Figure 2.8: Comparison of ON1's temporal coding with the temporal structures of behaviourally relevant sounds. **A.** Mean normalized information-transfer function of ON1 for RAM stimuli with 4.5 kHz carrier (mean stimulus intensity 73. 6 dB SPL, 20 dB above threshold), together with the spectrum of the amplitude envelope of the calling song of *T. oceanicus* (derived by FFT analysis of 10s-long song segments from each of 6 crickets). Also shown is the temporal selectivity of behavioural responses to song models (70 dB SPL; data from Pollack and El-Feghaly, 1993). **B.** Information transfer function for 30 kHz stimuli, (mean stimulus intensity 95.8 dB SPL, 30 dB above threshold) together with the ranges of pulse repetition rates produced by six species of insectivorous bat (Wimsalt 1970; Kulzer et al. 1984; Schnitzler and Kalko 2001; South-eastern Australian bat call library, http://batcall.csu.edu.au/batcall/batcall1.html), indicated by horizontal bars. The top two bars represent species that occur in the same region of Australia as *T. Oceanicus*. The remaining species are representative of genera that also occur in this region.

Bridge from chapter 2 to chapter 3

In chapter 2 we characterized the temporal coding properties of the ON1 neuron. We showed that the response properties vary with stimulus carrier frequency. ON1 provides contralateral inhibition to the ascending neurons 1 and 2. These neurons carry the auditory information to the brain. By increasing the bilateral contrast in the response of the ascending neurons, ON1 enhances the cues used by the brain to localize the sound. We suspect that ON1's frequency-specific response properties affect its impact on target cells.

In chapter 3 we first describe the coding properties of the ascending neurons in order to investigate the impact of ON1's inhibition on these neurons. More specifically, we examine the role of ON1's carrier-frequency-specific response pattern on the information about the stimulus being carried to the brain by the ascending neurons.

Chapter 3

Effect of the temporal pattern of contralateral inhibition on sound localization cues.

Marsat G, Pollack GS.

Journal of Neuroscience (2005); 25: 6137-6144;

Abstract

We studied the temporal coding properties of identified interneurons in the auditory system of crickets, using information theory as an analytical tool. The neuron AN1, which is tuned to the dominant carrier frequency (CF) of cricket songs, selectively codes the limited range of amplitude-modulation (AM) frequencies that occur in these signals. AN2, which is most sensitive to the ultrasonic frequencies that occur in echolocation calls of insectivorous bats, codes a broader range of AM frequencies, as occur in bat calls. A third neuron, ON1, which is dually tuned to both ranges of carrier frequency, was shown previously to have CF-specific coding properties, allowing it to represent accurately the differing temporal structures of both cricket songs and bat calls. ON1 is a source of contralateral inhibition to AN1 and AN2, enhancing binaural contrast and facilitating sound localization. We used dichotic stimulation to examine the importance of the temporal structure of contralateral inhibition for enhancing binaural contrast. Contralateral inhibition degrades the coding of temporal pattern by AN1 and AN2, but only if the temporal pattern of inhibitory input matches that of excitation. Firing rate is also decreased most strongly by temporally matched contralateral inhibition. This is apparent for AN1 in its mean firing rate; for AN2, high-frequency firing is selectively suppressed. Our results show that the CF-specific coding properties of ON1 allow this single neuron to enhance effectively localization cues for both cricket-like and bat-like acoustic signals.

Introduction

Sensory information processing often relies on precisely timed neural activity (Fricker and Miles, 2001; Lestienne, 2001; Cariani, 2004). This is particularly evident in the neural interactions leading to sound localization. For example, in the avian nucleus laminaris and the mammalian superior olivary complex, bilateral inputs converge and the timing of the inputs from

each side is an important factor in determining neuronal responses (Oertel, 1999). The timing of these inputs is determined by the timing and intensity of the sound as it reaches each ear, but also by the temporal response properties of the neurons that carry this information: precise temporal coding of the stimulus allows precise bilateral interaction (Carr, 1993; Brand et al., 2002). Natural stimuli, such as communication sounds, contain characteristic patterns of amplitude modulation (AM), and neurons are often specialized to represent precisely the temporal features of these stimuli (Rieke et al., 1995; Theunissen et al., 2000; Machens et al., 2001b; Nagarajan et al., 2002).

Crickets communicate with sounds that are amplitude-modulated at species-specific rates (Pollack, 1998). They also respond to echolocation sounds emitted by insectivorous bats, which differ from communication signals both in carrier frequency (CF: 4.5 kHz for *Teleogryllus oceanicus*, the species studied here; >20 kHz for bat sounds) and in rates of AM (<32 Hz for *T. oceanicus*, <200 Hz for bat sounds). An identified neuron early in the cricket's auditory pathway, the Omega Neuron 1 (ON1), is dually tuned, with enhanced sensitivity to both ranges of carrier frequency. We showed recently that ON1 is also dually tuned with respect to its coding of the stimulus amplitude envelope (Marsat and Pollack, 2004). When stimulated with cricket-like carrier frequency, ON1's spike train selectively codes the narrow range of AM rates that occur in cricket songs. When the stimulus carrier frequency is bat-like, ON1 codes a broader range of AM rates, corresponding to the temporal structures of echolocation sounds.

ON1 participates in sound localization by increasing bilateral contrast through contralateral inhibition of the paired Ascending Neurons (ANs) AN1 and AN2 (as well as of the contralateral ON1), which respectively carry information about cricket-like and bat-like sound frequencies to the brain (Pollack, 1998). These neurons have been shown to be crucial for phonotactic responses towards cricket songs and away from ultrasound, respectively (Nolen and Hoy, 1984; Schildberger and

Hörner, 1988). Positive phonotaxis depends strongly on the stimulus temporal pattern (Pollack, 1998). Analysis of temporal pattern appears to occur in the brain by circuits that receive afferent input from AN1 (Schildberger, 1984). Crickets can discriminate between patterns presented simultaneously from the two sides (Pollack, 1986), suggesting that the bilateral difference in representation of temporal patterns by the left and right AN1s influences orientation (Stable et al., 1989). The probability of responding to ultrasound stimuli does not depend on stimulus temporal pattern, although temporal pattern may affect sustained responses (Pollack and El Feghaly, 1993). Stimulus direction is determined from bilateral comparison of activity in AN2 (Nolen and Hoy, 1984; Samson and Pollack, 2002).

In this paper we describe the temporal coding properties of AN1 and AN2. We show that the timing of contralateral inhibition affects both the firing rate and the accuracy with which the sound pattern is represented in these ascending neurons (ANs).

Materials and Methods

Electrophysiology

Teleogryllus oceanicus were reared in the laboratory. Virgin females were used for experiments at age 10-20 days after final molt. They were anesthetized by chilling on ice and mounted on a support ventral-side uppermost. The prothoracic ganglion was exposed by ventral dissection, supported on a metal platform and bathed in physiological saline (Strausfeld et al., 1983).

AN1 and AN2 were recorded extracellularly from the cervical connective, which was cut anteriorly. The connective was desheathed and separated into medial and lateral bundles. The medial bundle was wrapped several times around a stainless steel hook electrode and covered with a mixture of petroleum jelly and mineral oil for electrical isolation. Spikes of AN1 and AN2 are easily identified by their relative

amplitudes (AN1<<AN2) and by frequency sensitivity (AN1 best frequency, 4-5 kHz; AN2, 15-30 kHz; see Faulkes and Pollack (2000), Moiseff and Hoy (1983) for further details). To reduce background activity we cut the pro-mesothoracic connectives. ON1 was recorded extracellularly from its soma-contralateral processes in the prothoracic ganglion, using blunt glass microelectrodes filled with 1M NaCl (resistance: 5-10 Mohm). ON1 can be identified in this recording configuration by its preference for electrode-contralateral stimuli, as well as its greater sensitivity, but longer latency, to 4.5 kHz stimuli as compared to ultrasound stimuli (Faulkes and Pollack, 2000). In this paper, "ipsilateral" refers to the side from which sound most effectively excites the neuron. For ON1, this is ipsilateral to the soma; for the ANs, this is ipsilateral to their ascending axons (Wohlers and Huber, 1982). Recordings were amplified by a Grass P15 amplifier (Astro-Med Inc., West Warwick, RI, for hook recordings) or a Getting 5A microelectrode amplifier (Getting Instruments, San Diego, CA) and digitized (16 bits, sampling rate 10 kHz; Digidata 1320A, Axon Instruments, Union City, CA).

Sound stimulation

Threshold was defined as the sound intensity that reliably elicits at least one spike per sound pulse (30 ms sound pulses, including 5 ms onset and offset ramps, presented at 2 Hz). Carrier frequency (CF) was either 4.5 kHz or 30 kHz.

Stimuli with Random Amplitude Modulation envelopes (RAM) were produced by multiplying a sinusoidal signal, of desired carrier frequency, with a low-pass-filtered Gaussian signal (<200 Hz) with a standard deviation of 5 dB. RAM stimuli were 15 s long with 0.1 s linear onset and offset ramps, and were separated by at least 45 s of silence. Stimuli were generated by a National Instruments (Austin, TX) AD/DA board with 12 bits of resolution, at a sampling rate of 100 kHz.

For free-field stimulation, the cricket's front legs (which bear the ears) were held flexed against the pronotum in a position similar to that assumed during flight. Sound was broadcast from loudspeakers situated to the cricket's left and right, perpendicular to the longitudinal axis. For closed-field stimulation, the legs were held horizontally and were inserted in cylindrical chambers containing earphones (Radio Shack, Optimus Nova 401). The "acoustic" trachea linking the two ears was severed to ensure stimulus isolation (Michelsen and Löhe, 1995). The chambers were 14 mm in diameter and 3 mm in length, and had calculated resonance frequencies >50 kHz (Filippi, 1999). The chambers were sealed with wax. Thresholds of AN1 and AN2 were at least 50 dB higher for contralateral than for ipsilateral stimuli. In closed-field experiments, stimuli at the ear ipsilateral to the ANs were either 65 dB SPL, 4.5 kHz, or 80 dB SPL, 30 kHz. Stimuli at the ear ipsilateral to ON1 were 8 dB higher than those to the AN-ipsilateral ear, simulating a sound source on the ON1-ipsilateral side of the cricket. These stimulus intensities were chosen because they evoked robust responses in all three neurons, and they fall within the intensities ranges that cricket are likely to encounter in the field (Nocke, 1972; Miller and Surlykke, 2001).

For both stimulation methods, sound level was calibrated using Brüel and Kjaer (Naerum, Denmark) instruments (4135 microphone, 2610 sound-level meter).

Data analysis

We quantified the information available in the neuron's spike train about modulations in stimulus amplitude by calculating information transfer functions. The exact information content can be evaluated based on the variability between responses to repeated presentations (n=4) of the identical RAM stimulus. Highly similar patterns of spiking across responses indicate accurate temporal coding whereas responses bearing

little similarity in firing pattern will carry little information about the stimulus pattern (see Rieke et al., 1997 for general reference).

Spike timing was compared between pairs of responses by calculating response-to-response coherence (Roddey et al., 2000). Spike trains, ($r(t)$), expressed as binary events, were separated into overlapping, Hanning-windowed, 300 ms segments and then converted to the frequency domain, ($R(f)$), using the fast Fourier transform. The resulting arrays for a pair of responses ($R_i(f)$ and $R_j(f)$) were used to calculate coherence:

$$Coh=\sqrt{\langle R_i(f)*R_j(f)\rangle\langle R_j(f)*R_i(f)\rangle / \langle R_i(f)*R_i(f)\rangle\langle R_j(f)*R_j(f)\rangle},$$

where '*' indicates the complex conjugate of the variable it follows, and $\langle\rangle$ indicates average across the 300 ms response segments. This calculation was performed for all pair-wise combinations of responses to the same stimulus and averaged across response pairs, yielding $\overline{Coh}$. Information was calculated as $I(f) = -\log_2(1- \overline{Coh})$. Assuming that the neuron's performance is deteriorated only by Gaussian additive noise that is independent of the signal, this measure represents the total information content of the responses (Borst and Theunissen, 1999). We showed earlier (Marsat and Pollack, 2004) that the distributions of response and noise were Gaussian for ON1.

Both linear and non-linear coding can contribute to information coding. If coding is truly linear, a linear model will capture all the information transmitted by the neuron, otherwise, the linear model yields a lower-bound of information transmission. We assessed the degree of nonlinear coding by comparing the information transfer function calculated as above with a lower-bound estimate (Borst and Theunissen, 1999).

Lower-bound information transfer functions were calculated using reverse reconstruction. We used the same standard technique described in detail elsewhere (Marsat and Pollack, 2004; see also Theunissen et al., 1996; Clague et al., 1997). Arrays representing firing rate, $r(t)$ and the

stimulus envelope, $s(t)$, were expressed as variations around their respective means, yielding $r'(t)$ and $s'(t)$.These arrays were segmented and converted to the frequency domain as described above, yielding $R'(f)$ and $S'(f)$. The frequency-domain representation of the linear reverse filter for response i was calculated as: $H_i(f)=\langle R_i'(f)*S_i'(f)\rangle / \langle R_i'(f)*R_i'(f)\rangle$. $H_i(f)$ was converted to the time domain, $h_i(t)$, using the inverse Fourier transform. $h_i(t)$ was convolved with $r_i(t)$ to reconstruct the neuron's estimate of the stimulus, $est_i(t)$. Noise, $n_i(t)$, was computed as $s_i(t)$ - $est_i(t)$. Signal-to-noise ratio, $SNR_i(f)$, was computed as the power spectrum of $est_i(t)$ divided by that of $n_i(t)$, $SNR_i(f)$ was averaged for all i and information transfer was calculated from $\overline{SNR}(f)$ according to the equation: $I(f)=\log_2(1+\overline{SNR}(f))$. We quantified the breadth of information transfer functions by their half-widths, defined as the range of AM frequencies where information rate is higher than half the maximum.

Our calculations assume that response statistics are stationary over time (Rieke et al., 1997) yet the neurons studied here adapt markedly shortly after sound onset. Therefore responses were analyzed starting 5 s after sound onset to restrict our analysis to the portion where firing rate is stable.

Data analysis was performed with Matlab 6.5 (Mathworks, Natick, MA). Statistical tests on proportions were performed on arcsine, square root-transformed data (Zar, 1999). We used Statistica 5.5 (Statsoft, Tulsa, OK) for all tests of significance.

Results

Temporal coding in the ascending neurons

The information content in a neuron's response about the temporal structure of a stimulus can be characterized by the information transfer function. We computed information transfer functions for AN1 and AN2 for responses to RAM stimuli with CF of 4.5 kHz and 30 kHz, respectively.

Peak information-transfer rate for AN1 occurs at AM frequencies ranging from 12 ± 3.1 Hz to 23.3 ± 12.1 Hz, shifting to higher frequencies with increasing intensity (ANOVA, p=0.01; Fig. 3.1A). This corresponds to the range of sound-pulse rates that are most effective at eliciting positive phonotaxis (Pollack and El-Feghaly, 1993; Hennig and Weber, 1997). The information-transfer rate drops sharply at approximately 30 Hz. As a result, AN1 codes only a rather limited range of AM frequencies (range of half widths: 34.6 ± 3.4 Hz to 37.1 ± 3.9 Hz), corresponding to the range of AM frequencies that occur in conspecific songs (ca. 8-32 Hz; Balakrishnan and Pollack, 1996). Peak rate decreases with increasing stimulus intensity, from 2.1 ± 0.1 bits/s at 15 dB above threshold to 1.2 ± 1.2 bits/s at 35 dB above threshold (ANOVA, p=0.003). Mean firing rate increases with intensity (ANOVA, p=0.0007), saturating at 25 dB above threshold (Tukey test, p=0.4).

For AN2, peak information-transfer rate occurs at AM frequencies between 7.9 ± 1.9 Hz and 11.9 ± 1.5 and decreases gradually with increasing AM frequency (Fig. 3.1B). With increasing intensity, both the height and breadth of the information-transfer function increases (peak: from 1.9 ± 0.2 to 2.9 ± 0.1 bits/s, ANOVA, p=0.004; half-width: from 46.3 ± 1.7 Hz to 64 ± 6.8 Hz, ANOVA, p=0.01). Thus, stimulus intensity affects coding accuracy of AN1 and AN2 differently. For AN1, total information decreases with increasing intensity, whereas it increases for AN2 (Fig. 3.1C; ANOVA, for AN1, p=0.04; for AN2, p=0.002).

These information-transfer rates were calculated making no assumptions about the nature of the neural code (see Methods). We also calculated information rates based on a linear model. The difference between total information and that accounted for by a linear model represents the amount of non-linear coding (Fig. 3.1C). AN1 and AN2 differ in the amount of non-linear coding. For AN2, linearly coded information accounts for less than a third of the total information content,

whereas more than half of AN1's information content can be accounted for by a linear code (ANOVA, neuron effect, $p<0.0001$).

Contralateral inhibition and coding in the ANs.

ON1 provides contralateral inhibition to AN1 and AN2, thereby enhancing bilateral contrast for both cricket-like and bat-like stimuli. Previous work showed that ON1 accounts for all measurable contralateral inhibition of the ANs (Faulkes and Pollack, 2000). To assess the influence of contralateral inhibition on temporal coding by the ANs, we recorded simultaneously from AN1 and AN2 and from the ON1 that inhibits them. Because the excitatory input to the ANs and to ON1 originates in opposite ears, we could control independently excitation and contralateral inhibition of the ANs using dichotic stimulation (Fig. 3.2A).

The effects of contralateral inhibition on the ANs are illustrated in Fig. 3.2. Binaural stimulation, and the resulting activation of ON1, results in decreased firing rate in the ANs relative to that during monaural stimulation. This is particularly obvious, in the excerpts shown, following the two conspicuous increases in stimulus amplitude (shaded areas).

As we reported previously (Marsat and Pollack, 2004), ON1 codes a narrow range of AM rates when stimulated with cricket-like CF, and a broader range for ultrasound stimuli. A similar difference in coding of stimuli with these two CFs, but represented by distinct neurons, is apparent in the responses of AN1 and AN2. Coding of 4.5 kHz stimuli by AN1 (whether stimuli were monaural or binaural) spans a similar range of AM frequencies as are coded by ON1 for the same CF (Fig. 3.3A). Similarly, coding of 30 kHz stimuli by AN2 and by ON1 extends to higher AM frequencies, although ON1's information-transfer curve is broader than that of AN2 (Fig. 3.3B). Thus, in a manner similar to the CF-specific coding of ON1, coding of bat-like CF, by AN2, is broader than coding of cricket-like CF, by AN1 (AN1 half-width: 38.1 ± 4.9 Hz vs. AN2: 68.5 ± 9.5 Hz; paired t-test, $p<0.0001$).

The effects of contralateral inhibition on information-transfer rates of the ANs reflect these CF-related differences in coding. Contralateral inhibition decreases coding accuracy of AN1 most severely for AM frequencies below 40 Hz (Fig. 3.3A, C). This is due, of course, to the poor coding of higher AM frequencies by AN1, leaving little room for further decrease in information-transfer rate. The decrease in coding accuracy of AN2 extends up to 70 Hz (Fig. 3.3B, C). Thus contralateral inhibition produces a larger decrease in information content at high AM frequencies for AN2 than for AN1 (ANOVA, $p=0.02$; Tukey $p<0.05$ for AM frequencies between 43Hz and 80 Hz). Contralateral inhibition also decreased mean firing rate in AN1 and AN2, by 18% and 22% respectively.

ON1's spiking pattern and inhibitory influence on the ANs.

Contralateral inhibition might depend only on ON1's mean firing rate. Alternatively, the precise timing of ON1 spikes relative to excitatory input to the ANs might affect its inhibitory impact. We examined these possibilities by controlling separately the temporal patterns of stimuli at the two ears.

Contralateral inhibition resulting from ON1-ipsilateral stimulation with a constant tone had no effect on coding accuracy of AN-ipsilateral RAM stimuli for either AN1 or AN2, although it did reduce the spike frequencies of the ANs (Fig. 3.4A). Although the ON1-ipsilateral stimulus had constant amplitude, ON1's spike train might, in principle, still reflect the temporal pattern of the stimulus presented to the AN-ipsilateral ear, due to temporally patterned inhibition from the AN-ipsilateral ON1 . In fact, however, there was no statistically significant coding of the AN-ipsilateral RAM stimulus by ON1 ($p>0.05$, jackknife resampling; Efron and Tibshirani, 1993), perhaps because the higher ON1-ipsilateral stimulus level (see Methods) masked any effects of temporally patterned inhibition. Firing rate of ON1 was similar for RAM and constant-amplitude stimuli (4.5 kHz RAM: 52.4 ± 5.3 spks/s vs. tones: 51.8 ± 5.1 spks/s paired t-test, $p=0.8$; 30 kHz

RAM: 43.9 ± 2.7 spks/s vs. tones: 40.1 ± 2.3 spks/s, p=0.04), suggesting that the lack of effect on coding by the ANs was due specifically to disturbance of the normal temporal relationship between excitatory and inhibitory inputs. We tested this hypothesis by presenting different RAM stimuli (but with identical bandwidth and standard deviation) to the two ears. Under these stimulus conditions, ON1 codes the ON1-ipsilateral AM envelope with accuracy similar to that shown in Fig. 3.3 (data not shown). As for contralateral stimulation with constant tones, contralateral stimulation with a different RAM stimulus caused a decrease in firing rate of the ANs, but had no effect on their temporal coding (Fig. 3.4B).

These findings suggest that ON1s differential temporal coding of low-frequency and ultrasound stimuli may fine-tune the temporal structure of contralateral inhibition so as to match the different temporal coding properties of AN1 and AN2. We explored this possibility by presenting RAM stimuli with identical amplitude envelopes, but different CFs, to the two ears. When the AN-ipsilateral ear is stimulated with ultrasound and the ON1-ipsilateral ear with cricket-like CF, information transfer in AN2 is decreased only for the narrow range of AM frequencies that are well coded by ON1 (Fig. 3.4C, bottom), rather than over a broad range, as occurs for ON1-ipsilateral ultrasound stimuli. Unlike the situation described earlier, where a floor effect explained the restricted range over which coding by AN1 was affected (Fig. 3.3A, C); here the limited range of effectiveness is due to the temporal pattern of contralateral inhibition.

By contrast, the CF of the contralateral stimulus has only a minor effect on the decrease in coding of a low-CF RAM by AN1 (Fig. 3.4C, top). This is not surprising given that, even for ultrasound stimuli, ON1's coding includes the range of low AM frequencies that are well coded by AN1 (Fig. 3.3).

We summarize the effects of contralateral inhibition on the responses of the ANs in Fig. 3.5. The decrease in AN1's information content was greatest when the stimuli to the two ears had the same

amplitude envelope. This decrease did not differ, however, for 4.5 kHz and 30 kHz contralateral stimuli (Fig. 3.5A). Similarly, the decrease in firing rate was greatest (around 18 %) for contralateral stimuli with the same pattern, independently of the CF of the contralateral stimulus (Fig. 3.5 B). For AN2, both the temporal pattern and the carrier frequency of the contralateral stimulus affect the decrease in information transfer rate. Interestingly, the decrease in AN2's firing rate (lower by about 22 %) was independent of both the pattern and the CF of the contralateral stimulus.

We also examined the importance of the timing of contralateral inhibition by comparing the moment-to-moment variations in firing rates of ON1 and the ANs. We recorded simultaneously from ON1 and the ANs for both monaural stimulation (of the ear driving the ANs) and for binaural stimulation. For a pair of binaural/monaural responses, the spike trains were transformed to instantaneous firing rates (inverse of inter-spike intervals). We computed the difference in instantaneous firing rate of the ANs between the two stimulus conditions (binaural-monaural). This new variable reflects the effect of contralateral inhibition (and noise). We generated a similar variable for ON1, reflecting its stimulus-driven spiking. An example of the relationship between these two variables is shown in Fig. 3.6A. We calculated the coherence between the two variables, a measure of their temporal correlation, as described in the Methods.

For low-carrier-frequency ON1-ipsilateral stimuli, changes in firing rate of ON1 and of the ANs are coherent only at low modulation frequencies (Fig. 3.6B). The coherence is maximal for modulation frequencies around 16 Hz. For ultrasonic ON1-ipsilateral stimuli, modulations in firing rate of ON1 and of the ANs are coherent over a wider range of modulation frequencies (Fig. 3.6B). This analysis confirms that contralateral inhibition affects the temporal structure of responses of the ANs only for modulation rates that are well coded by ON1.

Inhibition and high frequency firing in AN2.

Evasive behaviour is triggered by high firing rate (>190 Hz) in AN2 (Nolen and Hoy, 1984). We examined the inter-spike-interval (ISI) distribution of AN2's response to evaluate the impact of contralateral inhibition specifically on periods of high frequency firing. Ultrasound avoidance occurs with short latency (Nolen and Hoy, 1986), but also may persist for several seconds (e.g. Pollack and El-Feghaly, 1993). Accordingly, we examined separately the ISI distribution shortly after sound onset (0-1 s; Fig. 3.7A) and during the sustained portion of the response (1-14 s; Fig. 3.7B). For monaural stimulation with a 30 kHz RAM stimulus, short ISIs (<5ms) are frequent during both time periods. In the sustained portion of the response, after adaptation is established (Samson and Pollack, 2002), AN2 spikes occur in bursts of high frequency firing separated by more sparsely spaced spikes, as indicated by the bimodal distribution of ISIs typical of bursting neurons (Fig. 3.7B).

Although the CF of contralateral stimulation has no effect on the decrease in AN2's mean firing rate (Fig. 3.5), it has a profound effect on its ISI distribution. In the presence of 30 kHz-driven contralateral inhibition, AN2's initial ISI distribution has fewer ISIs between 1 and 5 ms but more between 12 and 14 ms (ANOVA and Tukey-test, $p<0.05$); thus, contralateral inhibition decreases the proportion of short ISIs (Fig. 3.7A, inset; $p<0.05$; ANOVA, followed by Tukey test). This change in the ISI distribution occurs only when the ON1-ipsilateral ear is stimulated with ultrasound. When the contralateral inhibition is driven by 4.5 kHz stimuli, the proportion of ISIs shorter than 5 ms is similar to that for monaural stimulation ($p>0.05$). A similar influence of ON1's CF-specific inhibition is seen during the adapted portion of the response. Only contralateral inhibition driven by 30 kHz stimuli decreases the proportion of short ISIs (Fig. 3.7B, inset; $p<0.05$).

Discussion

AN1 and AN2, which are tuned respectively to the CFs of cricket songs and bat sounds, have temporal coding properties that are matched to the structures of these signals. We showed previously (Marsat and Pollack, 2004) that ON1's temporal coding properties differ for cricket-like and bat-like CFs, and in the present paper we show that this has functional consequences. The correspondence between coding by ON1 and by the ascending neurons results in more effective suppression of information transmission. Faulkes and Pollack (2000) also studied the effects of the timing of contralateral inhibition on responses of AN1. Using single brief sound pulses, they found that contralateral inhibition did not affect first-spike latency of AN1. However, it is clear from their data (e.g. Fig. 3.4A of their paper) that the temporal organization of succeeding spikes was severely affected. The matched coding properties of ON1 and the ANs also result in greater decrease in firing rate of the ascending neurons. For AN1 this is apparent in its mean firing rate and for AN2 in the frequency of short inter-spike intervals.

Contralateral inhibition affects ascending information about cricket song.

Activity of AN1 (and to a lesser extent, of AN2) is important for both recognition and localization of cricket songs. The roles of these neurons in localization have been demonstrated by hyperpolarizing them while crickets performed phonotaxis towards song models. Hyperpolarizing AN1 on one side caused crickets to orient towards the other side independent of the location of the sound source, showing that the direction of orientation is influenced by bilateral comparison of activity in the AN1 pair. Hyperpolarization of AN2 led to similar, though less pronounced, deviations towards the other side (Schildberger and Hörner, 1988). Song recognition in crickets is based mainly on stimulus temporal pattern (Pollack, 1998), and AN1is the main source of afferent input to temporal-

pattern-filtering circuits in the brain (Schildberger, 1984). Its selective coding of temporal pattern implies that these brain circuits will receive accurate information about stimulus structure only for a limited range of AM rates, similar to those that occur in cricket song.

Contralateral inhibition degrades temporal coding by AN1, and thus will result in a bilateral difference in the quality of information about temporal pattern coded by the AN1 pair. Stabel et al. (1989) showed that crickets orient towards the side where the temporal pattern of the attractive stimulus is best represented by the spike trains of the ANs, rather than simply to the side where mean firing rate is highest. This suggests that the degradation of temporal coding that we describe will affect orientation.

The pathways by which ascending activity affects phonotaxis towards cricket song are not clear. Earlier studies suggested that phonotaxis direction might be determined by comparing the outputs of bilaterally paired recognition circuits in the brain (Pollack, 1986; Stabel et al., 1989). Von Helversen and von Helversen (1995) discuss the possible selective advantages of this interaction between recognition and localization. More recent work, however, shows that the motor drive for phonotaxis involves reflex-like circuitry that is not directly routed through recognizers in the brain (Hedwig and Poulet, 2004). Recognition circuits may nevertheless influence orientation through descending modulation of local circuitry, and this descending influence might be affected by bilateral differences in information content of the ANs.

Precise contralateral inhibition and localization of bat sounds

Both AN2 and ON1 (when stimulated with ultrasound) code relatively broad ranges of AM frequencies. Furthermore, they both encode ultrasound stimuli in a largely non-linear manner (see Marsat and Pollack, 2004 for ON1), unlike the responses to cricket-like CF of AN1 and ON1, where nonlinear coding is less pronounced. This similarity of their coding

properties allows ON1 to provide temporally matched contralateral inhibition to AN2. As for AN1 (see above), information transfer was suppressed maximally when the temporal pattern of contralateral inhibitory input to AN2 matched AN2s response pattern. The initiation of negative phonotaxis is not temporal-pattern-selective, but sustained responses to ultrasound do vary with stimulus temporal pattern (Pollack and El Feghaly, 1993); thus the temporal information in AN2's spike train might affect ultrasound elicited behaviour.

The key feature of AN2's response for triggering bat avoidance is high instantaneous firing rate (Nolen and Hoy, 1984). We show that contralateral inhibition selectively affects high-frequency firing in AN2, but only when ON1's response matches the temporal pattern of that of AN2. Contralateral inhibition is therefore expected to enhance the bilateral difference in AN2's responses specifically during periods of high instantaneous firing rate.

Precisely timed contralateral inhibition is important for directional processing in other systems. In locusts, the response of an identified interneuron switches from nearly complete suppression to nearly maximal excitation with a shift in binaural stimulus timing of as little as 2 ms (Rheinlaender and Mörchen, 1979). In the gerbil medial superior olive as well, sensitivity to interaural timing difference is shaped by temporally precise inhibition (Brand et al., 2002; Grothe, 2003 for review). Similarly, sensitivity to interaural intensity difference in the lateral superior olive and inferior colliculus of bats depends on the latency and duration of contralateral inhibition (Park et al., 1996; Park, 1998; Oswald et al., 1999; Irvine et al., 2001).

The distinct coding properties of ON1 for cricket-like and bat-like stimuli, which we described previously (Marsat and Pollack, 2004), are also seen at the level of the ANs with which ON1 interacts. We show that contralateral inhibition is most effective when the responses of ON1 and of its targets are temporally matched. Thus, ON1s response properties allow

this single neuron to effectively enhance binaural contrast for two distinct, behaviourally relevant, stimuli.

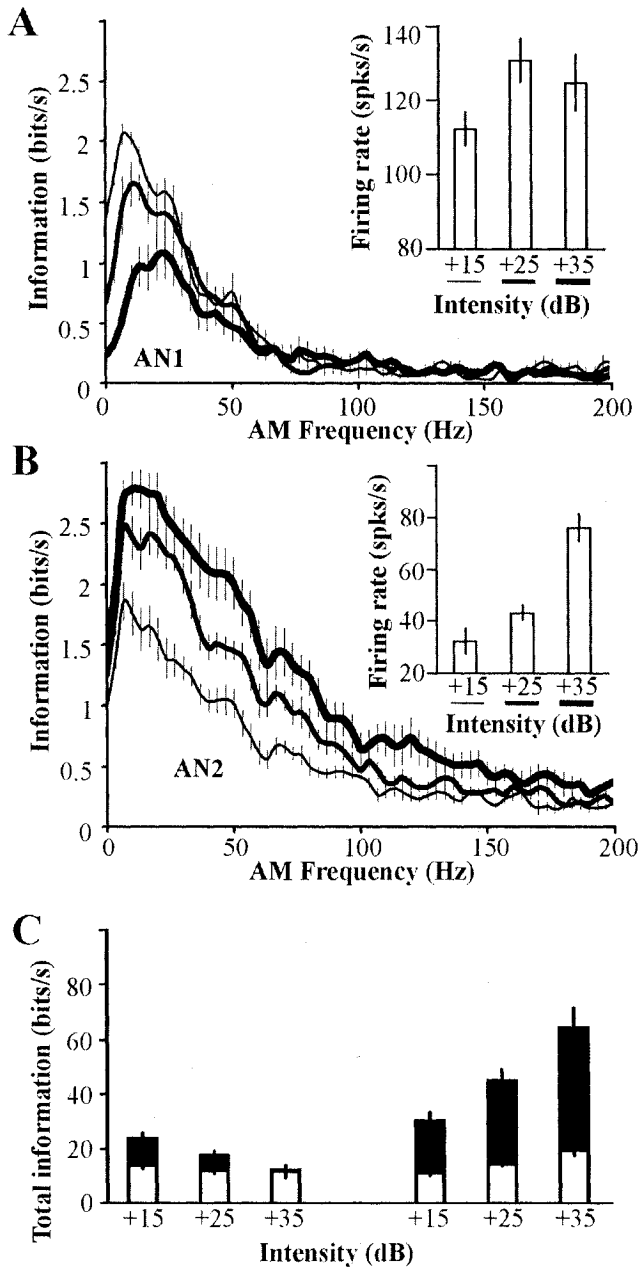

Figure 3.1. Temporal coding by AN1 and AN2. RAM stimuli were presented with mean intensities 15, 25 or 35 dB above threshold, with CF of 4.5 kHz for AN1 and 30 kHz for AN2. AN1's mean threshold (± sd): 46.1 ± 4.2 dB SPL; AN2's threshold: 53.2 ± 5.1 dB SPL. **A.** Mean (± se; n= 7) information transfer rate of AN1; inset shows mean firing rate as a function of stimulus intensity. **B.** Mean (± se; n= 8) information transfer rates of

AN2; inset as in A. **C.** Mean (± se) total information content of AN1 and AN2 spike trains (areas under the curves in A and B). Open portions of bars show information content accounted for by a linear model of coding; filled portions represent the degree of nonlinear coding (see Methods). Total information was calculated by summing information rates only for those AM frequencies at which information rate differed significantly from zero, as assessed by jackknife resampling (Efron and Tibshirani, 1993).

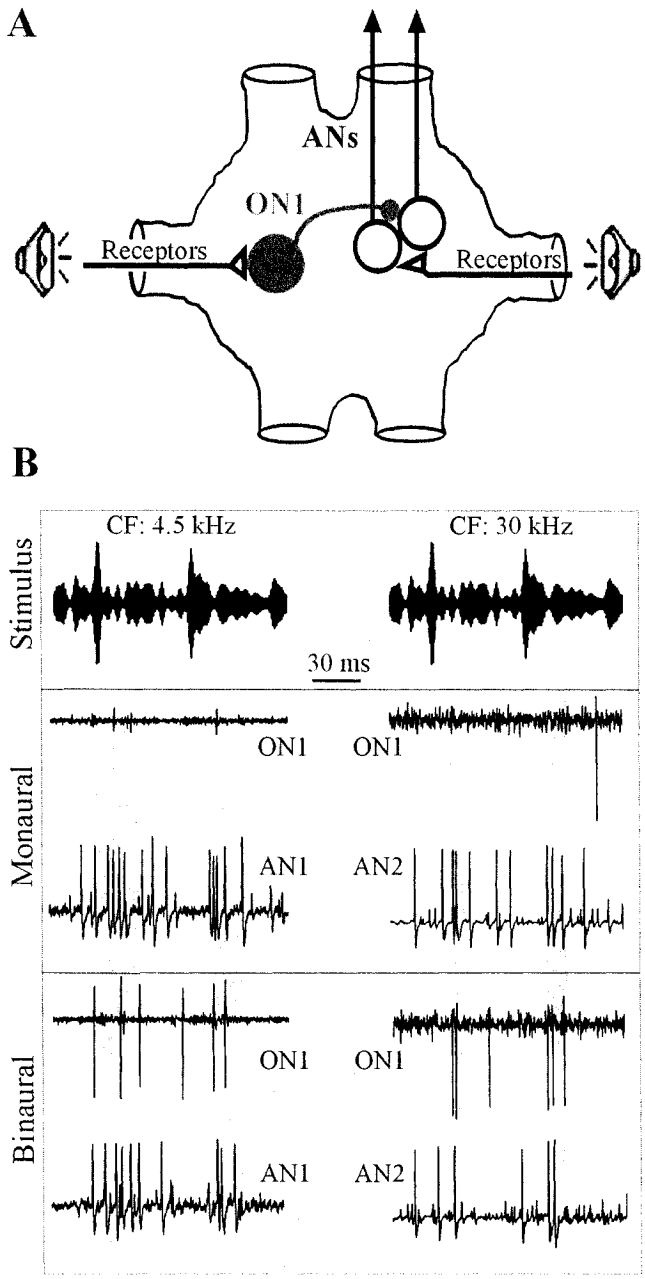

Figure 3.2. Dichotic stimulation and responses of AN1, AN2 and ON1. **A.** Schematic drawing of the connections between receptors, AN1, AN2 and ON1. All three interneurons exist as mirror-image pairs; only the recorded neurons are shown. **B.** Excerpts of the responses of AN1, AN2 and ON1 to RAM stimuli during monaural and binaural stimulation. Responses to 4.5 kHz and 30 kHz are from different experiments. The shaded areas highlight increased spiking of ON1, and decreased spiking of the ANs, for binaural stimulation.

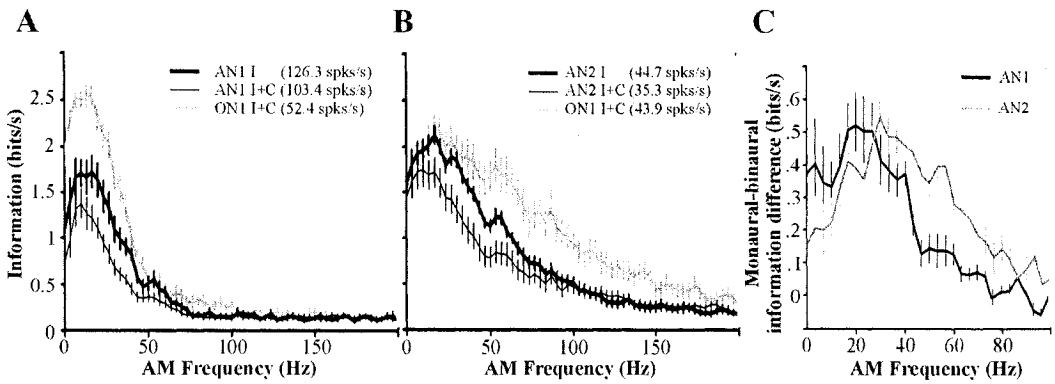

Figure 3.3. Temporal coding and the effect of contralateral inhibition. Stimuli were presented dichotically. AN-ipsilateral stimuli were either 4.5 kHz, 65 dB SPL (for experiments on AN1) or 30 kHz, 80 dB SPL (for AN2 recordings). ON1-ipsilateral stimuli, if present, had the same carrier frequency as the AN-ipsilateral stimulus, and sound level was 8 dB higher to mimic free-field stimulation from the ON1-ipsilateral side. **A, B**. Mean information transfer functions (± se; n= 13) of AN1 (A), AN2 (B) and ON1 are shown for monaural (labelled I; denoting stimulation from the AN-**I**psilateral ear only) and binaural stimuli (I+C; both the AN-**I**psilateral and the AN-**C**ontralateral ear are stimulated). During monaural stimulation, ON1 fired at similar rate as during silence (<8 spks/s) and did not code the stimulus (data not shown). Inset: mean firing rates. **C.** Differences between information-transfer curves for monaural and binaural stimulation.

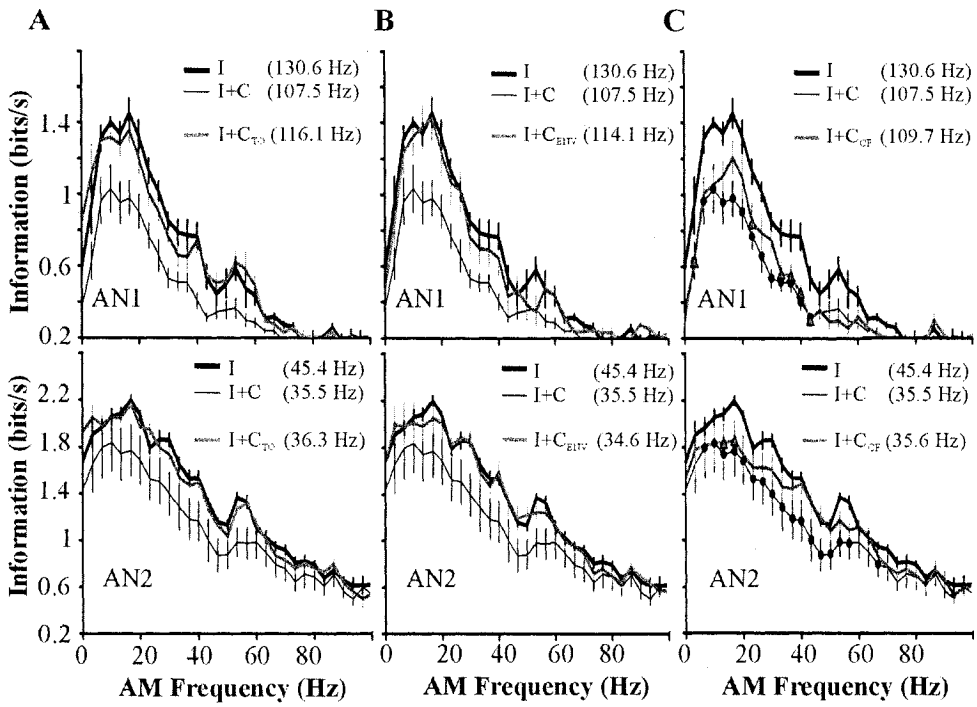

Figure 3.4. Temporal pattern of contralateral inhibition and information transfer rates. In each panel, mean information-transfer curves (± se; n= 9) are shown for monaural presentation of a RAM stimulus (I; thick black lines), and for binaural stimulation with the same RAM stimulus (I+C; thin black lines). The gray lines are the transfer functions for binaural stimulation with the following stimuli presented to the ON1-ipsilateral ear: **A.** A constant tone with same CF as the AN-ipsilateral RAM stimulus ($I+C_{TO}$); **B.** A RAM stimulus with different AM envelope, but identical bandwidth, standard deviation, and CF as the AN-ipsilateral stimulus ($I+C_{ENV}$); **C.** A RAM stimulus with the same AM envelope as the AN-ipsilateral stimulus, but with different carrier frequency ($I+C_{CF}$). As ON1's mean firing differs for stimuli with the same mean intensity relative to threshold but different CF (Marsat and Pollack, 2004), we adjusted the intensity of the ON1 ipsilateral stimulus so that firing rate was similar to that for I+C stimulation. Points that are indicated by filled circles (I+C) or open triangles ($I+C_{CF}$) differ significantly from the corresponding points for

monaural stimulation (I; ANOVA followed by Tukey, $p<0.05$). Firing rates, shown in insets, were lower for all binaural conditions compared to the corresponding monaural one (ANOVA followed by Tukey, $p<0.05$).

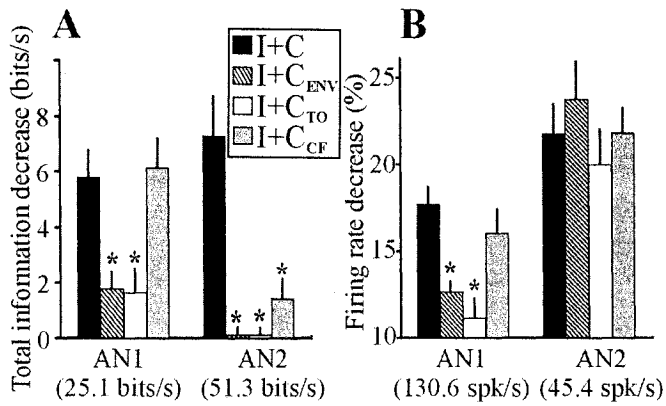

Figure 3.5. Summary of effects of contralateral stimulation. **A.** Mean decrease (± se) in total information between responses to monaural and binaural stimulation. Total information for monaural stimulation shown in parentheses. **B.** Mean percent decrease (± se) in mean firing rates for binaural stimulation compared to monaural stimulation. Firing rates for monaural stimulation shown in parentheses. Asterisks indicate significant differences from the I+C condition (black bars); ANOVA followed by a Tukey test, $p<0.05$. Notation for stimulus conditions (legend) as in Figs. 3.3 and 3.4.

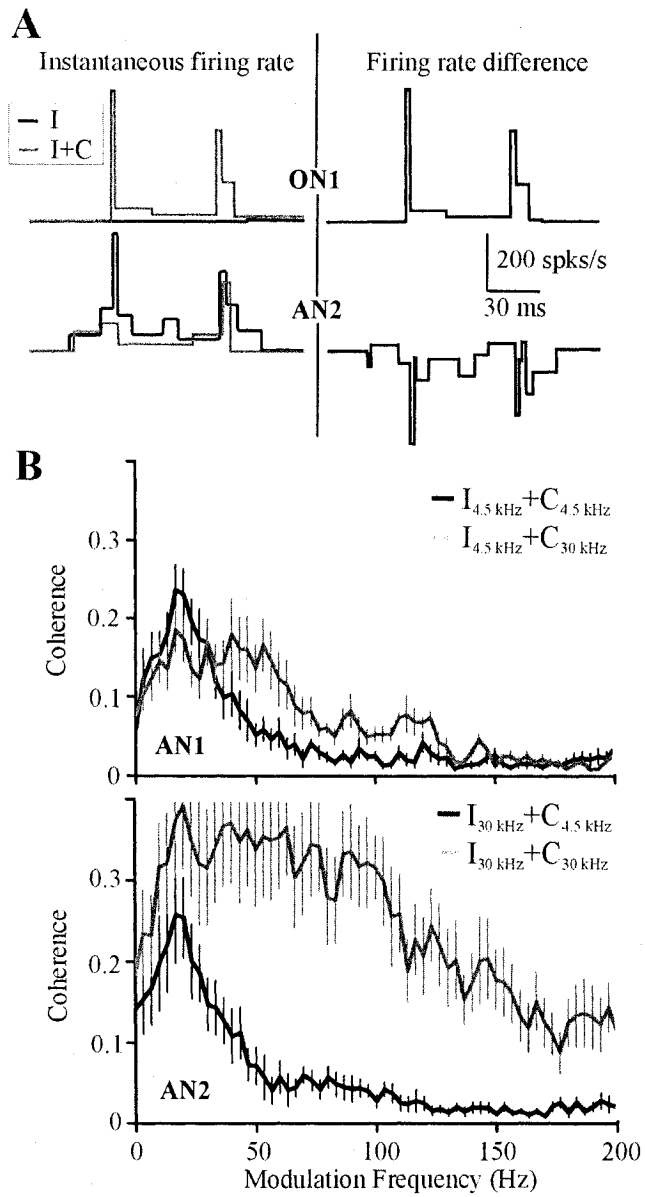

Figure 3.6. Coherence between variations in instantaneous firing rates of ON1 and ANs. **A.** Instantaneous firing rate of ON1 and AN2 (for excerpts shown in Fig. 3.2B) during monaural and binaural stimulation (left panel) The difference in instantaneous firing rate between response to binaural and monaural stimulation is shown on the right. **B.** Coherence of firing rate differences (as shown in A, right panel) between ON1 and AN1 (top) and ON1 and AN2 (bottom). ON1-ipsilateral stimuli had CF of either 4.5 kHz (black lines) or 30 kHz (gray lines); AN1- and AN2-ipsilateral stimuli were 4.5 kHz and 30 kHz respectively. Curves are means ± se; n= 9.

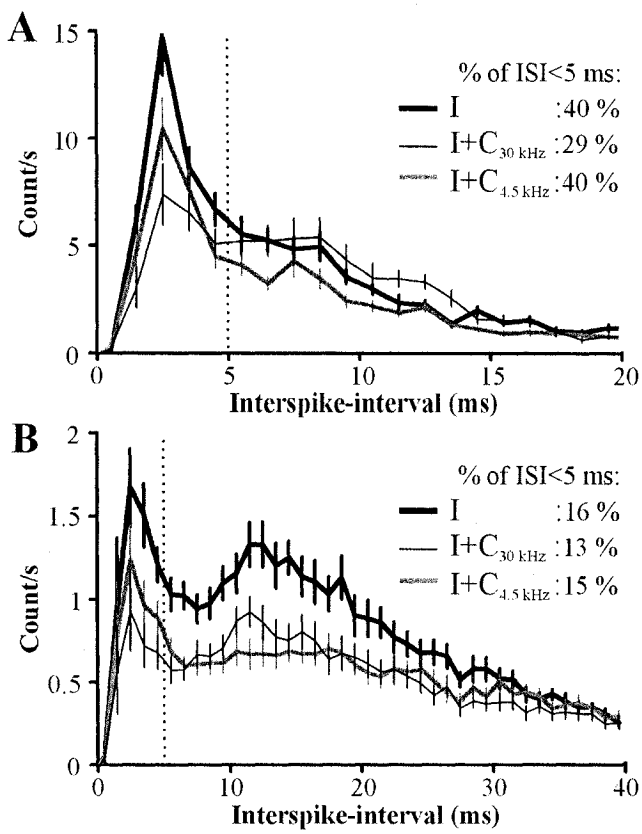

Figure 3.7. Effects of contralateral inhibition on ISI distribution of AN2 responses. Histograms show the mean number of ISIs per second, bin width: 1 ms. **A, B:** Mean (± se; n=9) ISI distributions for the initial portion of the response (0-1 s after sound onset) and the adapted portion (1-14 s), respectively. Insets: percent of ISIs < 5ms. We indicate with a dotted line the 5 ms mark. Stimulus notation as for Figs. 3.3, 3.4.

Bridge from chapter 3 to chapter 4.

We showed in chapter 3 that ON1's responses properties match those of its targets thereby maximizing its inhibitory impact. In response to ultrasound, ON1 inhibits particularly well the high frequency bursts of spikes in AN2. Bursts of spikes are part of the response of sensory neurons in other systems as well and it was shown that burst often signal the occurrence of behaviourally relevant stimuli. Therefore we hypothesized that bursts in AN2 are an important aspect of AN2's coding properties that could have a direct impact on behavioural responses.

Flying crickets respond to ultrasound by steering away from the sound source. This avoidance response is triggered by high frequency firing in AN2. We suspect that the behavioural response to dynamic stimuli will reflect the bursting properties of AN2. In chapter 4 we show that bursts do indeed code for behaviourally relevant features of ultrasound stimuli.

Chapter 4:

A behavioural role for feature detection by sensory bursts

Marsat G, Pollack GS.

Abstract

Brief episodes of high-frequency firing of sensory neurons, or bursts, occur in many systems, including mammalian auditory and visual systems, and are believed to signal the occurrence of particularly important stimulus features, i.e., to function as feature detectors. However, the behavioural relevance of sensory bursts has not been established in any system. Here, we show that bursts in an identified auditory interneuron of crickets reliably signal salient stimulus features and reliably predict behavioural responses. Our results thus demonstrate the close link between sensory bursts and behaviour.

Introduction

Bursts occur in a number of sensory systems (Eggermount and Smith, 1996; Yu and Margoliash, 1996; Sherman, 2001; Martinez-Conde et al., 2002; Chacron et al. 2004; Krahe and Gabbiani, 2004), and it has been proposed that they constitute a specific neural code, signalling the occurrence of behaviourally relevant sensory events. The possible coding functions of sensory bursts have been studied particularly thoroughly in the lateral geniculate nucleus (LGN) of mammals, and in the electrosensory lateral line lobe (ELL) of weakly electric fish. Bursts by relay cells of the LGN signal large changes in light intensity, typical of natural moving scenes (Lesica and Stanley, 2004). In pyramidal cells of the ELL, bursts preferentially encode slow modulations in the amplitude of the fish's electric field, similar to the field distortions that are caused by prey (Oswald et al., 2004). In these examples, bursts extract and signal features of the stimulus that are thought to be behaviourally important (Guido et al., 1995; Lesica and Stanley, 2004; Oswald et al., 2004), but the link between bursting and behaviour remains elusive. Indeed, a behavioural role of sensory bursts has not yet been established for any system.

Echolocating bats hunt flying insects using ultrasonic probes and crickets, like many nocturnally flying insects, respond to ultrasound stimuli with avoidance responses (Hoy, 1992), a behaviour that is triggered by an identified ultrasound-sensitive interneuron, AN2. AN2 occurs as a bilateral pair. Each AN2 receives excitatory input from one ear in the prothoracic ganglion. Its axon ascends ipsilaterally to the brain, where descending motor commands originate (Brodfuehrer and Hoy, 1989). Earlier work showed that high-frequency firing of AN2, which occurs at the onset of an ultrasound stimulus, is required for behavioural responses (Nolen and Hoy, 1984). However, bat-insect encounters may last for several seconds, during which the insect is exposed to continuous, dynamic, stimulation with ultrasound (Simmons, 2005); thus the need for AN2 to detect behaviourally relevant features of ultrasound stimuli and trigger avoidance responses persists at least for several seconds after the onset of a dynamic stimulus. AN2's response to long lasting stimuli includes both isolated action potentials and bursts. Using signal-detection theory, we show that bursts, but not isolated spikes, detect salient amplitude increases with high accuracy. Moreover, only bursts reliably signal the location of the stimulus, which must be coded to elicit properly directed behavioural responses. Most importantly, we show that bursts, but not isolated spikes, reliably predict behavioural responses.

Materials and Methods

Behavioural recordings. *Teleogryllus oceanicus* females, aged 7 to 14 days after the final molt, were anesthetized by chilling on ice; wings, hind- and mid-legs were removed to facilitate behavioural and neurophysiological recordings. Crickets were tethered dorsally and placed ventral-side up in a wind stream to elicit flight behaviour, which can be identified, despite the absence of wings, by beating of the wing stumps and by the characteristic flight posture assumed by the antennae and front legs. Abdominal steering movements associated with ultrasound

avoidance were monitored by casting a shadow of the abdomen on to a photocell array, the voltage output of which varied roughly linearly with lateral displacement of the abdomen (mean slope (± sd; n=3) = 11.8 ± 1.3 mv/mm; R2=0.85). This measurement quantifies the sign and strength of the motor output, but, because the precise relationship between abdominal displacement and flight path is unknown, it does not describe the angle towards which the cricket attempts to turn. Signals were digitized for off-line analysis (16 bits; 10 kHz sampling rate, PCI-6251 AD/DA board, National Instruments, Austin, TX).

Electrophysiology. Twenty to forty minutes after the behavioural assay, the cricket was prepared for in vivo electrophysiology as described elsewhere (Marsat and Pollack 2004). AN2 was recorded extracellularly, and bilaterally, from the cervical connectives with stainless-steel hook electrodes. Recordings were amplified with a Grass P15 amplifier (Astro-Med, West Warwick, RI) and digitized as described above. AN2's action potentials were easily recognized by their large amplitude and lowest threshold to ultrasound.

Sound stimulation. Sound was broadcast from either of two loudspeakers situated to the right and left of the cricket, perpendicular to the long axis. Stimuli (duration 15 s) had carrier frequency of 30 kHz and Gaussian amplitude envelopes (low-pass-filtered at 200 Hz; standard deviation 6 dB except where otherwise noted). Stimuli were generated digitally at sampling rate of 120 kHz. Except where specified otherwise, mean stimulus level was 85 dB SPL, corresponding to approximately 20-25 dB above threshold. Stimuli were preceded by at least 1 minute of silence.

Spike train separation. All analyses are for responses to axon-ipsilateral stimuli, except for those in figure 4.3, where ipsi- and contralateral responses are compared. We excluded from our analyses the first second of responses (both behavioural and physiological), during which AN2's

firing rate and behavioural responses adapt. Spike trains, expressed as series of ones (for time points at which spikes occur) and zeros, were down-sampled to 2 kHz and separated into two new series, consisting either only of isolated spikes (i.e. the points at which spikes-within-bursts occurred were set to zero) or only of spikes within bursts (ISI ≤ 6.5 ms). For the analyses presented in all figures except Fig. 4.3 a and b, only the first spike in each burst was retained, thereby reflecting the timing of the bursts but not their internal structure.

Feature detection. We performed standard feature-detection analysis as described in detail elsewhere (Metzner et al., 1998). We describe the procedure here only for the burst-containing train; the identical procedure was followed for the isolated-spike train. A stimulus vector, s, was defined for each successive time point in the burst train as the amplitude envelope of the 150 ms-long stimulus segment preceding that point. Each s was assigned to one of two ensembles according to whether or not, at the reference point, a burst occurred. The means of these ensembles correspond to the burst-triggered and no-burst-triggered averages (BTA, NTA). The difference between these ensembles was assessed using a Euclidian classifier. The feature vector, f, was defined as BTA - NTA. We projected s on to f to quantify their similarity, yielding the conditional probability distributions $P(f \cdot s \mid \text{burst})$ and $P(f \cdot s \mid \text{no burst})$. Receiver operating characteristic curves were generated by varying a threshold similarity level, T. For each threshold value the probability of detection (PD) is calculated as the sum of $P(f \cdot s > T \mid \text{burst})$, and the probability of failure (PF) as the sum of $P(f \cdot s > T \mid \text{no burst})$. The error level for each threshold value is ½ PF + ½ (1- PD). We report the minimum error level across values of T.

Behaviour analysis. Recordings of abdomen movements were high-pass filtered with a cutoff frequency of 0.5 Hz to eliminate slow drifts in abdomen position (Pollack and Plourde, 1982) and focus on the rapid

abdomen flexions associated with the avoidance steering response during flight. The behavioural responses were either averaged across repetitions of the same stimulus to calculate spike- and burst-triggered averages, or quantified for individual abdominal movement recordings. We quantified behaviour in two ways. First, we used the standard deviation of the abdominal-movement recording as a measure of the response. This reflects the strength and frequency of abdomen deflections, including both "correct" responses, i.e. away from the sound source, and misdirected responses. Second, in order to examine separately correct and misdirected responses, we measured the area under the half-rectified recording of abdomen position separately for deflections away from and towards the sound source. The method based on standard deviation and that based on half-rectified recordings that retained only responses directed away from the source yielded nearly identical results, suggesting that responses were directed mainly away from the sound source. This is confirmed by comparison of half-rectified responses directed towards and away from the sound source (see Supplemental Fig. 4.2). Only the results based on standard deviation are presented here; those based on rectified recordings are available in the supplementary material.

Statistical treatment. Response measures (both electrophysiological and behavioural) of individual crickets to a given stimulus were averaged. Averages of these values across crickets are reported in the results, and were used for statistical analyses, except for Fig. 4.5b. Proportions were arcsine-square root-transformed (Zar, 1999) before being subjected to statistical tests.

Results

Responses to long-lasting stimuli with Gaussian amplitude envelopes consist, after a rapid adaptation phase (Samson and Pollack, 2002), of both isolated spikes, separated by relatively long and variable inter-spike

intervals (ISIs), and of bursts, consisting of groups of spikes separated by short ISIs (typically 3-4 ms; Fig. 4.1a). Bursting is reflected in ISI histograms (Fig. 4.1b) as a narrow peak of short ISIs that is distinct from the broader peak of longer ISIs. The proportion of spikes within bursts (operationally defined as spikes occurring with ISI < 6.5 ms) increases with sound level (from 12 ± 1.3 % for 10 dB above threshold to 29 ± 4.1 % for 30 dB above threshold; means ± SD; ANOVA, p=0.012, n=9; Fig. 4.1b). Bursting also increases with modulation depth (from 1 ± 0.2 % for envelope s.d. of 1 dB to 37 ± 5.2 % for s.d. of 7 dB; ANOVA, p=0.001, n=6; Fig. 4.1c).

Bursts function as feature detectors.

We first asked whether, as in other systems, bursts in AN2 might function as feature detectors. Spike-triggered and burst-triggered averages of pre-spike or pre-burst segments of the stimulus envelope show that both bursts and isolated spikes are time-locked to increases in stimulus amplitude (Fig. 4.2a). However, bursts occur following large increases in stimulus amplitude, whereas isolated spikes follow smaller peaks. The amplitude increase required to elicit bursts scales with mean stimulus amplitude and modulation depth, such that for a variety of stimuli, bursts occur following conspicuous amplitude increases, as indicated by peak pre-burst amplitudes that extend at least one standard deviation beyond the mean. Moreover, the peak of the burst-triggered average, but not of the spike-triggered average, is preceded by a period of low stimulus amplitude, as indicated by the dip below the mean level approximately 15 ms before the burst.

We used signal-detection measures (Metzner et al., 1998) to quantify the performance of bursts and isolated spikes as feature detectors. Receiver operating characteristic curves (Fig. 4.2b) show the reliability with which portions of the stimulus resembling features that are putatively associated with bursts or with isolated spikes are in fact followed

by these responses. Bursts perform well as feature detectors, whereas isolated spikes do so poorly. Minimum error rate, which includes both failure to identify a feature when it occurs and erroneous identification of a feature when there is none, is 9 ± 1.6 % for bursts and 33 ± 3.1 % for isolated spikes for the data set shown in Fig. 4.2b (means ± SD; paired t-test, $p<10\text{-}5$; n=16 neurons). Although burst rate varies with mean stimulus amplitude and modulation depth (Fig. 4.1b,c), the accuracy of feature detection by bursts and isolated spikes remains constant over a wide range of stimulus statistics (Fig. 4.2c, ANOVA on minimum error level, $p=0.23$ and $p=0.34$ for bursts and isolated spikes respectively; n=6 neurons).

Bursts encode localization cues

Ultrasound-avoidance responses are directed away from the sound source. Thus, if bursts are instrumental in driving behaviour, they should not only detect a stimulus, but also code for its location. Localization of ultrasound is based on bilateral differences in the responses of the left and right AN2s (Pollack, 1998). We quantified localization cues by recording simultaneously from both neurons. Fig. 4.3a shows firing rates of the two neurons, calculated separately for isolated spikes and for spikes within bursts. The bilateral difference is striking for bursts, but is less evident for isolated spikes. Using sliding windows (1 to 100 ms wide, a range that includes behavioural latencies (Nolen and Hoy, 1986) and thus the integration times of downstream circuits), we calculated separately, for bursts and isolated spikes, the binaural difference in mean spike count per window (excluding windows that contained no spikes on either side). Bilateral spike-count difference is greater for bursts than for isolated spikes over the entire range of window widths (ANOVA, $p=0.001$, Tukey test, $p<0.05$ for all points; Fig. 4.3b); indeed the difference for isolated spikes does not differ significantly from zero for any window width (one sample t-test, $p>0.05$). Another possible sound-localization cue is the

bilateral timing difference. Figure 4.3c shows the temporal distribution of spikes or bursts in the AN2 contralateral to the sound source relative to those in its ipsilateral counterpart. We focus on bilateral differences within the range ± 10 ms, which encompasses the range of previously measured binaural latency differences of AN2 for trains of discrete sound pulses (Samson and Pollack, 2002). For 23% of ipsilateral bursts, a contralateral burst occurs within ±10 ms (the area under the curve). The sound-ipsilateral burst leads in 85 ± 5.1 % of these cases (unshaded area, significantly different from chance, one-sample t-test $p<10^{-4}$). Thirty-eight percent of ipsilateral isolated spikes are matched by contralateral isolated spikes, but the ipsilateral spike leads in only 61 ± 8.3 % of these cases , which does not differ significantly from that expected by chance (p=0.24). Thus, based both on spike count and on timing, only bursts provide reliable cues for sound direction.

Bursts predict behaviour

To study the role of bursts in behaviour, we compared neural and behavioural responses to dynamic stimuli. We recorded a conspicuous component of the ultrasound avoidance response, abdominal movements away from the sound source during tethered flight (Moiseff et al., 1978). Subsequently we recorded, in the same cricket, AN2's response to the same stimulus that was presented during behavioural tests. Visual comparison of behavioural and neural responses suggests that conspicuous abdominal movements tend to follow stimulus segments that elicit bursts in AN2 (highlighted in black in Fig. 4.4a). This is confirmed by the burst-triggered average of abdominal position (Fig. 4.4b), which shows that a large abdominal flexion begins ca. 40 ms after a burst. This value is similar to that reported by Nolen and Hoy (1984) for the latency between the first AN2 spike of a response and activation of abdominal steering muscles (49 ± 16 ms). Abdominal movements following isolated spikes are much less pronounced.

To examine the relationship between spike-train structure and behaviour more directly we manipulated the frequency of occurrence of bursts and isolated spikes. The relative frequency of bursts increases both with mean stimulus amplitude and with modulation depth (Fig. 4.1c). We chose stimuli (n=8) that differed in mean amplitude and/or in modulation depth, such that both burst rate and isolated-spike rate varied across responses to these stimuli, but were not correlated with each other (R^2=0.03, p=0.24; also see Supplementary Fig. 4.1a). We quantified the behavioural response as the standard deviation of the abdominal-movement recording (Fig. 4.5a). Behaviour varies strongly as a function of burst rate (Fig. 4.5b; R^2=0.77, $p<0.10\text{-}5$), but is independent of the isolated-spike rate (R^2=0.016, p=0.4; also see Supplementary Fig. 4.1 b, c and 4.2). These results argue strongly that AN2 bursts, but not isolated spikes, are responsible for the behavioural responses.

Discussion

We have shown that bursts in AN2 signal the occurrence of salient peaks in stimulus amplitude, encode sound direction, and predict behavioural responses, all with high reliability. These findings provide strong evidence that bursts are functionally important.

Bursting occurs over a range of stimulus amplitudes and modulation depths, but in all cases, bursts are triggered by the most conspicuous increases in amplitude. Thus, the stimulus feature that triggers bursts scales with stimulus statistics. Moreover, although the frequency of bursting varies across stimuli, the high accuracy of feature detection remains constant. This stimulus-dependent change in AN2's response properties is functionally similar to the adaptation that has been described in a number of sensory systems (Smirnakis et al., 1997; Kvale and Schreiner, 2004; Dean et al., 2005), which allows accurate detection and encoding of changes in a stimulus over a wide range of stimulus statistics.

In addition to detecting large amplitude increases, bursts reliably signal the location of the sound source through bilateral differences in bursting of the two AN2s. These differences were apparent both in spike count and in burst timing, both of which can provide cues for sound localization. It is not yet known, for responses to ultrasound, whether one or the other of these cues dominates in the determination of response direction. For positive phonotaxis to cricket songs, bilateral timing difference is less important than differences in response strength (Pollack, 2003; Hedwig and Poulet, 2005). Moreover, in our experiments, for more than three-quarters of the bursts in the sound-ipsilateral AN2, there was no burst in the contralateral neuron within a 10ms window, thus obviating the need to compare binaural timing. The strong bilateral difference in bursting is due, in part, to contralateral inhibition. An identified interneuron, ON1, is excited by input from one ear and inhibits the AN2 that is excited by the other ear (Selverston et al., 1985). We showed previously that contralateral inhibition selectively suppresses high firing rates in AN2 (Marsat and Pollack, 2005), and thus should enhance binaural contrast preferentially for bursts.

Isolated spikes were common in AN2's responses to the stimuli we used, yet they had little, if any, behavioural impact. AN2 also responds to cricket songs (Libersat et al, 1994) and contributes to behavioural responses to these stimuli (Schildberger and Hörner, 1988). Thus, isolated spikes may play a role in encoding these signals. AN2's role in bat evasion is known to be context dependent; it triggers avoidance steering only during flight (Nolen and Hoy, 1984). If isolated spikes play a role in responses to cricket song, then this would be another instance of the context-dependency of this neuron's behavioural impact, the context in this case being the nature of the stimulus. For bat-evasion responses, however, isolated AN2 spikes may simply be "noise", which is filtered out by the fact that only bursts elicit strong behavioural responses. Noise filtering by bursts has been shown in other systems where, due to synaptic

summation or facilitation, bursts are particularly effective in driving their target cells (Boyan and Fullard, 1988; Lisman, 1997; Swaldow and Gusev, 2001). The same may be true of AN2's interactions with its target neurons.

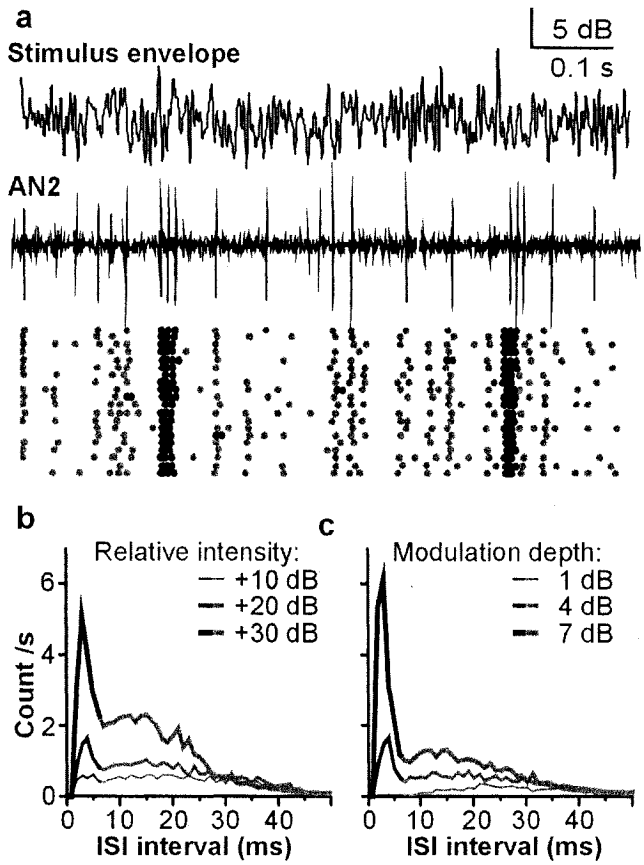

Figure 4.1. Bursts in AN2 in response to amplitude modulated stimuli. **a.** Excerpt of the response of AN2 to a Gaussian-envelope stimulus, beginning 4 s after stimulus onset. The top trace shows the amplitude envelope of the stimulus (mean sound level 85 dB SPL; standard deviation 6 dB). The middle trace is AN2's response. The bottom plot shows responses to 20 repetitions of the same stimulus. Grey dots represent isolated spikes; black dots indicate spikes within bursts. **b.** Interspike-interval (ISI) distributions of responses to stimuli that differ in mean sound level (standard deviation of amplitude envelope: 5 dB, n=9). Mean firing rates ± SD are: 21.9 ± 2.3 Hz, 32.7 ± 2.7 Hz and 61.7 ± 4.6 Hz for stimuli 10 dB, 20 dB and30 dB above threshold respectively **c.** ISI distributions of responses to RAM stimuli with different modulation depths (stimulus intensity: 85 dB SPL; n=6). In b and c, ordinate shows number of ISIs per

second; bin width, 1 ms. The black portions of the curves represent ISIs of spikes within bursts (ISI ≤ 6.5 ms). Mean firing rates ± SD are: 12.2 ± 3.1 Hz, 26.2 ± 3.8 Hz and 48.7 ± 5.7 Hz for stimuli with amplitude envelope SD of 1 dB, 4 dB and 7 dB respectively.

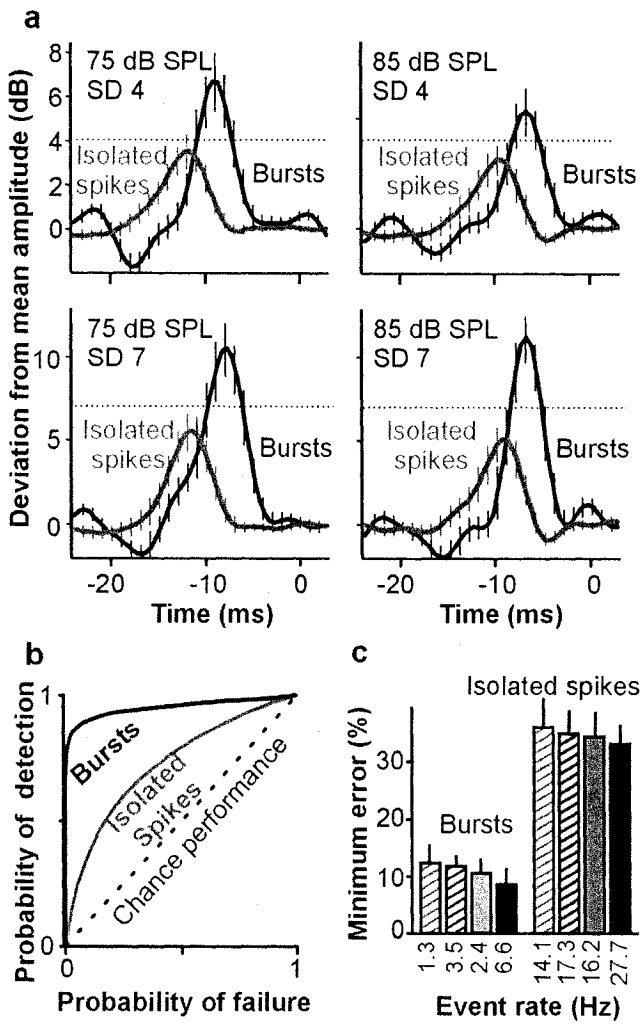

Figure 4.2. Coding of stimulus features by bursts and isolated spikes. **a.** Spike-triggered averages of the stimulus envelope preceding isolated spikes (grey) or bursts (black) for stimuli with different mean sound levels and modulation depths (mean ± SD, n=6 neurons). Modulation depth is quantified as the standard deviation (SD) of the stimulus and is indicated on the plots by dotted lines. Values represent departures from mean stimulus level (indicated on each panel). **b.** Receiver operating characteristic curves, which plot the probability of correct detection of a feature (i.e. a feature-containing stimulus segment is followed by the appropriate event) against the probability of failure (absence of event

following the putative feature), as the stringency for feature identification is varied. The dotted line indicates chance feature detection; performance increases with the degree of departure from this. Stimulus: 85 db SPL, envelope SD 6 dB (mean of 16 neurons). **c.** Minimum error level (mean ± SD, n=6 neurons) for stimuli with different mean intensities (grey: 75 dB SPL; black: 85 dB SPL) or modulation depths (hatched: envelope SD of 4 dB; solid: envelope SD of 7 dB). Burst rate or isolated spike rate is indicated for each stimulus.

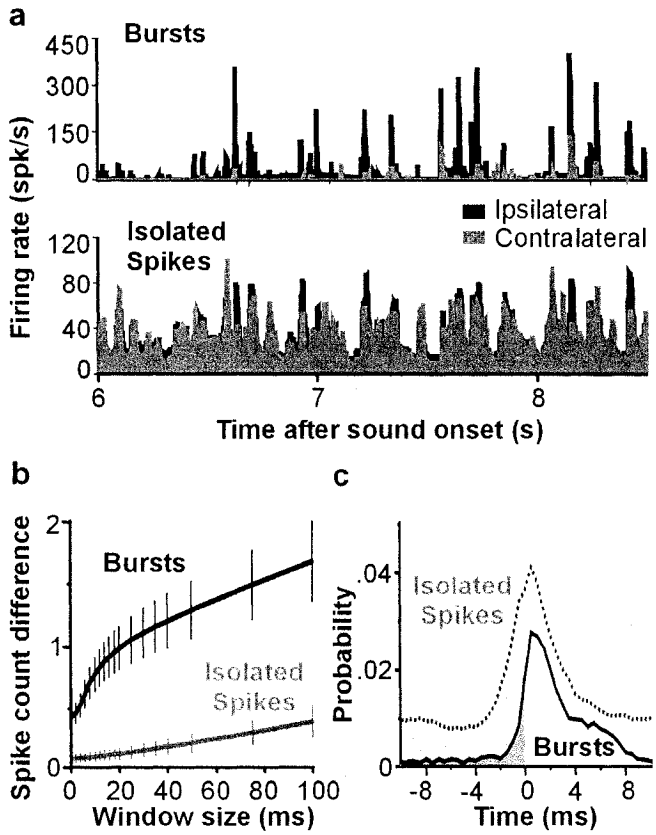

Figure 4.3. Directionality of AN2's response. **a.** Mean instantaneous firing rates (calculated as ISI-1; example from one experiment, n=20 stimulus repetitions) based either on spikes within bursts (top panel) or on isolated spikes (bottom panel). Both AN2s were recorded simultaneously. **b.** Bilateral spike count difference (mean ± SD, n=16 neurons) based on isolated spikes or bursts, calculated for sliding windows of different widths. **c.** Probability of occurrence of isolated spikes (dashed line) or bursts (solid line) in the sound-contralateral AN2 relative to the timing of an isolated spike/burst in the ipsilateral AN2 (bin width: 0.5 ms). Shading indicates contralateral-leading events.

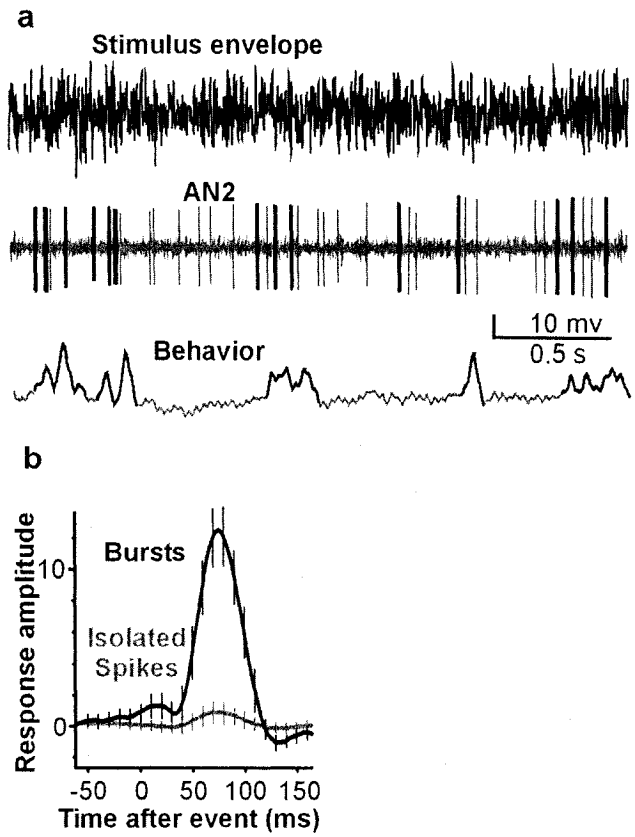

Figure 4.4. Behavioural impact of bursts and isolated spikes of AN2. **a.** Excerpts of behavioural and neural responses, each beginning 4 s after onset of the identical Gaussian-envelope stimulus. Note: the neural responses were recorded after completion of the behavioural measurements. Top: stimulus amplitude envelope; middle: response of the sound-ipsilateral AN2; bottom: abdominal movement; vertical scale indicates voltage ouptut of the recoding device (see Methods). Bursts in AN2, and conspicuous abdominal movements away from the sound source, are highlighted in black. **b.** Amplitude of abdominal movement (mv output of recording device, mean ± SD, n=16 experiments) following an isolated spike (grey) or a burst (black) in AN2. Positive values indicate abdomen flexion away from the sound source.

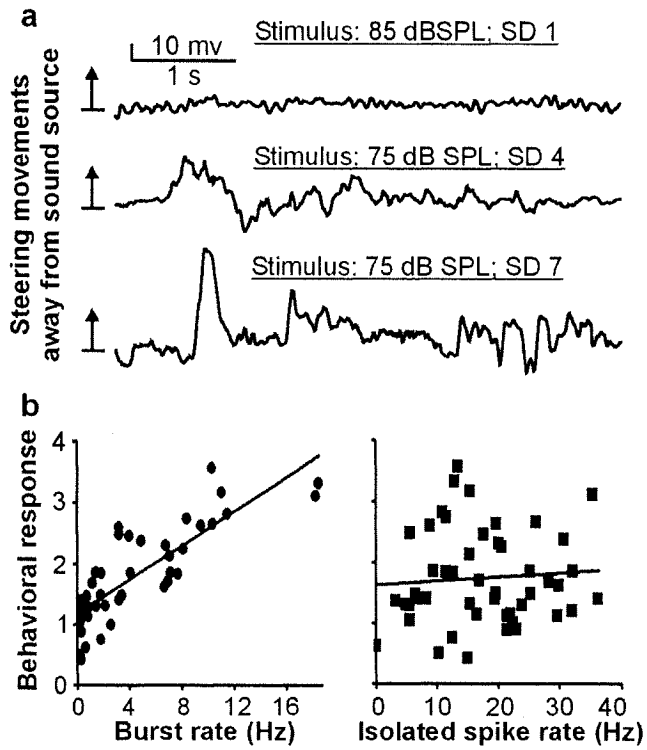

Figure 4.5. Behavioural responses vary with burst rate. **a.** Excerpts of behavioural responses to stimuli that had the same modulation envelope but different mean intensity or modulation depth (indicated above each recording). The traces show abdominal movements (individual responses of the same cricket to different stimuli) beginning six seconds after sound onset (scale as in Fig. 4.4). In this animal, the mean response of the sound-ipsilateral AN2 in response to these stimuli was, from top to bottom: 0.7, 7.2 and 10.4 bursts/s and 20.3, 19.1 and 26.4 isolated spikes/s. **b.** Behavioural response, quantified as the standard deviation of abdominal movements (mv output of recording device), as a function of the isolated-spike rate (right) and burst rate (left) in the sound-ipsilateral AN2. Data points are from 6 experiments, in each of which stimuli with different mean sound levels (70 dB SPL to 90 dB SPL) and/or modulation depths (envelope SD: 1 dB to 9 dB) were presented. Best-fit linear regression lines are shown. See also supplementary figures 4.1 and 4.2

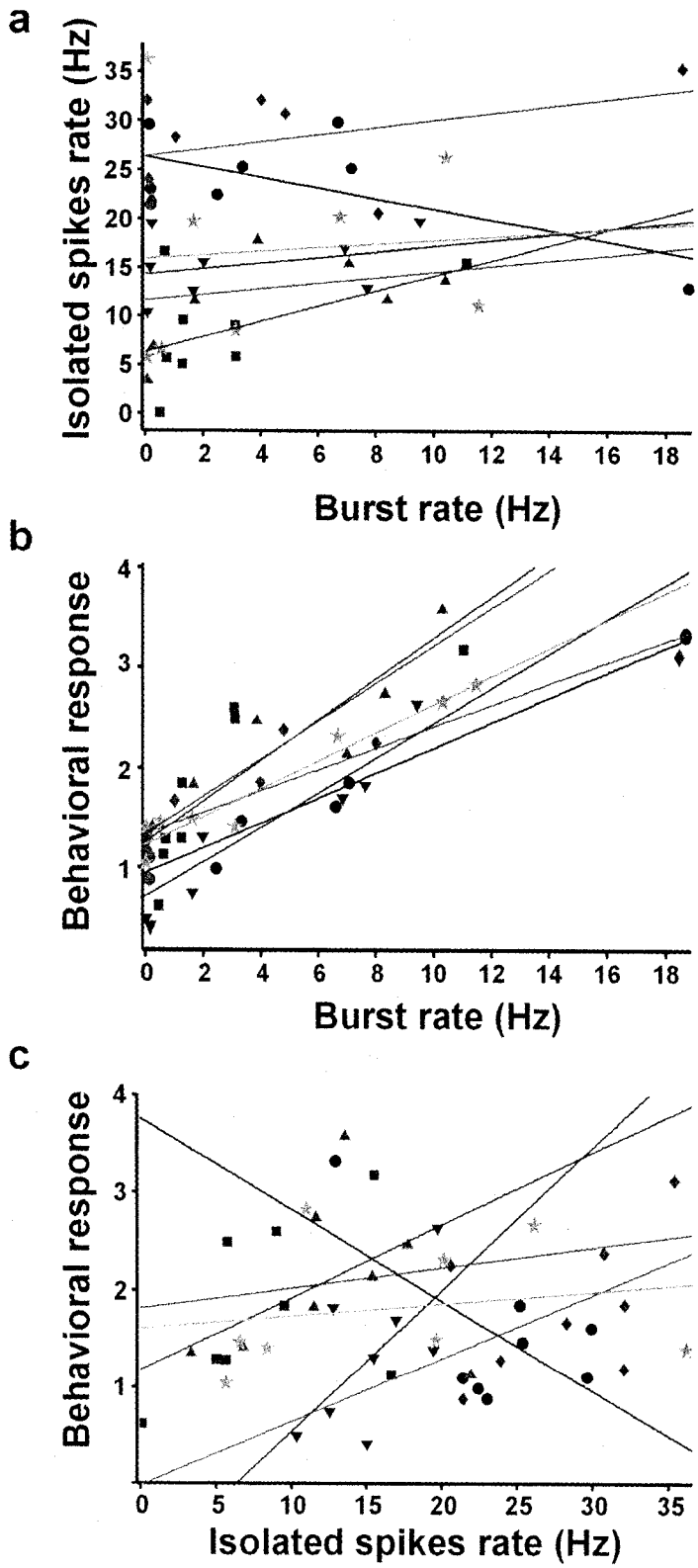
a
Isolated spikes rate (Hz)
0
5
10
15
20
25
30
35
0
2
4
6
8
10
12
14
16
18
Burst rate (Hz)
b
Behavioral response
1
2
3
4
0
2
4
6
8
10
12
14
16
18
Burst rate (Hz)
c
Behavioral response
1
2
3
4
0
5
10
15
20
25
30
35
Isolated spikes rate (Hz)

Supplemental Fig 4.1: Correlations between burst rate, isolated spike rate and behavioural response magnitude (measured as the SD of the abdomen movement trace). Stimuli with different mean sound levels and modulation depths were presented to each cricket (crickets are represented by symbols of different shapes and color; n=6). Each point represents the mean value (of isolated spike rate, burst rate or behavioural response) for a single type of stimulus (4 repetitions of each stimulus). Best-fit lines are shown for each cricket. a. Burst rate and isolated spike rates are not correlated across stimuli (R^2 range: 0.002 to 0.39; p: 0.09 to 0.69). b. Burst rate is positively correlated with behavioural response magnitude in all crickets (R^2 range: 0.67 to 0.96; p: 10^{-5} to 10^{-2}). c. Isolated spike rate is not correlated with behavioural response magnitude in any cricket (R^2 range: 0.003 to 0.4; p: 0.08 to 0.9).

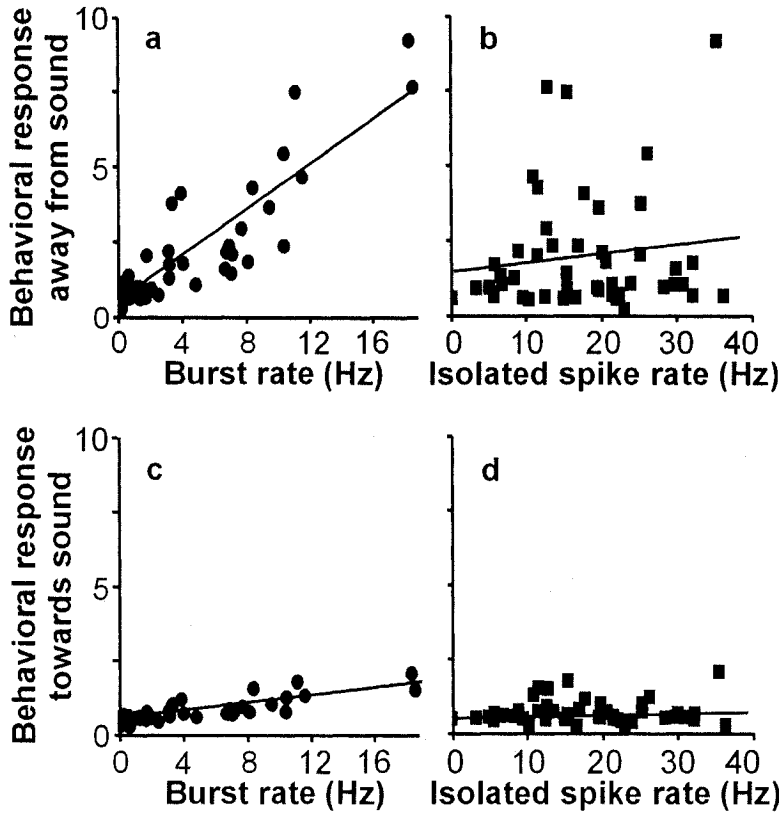

Supplemental Fig 4.2: Behavioural responses vary with burst rate and not isolated spike rate. Behavioural response, quantified as the area under the half-rectified recording of abdomen position (mv·s) away from (**a,b**) or towards (**c,d**) the sound source, as a function of the isolated-spike rate (**b,d**) and burst rate (**a,c**) in the sound-ipsilateral AN2. This measure of the behavioural response reflects the strength and frequency of abdomen movements away from or towards the sound source. Data points are from 6 experiments, in each of which stimuli with different mean sound levels (70 dB SPL to 90 dB SPL) and/or modulation depths (envelope SD: 1 dB to 9 dB) were presented. Best-fit linear regression lines are shown. Behaviour correlates strongly with burst rate (a: $R2 = 0.70$, $p<10\text{-}5$; c: $R2 = 0.69$, $p<10\text{-}5$), but not with isolated-spike rate (b: $R2 = 0.02$, $p=0.36$; d: $R2 = 0.01$, $p=0.42$). The relationship between behaviour and burst rate is steeper for responses away from the sound source (a; slope=0.38) than for responses directed towards the source (c; slope = 0.07; t-test, $p<10\text{-}5$).

Bridge from chapter 4 to chapter 5

In chapter 4 we showed that the behaviourally relevant information about ultrasound stimuli is carried by bursts in AN2 and that these bursts trigger avoidance responses. In particular, spatial information (localization cues) is more accurately encoded in bursts-bilateral contrast than in isolated-spikes bilateral contrast. Furthermore, we showed in chapter 3 that ON1's inhibition decreases the proportion of bursts in AN2's response. We hypothesize that ON1's response properties enable it to selectively enhance the bilateral contrast for AN2 bursts.

To test this hypothesis, we describe in chapter 5 the similarities between the response characteristics of ON1 and AN2. We also examine the temporal relationship between spiking in ON1 and AN2 to clarify the mechanism by which ON1 selectively enhances the bilateral contrast during bursting.

Chapter 5:
Efficient inhibition of bursts in the auditory system of crickets.

Marsat, G and Pollack GS

Abstract

Sensory processing, including sound localization, relies on precisely timed neural interactions. In crickets, auditory information about ultrasound is carried bilaterally to the brain by the AN2 neurons. The ON1 neuron provides contralateral inhibitory input to AN2, thereby enhancing bilateral contrast between the left and right AN2s. We examine how the structures of the spike trains of these neurons affect this inhibitory interaction. As previously shown for AN2, ON1 responds to salient peaks in amplitude with bursts of spikes. Spike bursts, but not isolated spikes, reliably signal the occurrence of specific features of the stimulus. ON1 and AN2 burst at similar times relative to the amplitude envelope of the stimulus. As a consequence, spikes within bursts in AN2 are more likely to be preceded by spikes in ON1 (mainly also in bursts) than are isolated AN2 spikes. The frequent coincidence of bursts in ON1 and AN2 compared with isolated spikes thus leads to a large decrease in burst rate. We conclude that the match in coding properties of ON1 and AN2 allows contralateral inhibition to be most efficient for portions of the response that carry the behaviourally relevant information, i.e. for bursts.

Introduction

Sensory processing often relies on precisely timed neural interactions. Sound localization provides a good example of the importance of the timing of inputs on neural responses. Sound localization in the horizontal plane relies largely on differences in timing and intensity of the sound as it reaches each ear (Rayleigh, 1876; Middlebrooks and Green, 1991) and these differences must be extracted and encoded by the nervous system. Neurons in the avian nucleus laminaris and the mammalian superior olivary complex are very sensitive to binaural differences, and this arises in large part from the relative timing of converging bilateral inputs (Oertel, 1999). This is true for cells detecting coincident excitatory inputs (Joris et

al., 1998), and a growing body of evidences indicates that temporally precise inhibition is also important in processing sound direction (Park et al., 1996; Irving et al, 2001; Brand et al., 2002; Grothe, 2003). The temporal structures of sound stimuli and the manner and precision with which these are encoded by auditory neurons underlie the temporal dynamics of neural interactions (Oertel 1999; Carr, 1993).

The AN2 neuron of crickets is an identified, bilaterally paired, ultrasound-sensitive interneuron that receives input from auditory receptors and carries ultrasound related information to the brain (Pollack, 1998). Crickets steer away from a source of ultrasound, a behaviour believed to allow avoidance of echolocating insectivorous bats (Hoy et al., 1989). High firing rate in AN2 is necessary and sufficient to trigger avoidance steering (Nolen and Hoy, 1984). In response to long dynamic stimuli, AN2 produces both bursts of spikes, with interspike intervals of a few ms, and isolated spikes separated by longer interspike intervals. Bursts, but not isolated spikes, reliably signal the occurrence of behaviourally relevant features of ultrasound stimuli and evoke avoidance responses (Marsat and Pollack, 2006).

The direction of the sound source, and thus of avoidance steering, is coded by the bilateral difference in bursting of the left and right AN2; the binaural difference in isolated spike rate does not reliably indicate the direction of the source (Marsat and Pollack, 2006). The bilateral difference in AN2 activity is enhanced by contralateral inhibition delivered by the ON1 neuron (Selverston et al. 1985; Horsemann and Huber, 1994; Faulkes and Pollack 2000). This inhibition is most efficient when the temporal patterns of the stimuli to both ears are identical. Under these conditions (which replicate the natural situation), contralateral inhibition selectively suppresses high firing rates in AN2's response (Marsat and Pollack, 2005). The goal of this study is to clarify how ON1's response pattern participates in creating a large bilateral contrast specifically for bursts. We examine the coding properties of ON1 and show that they are similar to

these of AN2: both neurons signal salient stimulus features through bursts. We compare the relative timing of bursts and isolated spikes between ON1 and AN2 and examine the influence of ON1's inhibition on AN2's response structure and coding performance.

Methods

Electrophysiology

Teleogryllus oceanicus were reared in the laboratory. Females were used for experiments at age 7-14 days after the final molt. After mounting the cricket on a support, the prothoracic ganglion was exposed by ventral dissection, supported on a metal platform and bathed in physiological saline (Strausfeld et al., 1983).

AN2 was recorded extracellularly from the cervical connective (which was cut anteriorly) using stainless steel hook electrodes. To reduce background activity we cut the pro-mesothoracic connectives. Spikes of AN2 are easily identified by their large amplitude and by the neuron's preferential sensitivity to ultrasound. ON1 was recorded extracellularly from its soma-contralateral processes in the prothoracic ganglion, using blunt glass microelectrodes filled with 1M NaCl (resistance: 5-10 Mohm). ON1 can be identified in this recording configuration by its preference for electrode-contralateral stimuli, as well as its greater sensitivity, but longer latency, to 4.5 kHz stimuli as compared to ultrasound (Faulkes and Pollack, 2000). In this paper, ipsilateral refers to the side from which sound most effectively excites the neuron, i.e. ipsilateral to AN2's ascending axon and ipsilateral to ON1's cell body. Recordings were amplified by a Grass P15 amplifier (Astro-Med Inc., West Warwick, RI, for hook recordings) or a Getting 5A microelectrode amplifier (Getting Instruments, San Diego, CA) and digitized (16 bits, sampling rate 10 kHz; Digidata 1320A, Molecular Devices, Union City, CA).

Sound stimulation

Threshold was defined as the lowest sound intensity that reliably elicits at least one spike per sound pulse (30 ms sound pulses, including 5 ms onset and offset ramps, presented at 2 Hz). Carrier frequency (CF) was 30 kHz except for figure 5.1 B where stimuli with a carrier frequency of 4.5 kHz were also used.

Stimuli with Random Amplitude Modulation envelopes (RAM) were produced by multiplying a sinusoidal signal of desired carrier frequency with a low-pass-filtered Gaussian signal (<200 Hz) with a standard deviation of 5 dB. RAM stimuli were 15 s long with 0.1 s linear onset and offset ramps, and were preceded by at least 45 s of silence. Stimuli were produced by a National Instruments (Austin, TX) AD/DA board with 12 bits of resolution, at a sampling rate of 100 kHz.

For free-field stimulation, the cricket's front legs (which bear the ears) were held flexed against the pronotum in a position similar to that assumed during flight. Sound was broadcast from loudspeakers situated to the cricket's left and right, perpendicular to the longitudinal axis. For dichotic, closed-field stimulation, the legs were held horizontally and were inserted in cylindrical chambers containing earphones (Optimus Nova 401, Radioshack). The chambers, which were 14 mm in diameter and 3 mm in height, were sealed with wax. The acoustic trachea linking the two ears was severed to ensure stimulus isolation (Michelsen and Löhe, 1995). In closed-field experiments, stimuli at the ear ipsilateral to the AN2 had a mean sound level of 80 dB SPL and stimuli at the ear ipsilateral to ON1 had mean sound levels of 88 dB SPL, simulating a sound source on the ON1-ipsilateral side of the cricket. For both stimulation methods, sound level was calibrated using Brüel and Kjaer (Naerum, Denmark) instruments (4135 microphone, 2610 sound-level meter).

Data analysis

Spike train separation. We excluded from our analyses the first second of responses, during which AN2 and ON1 firing rates adapt. Spike trains,

expressed as series of ones (for time points at which spikes occur) and zeros, were down-sampled to 2 kHz and separated into two new series, consisting either only of isolated spikes (i.e. the points at which spikes-within-bursts occurred were set to zero) or only of spikes within bursts (interspike-interval ≤ 6.5 ms). For the feature detection analysis, only the first spike in each burst was retained, reflecting the timing of bursts, but not their internal structure.

Feature detection. We performed standard feature-detection analysis as described in detail elsewhere (Metzner et al 1998). We describe the procedure here only for the burst-containing train; the identical procedure was followed for the isolated-spike train. A stimulus vector, s, was defined for each successive time point in the burst train as the amplitude envelope of the 150 ms-long stimulus segment preceding that point. Each s was assigned to one of two ensembles according to whether or not, at the reference point, a burst occurred. The means of these ensembles correspond to the burst-triggered and no-burst-triggered averages. The difference between these ensembles was assessed using a Euclidian classifier. The feature vector, f, was defined as the burst-triggered average minus the no-burst-triggered average. We projected s on to f to quantify their similarity, yielding the conditional probability distributions $P(f \cdot s \mid \text{burst})$ and $P(f \cdot s \mid \text{no burst})$. Receiver operating characteristic curves were generated by varying a threshold similarity level, T. For each threshold value the probability of detection (P_D) is calculated as the sum of $P(f \cdot s > T \mid \text{burst})$, and the probability of failure (P_F) as the sum of $P(f \cdot s > T \mid \text{no burst})$. The error level for each threshold value is $\frac{1}{2} P_F + \frac{1}{2} (1 - P_D)$. We report the minimum error level across values of T.

Data analysis was performed with Matlab 6.5 (Mathworks, Natick, MA). We used Statistica 5.5 (Statsoft, Tulsa, OK) for all tests of significance.

Results

Stimulus coding by bursts and isolated spikes

We recorded the response of ON1 and AN2 to amplitude modulated ultrasound stimuli with Gaussian amplitude envelopes. We described bursting by AN2 previously (Marsat and Pollack, 2006); we replicate these experiments here for comparison with ON1. The excerpt shown in figure 5.1A indicates that ON1 and AN2 possess similar bursting properties. The stereotypical interval between spikes within bursts is reflected in the interspike-interval (ISI) distribution by a narrow peak at ISI shorter than 6 ms (Fig 5.1B). ON1 responds both to ultrasound and to lower-frequency, cricket-like stimuli (carrier frequency of 4.5 kHz), yet, it produces bursts only for ultrasound stimuli (Fig 5.1B). The proportion of spikes within bursts increases, both for ON1 (in response to ultrasound) and AN2, as the mean intensity or the modulation depth of the stimulus is increased (Fig 5.1C; ANOVAs, $10^{-5}<p<10^{-2}$).

In many systems, bursts function as feature detectors, i.e. they signal the occurrence of specific stimulus features (Guido et al., 1995; Lesica and Stanley, 2004; Oswald et al., 2004). Bursts in AN2 reliably signal the occurrence of large increases in amplitude of an ultrasound stimulus, a feature that is important for behaviour (Marsat and Pollack 2006). ON1 also performs well as a feature detector. As for AN2, bursts in ON1 are triggered by relatively large peaks in amplitude, whereas isolated spikes follow smaller amplitude increases (Fig 5.2A, B). For ON1 as for AN2, the peak pre-burst stimulus amplitude follows a small decrease in amplitude approximately 15 ms before burst onset, suggesting that bursts are triggered by large contrasts in amplitude. The performance of a feature detector can be summarized as a receiver operating characteristic curve (ROC), which plots the probability of successful detection of a feature (in this case, occurrence of a burst or isolated spike following the burst-associated or isolated-spike-associated feature) against the probability of failure (Fig 5.2C, D). Both for ON1 and AN2, bursts perform well as feature

detectors, as indicated by the rapidly rising initial slope of the ROCs. Minimum error level, which include both failure to identify a feature when it occurs and erroneous identification of a feature when there is none, is similarly low for both ON1 and AN2 bursts (11 % and 12 % respectively). By contrast, isolated spikes perform significantly less well than bursts (paired t-test, $p<10^{-4}$ for both ON1 and AN2). The superior performance of bursts relative to isolated spikes is due in part to more precise timing of bursts relative to the stimulus feature that evokes them. This is confirmed in Fig. 5.2 E, F, where we show the scatter, across repeated presentations of the identical stimulus, of bursts and isolated spikes. The distributions are sharper and reach higher probability for bursts than isolated spikes. For example, for ON1, 65% of bursts occur within 4 ms of a burst in a reference response, compared with 43% of isolated spikes ($p<10^{-3}$). The corresponding values for AN2 are 46% (bursts) and 30% (isolated spikes; $p<10^{-3}$).

Inhibition of AN2 by ON1

ON1 provides contralateral inhibition to AN2 thereby enhancing the bilateral contrast in the responses of the AN2s. Previous work showed that ON1 accounted for all measurable contralateral inhibition (Faulkes and Pollack, 2000). However, this was assessed using only low-frequency stimuli; therefore we confirmed that the same is true for ultrasound responses (see Supplemental Fig. 5.1).

We hypothesized that coincident bursting in ON1 and AN2 underlies the selective suppression of bursts in AN2. To test this hypothesis, we recorded simultaneously from AN2 and from the ON1 inhibiting it. Stimuli were delivered dichotically in order to control independently the responses of ON1 and AN2 (Fig. 5.3A). During monaural stimulation, only AN2 was stimulated and ON1 fired only occasional spontaneous spikes (<8 spks/s). During binaural stimulation ON1 inhibited AN2 (Fig. 5.3B, compare AN2's monaural and binaural

response). In the excerpt shown, AN2 (during monaural stimulation) and ON1 produced bursts following the two large peaks in amplitude of the stimulus. In response to binaural stimulation most bursts in AN2 were inhibited, although the first spike of a burst sometimes escape inhibition; these now-isolated spikes are indicated by stars in figure 5.3B.

The timing relationship between spikes in ON1 and excitation of AN2 influences the effectiveness of contralateral inhibition (Marsat and Pollack 2005). To evaluate the temporal relationship between inhibitory and excitatory inputs to AN2, we compared the timing of ON1's response to binaural stimulation, which defines the availability of ON1 spikes through time, with AN2's response to monaural stimulation, which describes the time course of suprathreshold excitation. Figure 5.4A shows the timing of ON1 spikes relative to the timing of AN2 bursts. We used the last spike of AN2 bursts as the reference point, as ON1 spikes prior to that can influence AN2's response. The majority of ON1 spikes occurring prior to AN2 bursts are themselves in bursts, reflecting that bursts in both neurons are evoked, with high temporal precision, by the same stimulus features. ON1 spikes are most prevalent up to 15 ms before the end of AN2 bursts, corresponding approximately to the mean duration of AN2 bursts (12.3 ± 1.8 ms). We show later (Fig. 5.5) that the duration of the inhibitory influence of an ON1 spike is approximately 5 ms, suggesting that spikes occurring up to 17 ms before the end of an AN2 burst (AN2 burst duration + duration of ON1 influence) can affect AN2's response. Within this time window, on average 2.3 ON1 spikes occur before each AN2 burst, most of which (1.7) are part of a burst in ON1. Considering that AN2 bursts on average comprise 2.8 spikes, there are 0.82 ON1 spikes available to inhibit each AN2 spike within a burst.

Figure 5.4B shows the distribution of ON1 spikes relative to isolated spikes of AN2. The distributions for isolated ON1 spikes, and spikes within bursts, are similar. Overall, ON1 spikes are less probable before isolated spikes of AN2 than before AN2 bursts. Only 0.5 ON1 spikes occur during

a 5 ms window preceding an AN2 isolated spike. Thus, on a per-spike basis, there are more ON1 spikes available for contralateral inhibition of AN2 spikes within bursts than of isolated AN2 spikes (paired t-test, $p<10^{-4}$).

Figure 5.4 describes the availability of ON1 spikes for inhibiting AN2. To examine the impact of these spikes on AN2, we compared AN2 responses to monaural stimulation (i.e. with no inhibition) to those to binaural stimulation (with inhibition), relative to the timing of ON1 responses. Following the beginning of a burst in ON1, AN2 is less likely to produce spikes for approximately 10 ms (Fig. 5.5A). On average, 0.62 AN2 spikes are eliminated (hatched area). Considering that ON1's bursts are composed, on average of 2.4 spikes, each spike within an ON1 burst corresponds to a decrease of 0.24 spikes in AN2. Isolated ON1 spikes result in a similar decrease in AN2's response (Fig. 5.5B; -0.26 AN2 spikes per isolated ON1spike; paired t-test, p=0.24), with the inhibitory influence lasting for approximately 5 ms. Thus, on a per-spike basis, isolated ON1 spikes are similar in inhibitory impact to spikes within bursts.

We also examined independently the influence of ON1's inhibition on bursts and isolated spikes in AN2 (Fig. 5.5 C-F). Isolated ON1 spikes and spikes within bursts are similar in their effect on AN2 bursts (-0.22 and -0.31 AN2 spikes per ON1 spike respectively, paired t-test, p=0.09). Note that for AN2 bursts, the inhibitory effect is apparent even before the ON1 burst or isolated spike (Fig. 5.5C, D). If the first spike of an AN2 burst occurs before the ON1 response, and if this spike escapes inhibition (as occurs, e.g., in Fig. 5.3), then the burst with which it is associated will appear to have been suppressed before the inhibiting ON1 spike. The partially inhibited burst will now be classed as an isolated AN2 spike, and consequently the proportion of isolated spikes prior to the ON1 response will also be affected (Figs. 5.5E, F). These results emphasize that not all spikes of a burst need to be inhibited to suppress the burst.

The results shown in figure 5.4 and 5.5 suggest that ON1's inhibition leads to a pronounced decrease in the number of spikes within bursts in AN2 and a more subtle influence on isolated spike rate. Figure 5.6 A shows that, indeed, the number of spikes within bursts decreases by about half (paired t-test, $p<10^{-3}$) whereas isolated spike rate is relatively unaffected ($p=0.08$). Furthermore, not only the number of spikes within bursts, but also the number of bursts decreases, i.e. bursts are often eliminated altogether. Feature detection by AN2 bursts must therefore be affected since fewer features are being signalled through bursts. To confirm this, we compared AN2 performance as a feature detector for monaural and binaural stimulation, but using, in both cases, the features defined by the monaural responses (Fig. 5.6B). Contralateral inhibition results in a two-fold increase in error rate, paralleling the decrease in burst rate. Feature detection accuracy by isolated spikes is not altered.

Discussion

ON1's coding properties, in response to ultrasound, are similar to those of AN2. Both neurons produce bursts of spikes in response to salient peaks in stimulus amplitude. In both neurons, bursts perform well as feature detectors whereas isolated spikes do so poorly. These results confirm and extend those of Marsat and Pollack (2006).

The reliability with which inhibitory input from ON1 is timed relative to the excitatory input to AN2 can affect the impact of ON1's inhibition. Bursts in ON1 and AN2 are reliably associated with the same features of ultrasound stimuli, whereas the association between isolated spikes and stimulus features is less precise. This is demonstrated both by the higher probability of spiking at similar times relative to the stimulus envelope for bursts than for isolated spikes, and by the better performance of bursts as feature detectors. As a result, spikes within AN2 bursts are more likely to be preceded by firing in ON1 than are isolated AN2 spikes.

Studies in other sensory systems also showed that bursts are more reliable in their timing than isolated spikes. In the lateral geniculate nucleus of cats, burst timing is more reliable than isolated spike timing (Alitto et al, 2005). In the electrosensory lateral line lobe of electric fish, bursts in pyramidal cells are temporally correlated across neurons with nearby receptive fields, whereas this correlation is weaker for isolated spikes (M.J. Chacron and J. Bastian, personal comm.). It is therefore not surprising that bursts in ON1 and AN2 are reliable in their timing relative to the stimulus envelope and, because of this, have a high probability of coincidence between the neurons.

The possible advantages of bursts as a coding mechanism have been discussed extensively (Lisman 1997, Krahe & Gabbiani 2004). One advantage of bursts over isolated spikes is that, because of temporal summation and facilitation, they may have stronger impact on postsynaptic cells. Our results, however, suggested that on a per-spike basis, isolated ON1 spikes and spikes within bursts are similar in their ability to suppress AN2 spikes. We cannot rule out the possibility that bursting may result in facilitation of IPSPs, but if this does occur, it does not translate into a larger decrease in spiking.

In addition to the greater coincidence in burst timing between ON1 and AN2 compared with isolated spikes, our results reveal another feature of bursts that favours their efficient inhibition, namely, that not all of the component spikes need be eliminated to suppress the burst. Deleting one spike of a two-spike burst eliminates the burst entirely, whereas eliminating a single isolated spike will only slightly affect the overall isolated-spike rate.

In the lateral superior olive and the inferior colicullus of mammals contralateral inhibition also plays a role in shaping the sensitivity to interaural intensity differences (for review see Grothe, 2003). For example, a study on bats (Oswald et al., 1999) showed that many cells in the inferior colicullus received particularly effective inhibition during the onset

response to a tone whereas the prolonged response was less affected by inhibition, thus showing a reduced sensitivity to interaural intensity difference. The inhibitory input to these cells is transient and effective only shortly after a sharp increase in amplitude (i.e. the onset of a tone or a stimulus with rapid amplitude modulation). This situation is not unlike that of AN2 which is particularly well inhibited for brief periods of time in response to pronounced increases in stimulus amplitude.

The direction of the behavioural response to ultrasound is determined by the bilateral difference in the response of the AN2 pair (Pollack, 1998). We suggest here that this difference is enhanced by ON1's patterned inhibition. The AN2 contralateral to the sound will be strongly inhibited by ON1, leading to a decrease in burst rate. As bursts, but not isolated spikes, evoke steering responses (Marsat and Pollack, 2006), the lower burst rate in the AN2 contralateral to the sound should result in a weaker tendency to turn away from that side.

In summary, we showed that ON1 has the same bursting properties as AN2. This match in response structure allows ON1 to reliably inhibit bursts in AN2. ON1's inhibition affects AN2 burst rate more than its isolated spike rate both because coincidence of spiking in ON1 and AN2 is greater during AN2's bursts, and because a burst can be eliminated by suppression of only some of its spikes. This efficient decrease in burst rate implements a selective contrast enhancement that increases localization cues preferentially for portions of the stimulus that elicit bursts (i.e. for behaviourally relevant portions of the stimulus) compared with portions of the stimulus that elicit only isolated spikes.

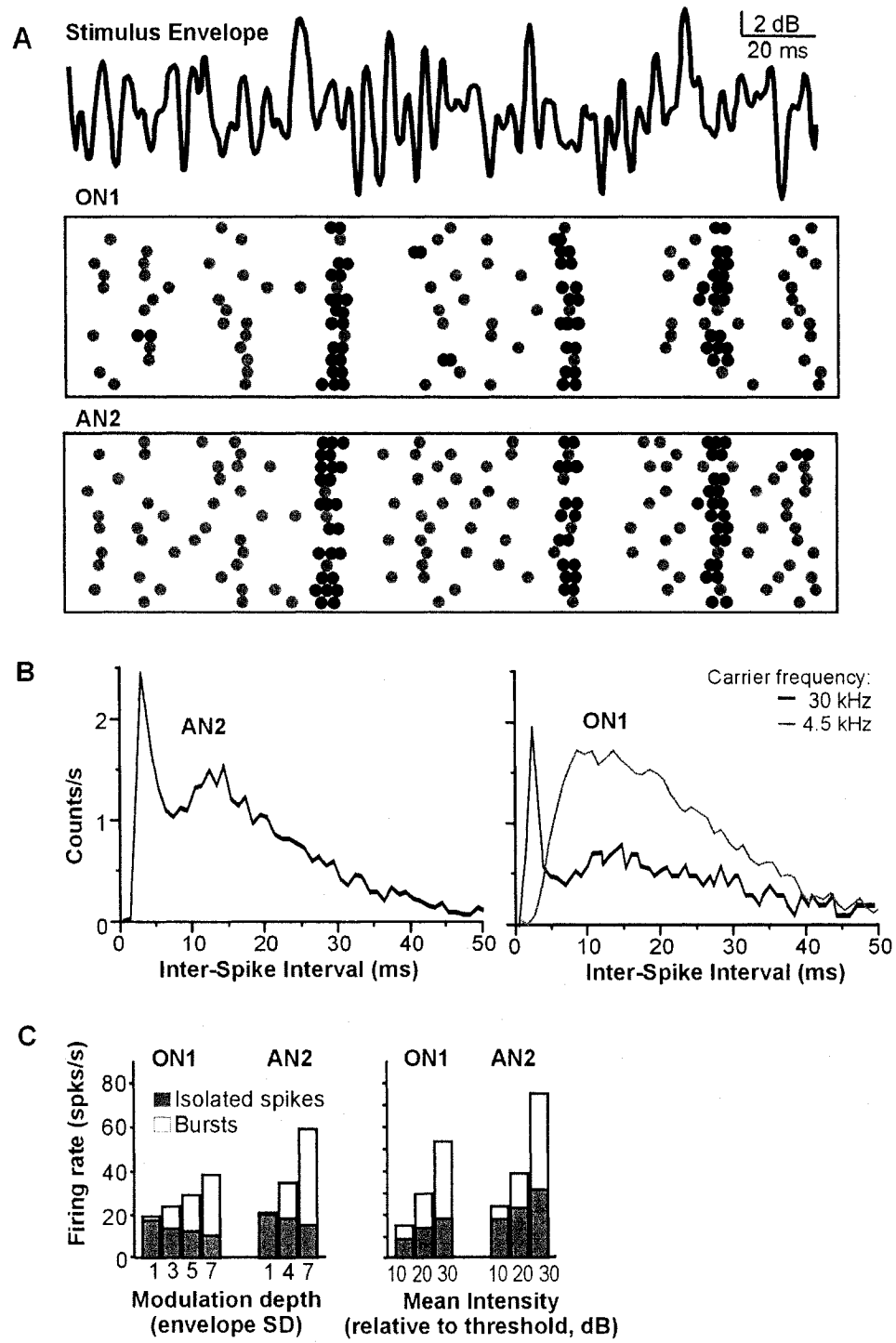

Figure 5.1: Bursting in ON1 and AN2. **A.** Excerpt of several responses of ON1 and AN2 to the same portion of an amplitude modulated stimulus (stimulus mean level: 20 to 25 dB above threshold; envelope SD: 5 dB). **B.** Interspike-interval distributions of ON1 and AN2's responses to amplitude

modulated stimulus (mean stimulus level: 20 to 25 dB above threshold; envelope SD: 5 dB; n=8 neurons for each curve). Mean (± SD) thresholds were 55.4 ± 4.2 dB SPL for AN2; 61.3 ±3.1 dB SPL for ON1's responses to ultrasound and 52.4 ± 3.2 dB SPL for ON1's responses to 4.5 kHz stimuli. Ordinate shows number of ISIs per second per 1 ms bin. **C.** Mean firing rates of ON1 and AN2 in response to stimuli with different modulation depth (mean intensity: 20 dB above threshold) or different mean intensity (envelope SD: 5 dB). The white part of each bar represents spikes within bursts and the grey part, isolated spikes (n= 8 for ON1 and n=6 for AN2).

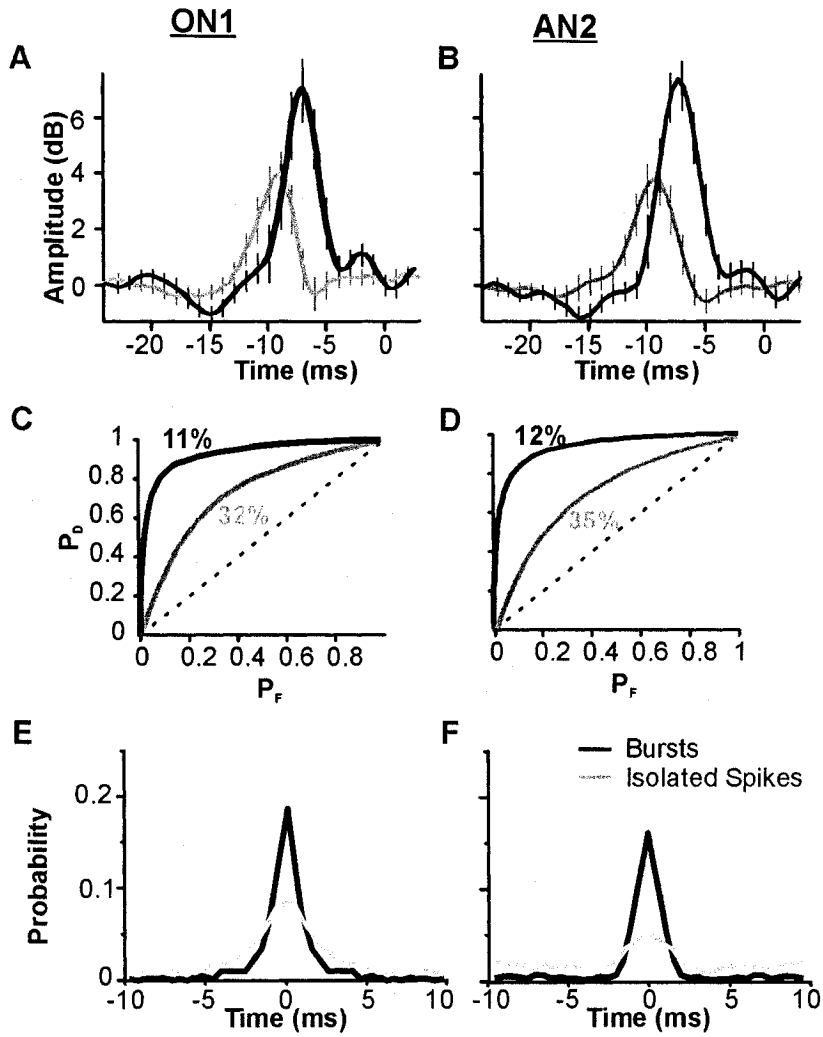

Figure 5.2: Feature detection by bursts and isolated spikes. **A,B.** Stimulus amplitude preceding isolated spikes (grey curve) or bursts (black curve; mean ± sd; n=8 neurons). Values represent departures from mean stimulus level (stimulus mean intensity: 20 dB above threshold; envelope SD: 5 dB; n=8 neurons). **C,D.** Receiver operating characteristic curves (means of 8 neurons) plot the probability of correct detection (P_D) against the probability of failure (P_F). The dotted straight line indicates chance feature discrimination; performance increases with the degree of departure from this. Minimum error rate is shown beside each curve. **E,F.** Probability of spiking or bursting at similar times relative to the amplitude envelope across several repetitions of the same stimulus (n=8 neurons). Bin width = 0.5 ms.

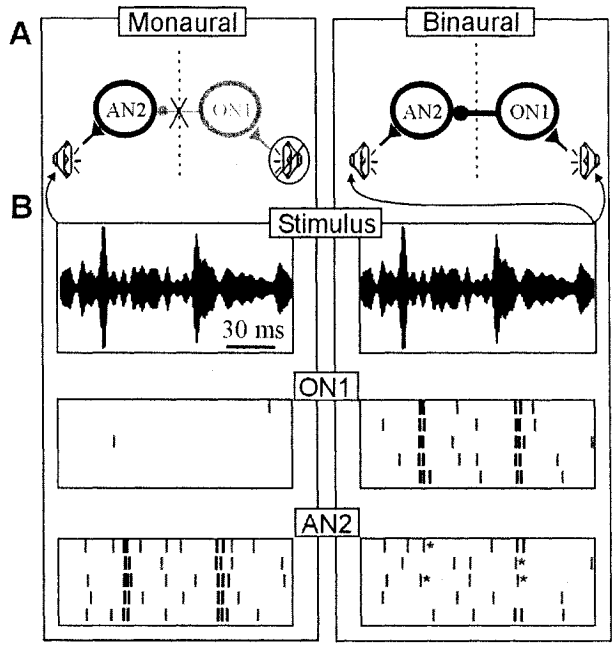

Figure 5.3: Dichotic stimulation and responses of AN2 and ON1. **A.** Schematic drawing of the connections between receptors, AN2 and ON1. During monaural stimulation (left), only the ear driving AN2 receives the stimulus and during binaural stimulation both ears are stimulated allowing ON1 to provide contralateral input to AN2. The interneurons exist as mirror-image pairs; only the recorded neurons are shown. **B.** Excerpts of several responses of AN2 and ON1 to RAM stimuli during monaural (left) and binaural (right) stimulation. Black bars indicate the timing of spikes within bursts and grey bars the timing of isolated spikes. We indicate with a star isolated spikes in the binaural response that correspond to an inhibited bursts (see results for details)

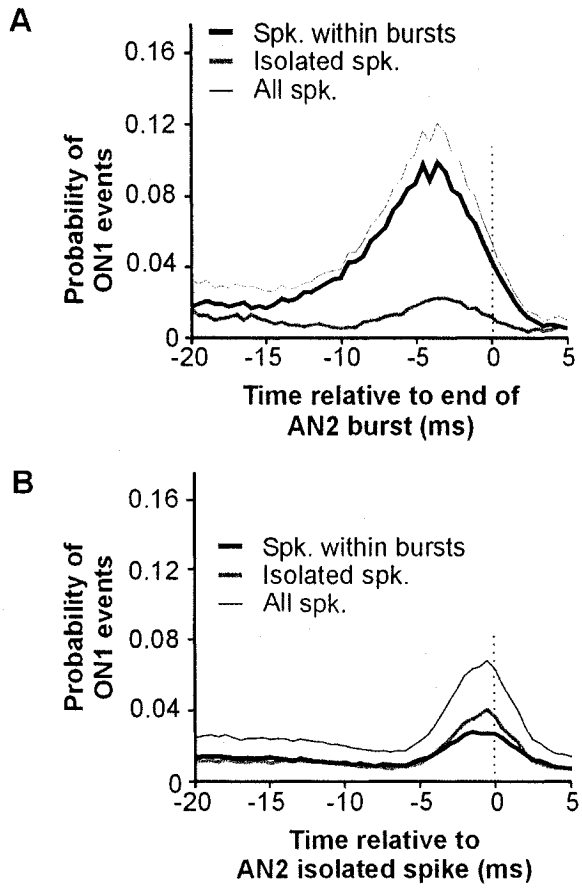

Figure 5.4: Temporal relationship between AN2 and ON1 events. **A.** Probability of spiking in ON1 relative to the timing of the last spike of an AN2 burst. We compared AN2's monaural response (i.e. when there is no contralateral inhibition) to the response of ON1 to binaural stimuli (i.e. the contralateral inhibition). Bin width 0.5 ms; n=9 crickets. **B.** As in A, but we compare the timing of spikes in ON1 relative to isolated spikes in AN2.

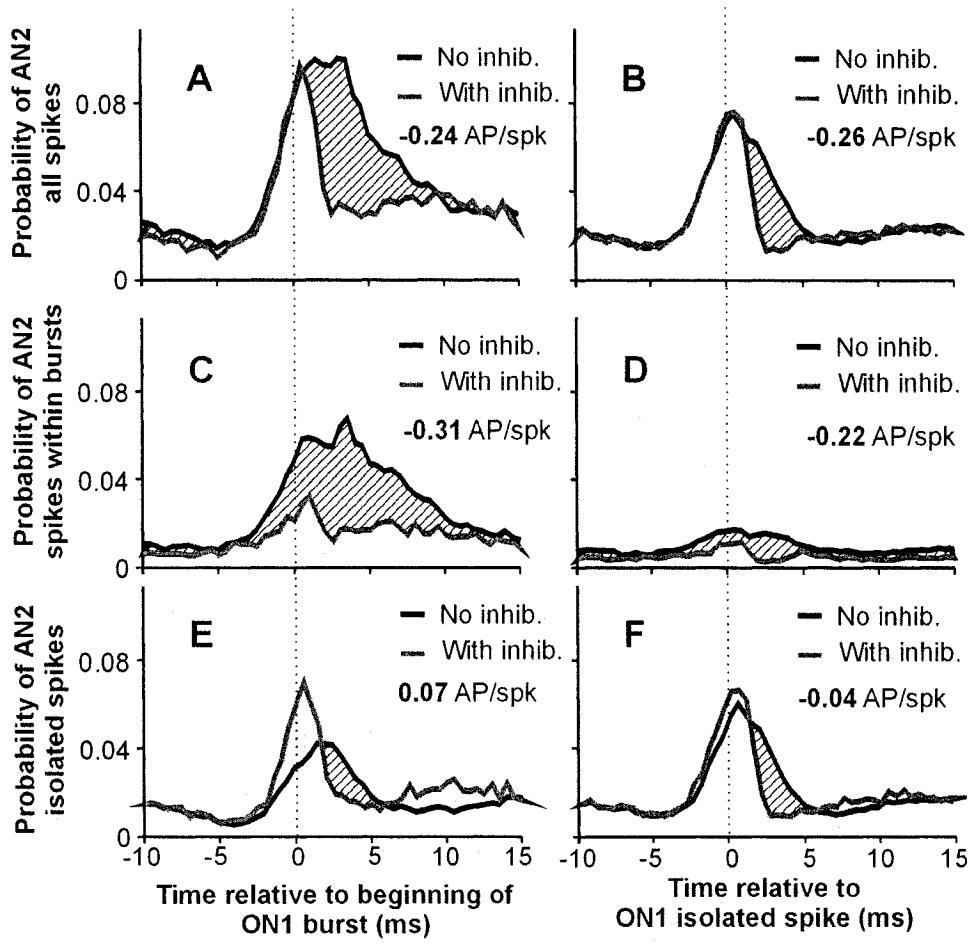

Figure 5.5: Influence of ON1's bursts and isolated spikes on AN2's probability of spiking. We compare the probability of spiking in AN2 during the monaural response (no inhibition) to the probability during binaural response (inhibition is present), relative to the timing of the beginning of an ON1 burst (**A,C,E**) or isolated spikes (**B,D,F**). The monaural distribution results from pair-wise comparisons of every AN2 monaural response with every ON1 binaural response in a given cricket. Results are averaged across crickets (n=9 crickets). For binaural distributions, pair-wise comparisons were done only on responses of ON1 and AN2 recorded simultaneously. Bin width 0.5 ms. We show in bold the overall change in AN2's spiking probability associated with a spike within a burst or an isolated spike, calculated for a time window ranging from -10 ms to 15 ms. Hatched areas indicate a decrease in spiking probability in the presence of ON1's inhibition and shaded areas show increases.

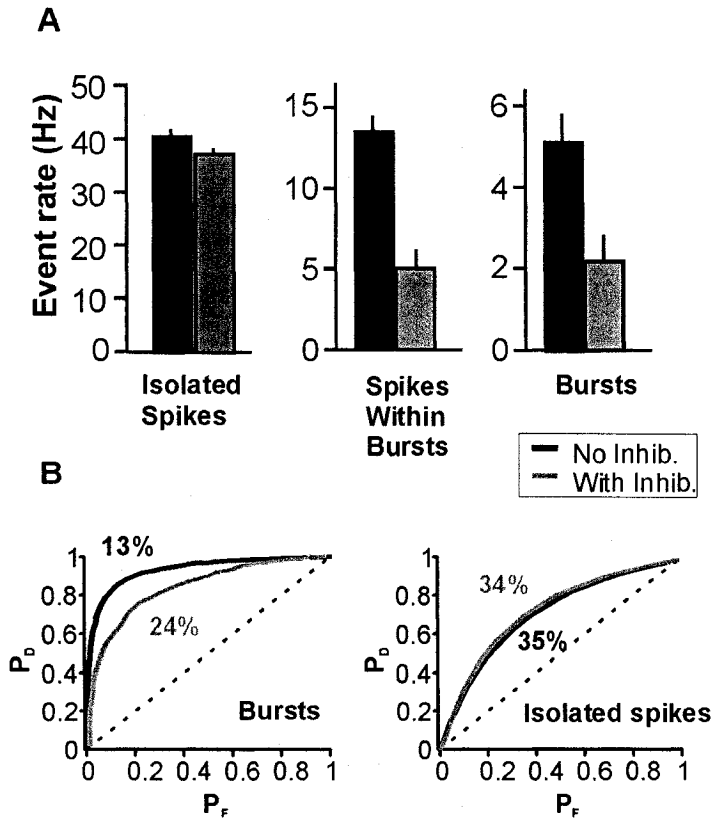

Figure 5.6: Effect of contralateral inhibition on accuracy of feature detection. **A.** Average isolated spike rate, burst rate and spikes-within-bursts rate of AN2 in response to monaural (no inhibition) and binaural (inhibited) stimuli. **B.** Receiver operating characteristic curves for AN2's bursts and isolated spikes during monaural and binaural stimulation. Minimum error rate is shown beside each curve.

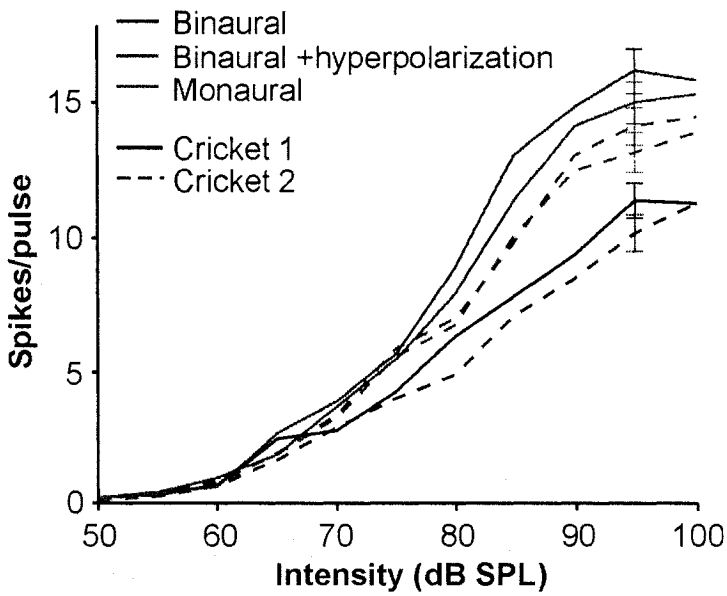

Supplemental figure 5.1: ON1's inhibition accounts for all measurable contralateral inhibition. The experimental configuration was similar as described in the methods: dichotic stimulation and dual recordings of ON1 and AN2 except that ON1 was recorded intracellularly. This experiment is similar to that of Faulkes and Pollack (2000) but uses ultrasound stimuli and thus confirms that ON1 accounts for all measurable contralateral inhibition also during ultrasonic stimulation. We compare the responses of AN2 to single sound pulses of varying intensity when it is stimulated monaurally (no contralateral inhibition), binaurally (all contralateral inhibition is present), and binaurally while ON1 was hyperpolarized in order to eliminate spiking. Data points are average spike counts for 10-20 repetition of each stimulus (representative SD are shown). No significant difference can be measured between monaural responses and binaural responses with ON1 hyperpolarized (ANOVA, $p= 0.25$); thus demonstrating that ON1 accounts for all contralateral inhibition.

Chapter 6: Conclusion

The experiments presented in this thesis investigate two aspects of auditory processing in the prothoracic ganglion of crickets: the coding properties of central interneurons and the role of these coding properties in shaping the neural information sent to the brain. We will summarize the relevance of these coding properties for processing behaviourally important stimuli, recapitulate how these coding properties influence auditory processing and discuss the role of contralateral inhibition on the elaboration of behaviour.

Coding of conspecific sounds and ultrasound: two neural codes

The cricket auditory system is specialized to process conspecific communication sounds and ultrasound stimuli such as those produced by echolocating bats. The auditory interneurons are tuned to the carrier frequencies of either or both kinds of sound. Previous studies that examined the selectivity of prothoracic interneurons for amplitude modulation rates used mainly trains of pulses presented at different rates to show that these neurons did not encode selectively behaviourally attractive AM rates (e.g. Schildberger, 1984). We used signal processing tools and information theoretic analysis to describe the responses to long dynamic stimuli with a wide range of temporal patterns. Our results quantify precisely the temporal filtering characteristics of three of the most studied prothoracic neurons: AN1, AN2 and ON1. These neurons encode AM frequencies up to a cut-off that varied depending on the carrier frequency. In response to ultrasound, ON1 and AN2 have rather broad temporal filtering properties that encompass frequencies up to more than 100 Hz. For communication-like carrier frequencies (~4.5 kHz) on the other hand, ON1 and AN1 have sharp filtering characteristics with a low-pass cut-off of around 30-40 Hz, which corresponds to the highest rates present in conspecific songs. These filtering properties reflect mainly the capacity of the neuron to synchronize its response to the stimulus' amplitude modulations. The firing rate is relatively unaffected by

modulation rate although responses to ultrasound have lower firing rates to stimuli with very slow or very fast amplitude modulation (below a few hertz and above ~60-70 Hz) which is likely due to adaptation (Samson and Pollack, 2002). The temporal filtering properties of individual receptors cannot account for the difference in filtering properties for low-frequency and ultrasound stimuli. We suggested that this difference could arise from differences in composition of the population of low-frequency and ultrasound tuned receptors: pooling of information from many low-frequency receptors could results in low-pass filtering whereas ultrasound receptors are less numerous and thus would impose less low-pass filtering.

Our analysis also clarifies how amplitude modulations are encoded by these neurons. The simplest code, namely a linear relationship between stimulus amplitude and response magnitude, describes partially the coding of stimuli with communication-like carrier frequencies. I speculate that the non-linearity of these responses could be accounted for by the threshold and saturation of the neurons: the linear relationship between amplitude and firing rate fails at low intensities because of the neuron's threshold and at high intensities because of the saturation of the response. Ultrasound responses are highly non-linear, thus a different coding strategy is used by the neurons responding to ultrasound. This non-linearity could arise from the presence of bursts of action potentials in the responses to ultrasound. In several sensory systems, bursts are described as feature detectors signalling the occurrence of specific patterns of amplitude modulation (Guido et al., 1995; Lesica and Stanley, 2004; Oswald et al., 2004). Feature detection analysis confirmed that bursts in ultrasound responses signal the occurrence of behaviourally relevant features of the stimuli: salient peaks in ultrasound amplitude. This neural code, by nature, is non-linear (Chacron et al., 2004) and thus may account for the observed non-linearity of the response.

Our characterization of the response properties of prothoracic interneurons revealed that two very different neural codes are used to encode low frequency sounds and ultrasound. These two carrier frequencies are encountered by the cricket in two different contexts: conspecific communication and predator avoidance. The behavioural responses to these signals have to be adapted to the constraints encountered during predator avoidance or mate finding. Ultrasound avoidance is a short-latency, reflex-like response that cannot rely on the evaluation of the signal during long time windows. Feature detection by bursts is an efficient neural code in that context: it is a short, easily identifiable signal that reliably indicates the occurrence of a peak in ultrasound amplitude. Brain circuits that control motor output can, in a short time, distinguish behaviourally relevant signals encoded by bursts from noise that elicits isolated spikes. The underlying mechanism could simply be a threshold mechanism, where the post-synaptic neurons respond only when the ISI is smaller than the burst limit (i.e. <6 ms). When a female cricket hears a conspecific calling song it must recognize the attractive pattern and track it for seconds or even minutes. The nervous system must analyse the song pattern carefully and localize its origin during long periods. The AN1 pair provide a rather faithful representation of the song pattern which is then processed by the brain. Since song recognition occurs in the brain, the information must be conserved for the brain circuit to analyse, but non-relevant temporal patterns (i.e. outside the range contained in the song) are filtered-out of the neural signal being sent to the brain. This selective encoding allows the recognition to be done higher up in the circuit but also the neural interactions in the prothoracic ganglion to be temporally matched only for behaviourally relevant patterns (see next section).

An interesting comparison of the coding properties of prothoracic neurons can be made with the three rules of efficient sensory processing hypothesized by Barlow (1961). The first rule hypothesizes that sensory

neurons must encode behaviourally relevant aspects of the environment. We showed that this is an appropriate description of the response properties of prothoracic interneurons: for conspecific carrier frequency they encode selectively song-like patterns and for ultrasound, salient peaks in amplitude, which elicit avoidance responses, are selectively and reliably encoded by bursts. The second hypothesis states that sensory relays must transform the signal according to the requirements of other parts of the nervous system. I argue that the prothoracic ganglion is a good example of this rule: for conspecific frequencies, the song pattern is represented faithfully so that brain neurons have an accurate description of the song to analyze; for ultrasound stimuli, behaviourally relevant features of the stimulus are extracted and signalled to the brain, which constitutes an early recognition mechanism reflecting the need for fast processing. Finally Barlow hypothesized that sensory encoding should aim at reducing a signal's redundancy. This principle is clearly relevant to ultrasound coding since the neurons signal only the occurrence of salient increases in stimulus amplitude and filter-out relatively constant stimuli. Conspecific song patterns are redundant since they are repetitions of stereotypic pulse patterns and this redundant information is encoded by prothoracic neurons. However, the location of the sound source will change constantly as the female approaches the male. Thus, to reach a singing male, the female's brain must continuously segregate the song from other sound sources. The ascending neurons must therefore continuously encode the redundant song pattern so it can be associated with the changing localization cues.

ON1's dual coding properties and bilateral contrast enhancement.

The specialization of the prothoracic neurons for coding behaviourally relevant sounds reaches an extreme in ON1 where this single neuron uses two different coding strategies depending on the carrier frequency of the signal. Similar dual coding properties have also been identified in

electric fish where pyramidal cells of the electrosensory lateral line lobe have different coding strategies for prey and conspecific signals (Chacron et al., 2003). These pyramidal cells and ON1 are, to my knowledge, the only two examples of neurons with dual, signal-specific, coding properties. The fact that two widely different systems have similar characteristics suggests that it is a general property of sensory systems to specialize their response properties for more than one type of signal. This dual specialization might be particularly useful in relatively small nervous systems because it allows a single neuron (or neuron type) to participate efficiently in the processing of several types of signal.

The role of ON1's inhibition is to enhance the bilateral contrast in the ANs (Horseman and Huber, 1994; Faulkes and Pollack, 2000). I showed that ON1's carrier frequency-specific response pattern allows the inhibitory input to match the ANs' response structures. I showed that this match in coding properties allows the bilateral contrast enhancement to be applied specifically to the behaviourally important features of the signal since these features are selectively encoded by ON1 and the ANs.

Contralateral inhibition plays an important role in sound localization in most vertebrate and invertebrate auditory systems. In mammals, for example, contralateral inhibition underlies the processing of interaural intensity differences and also plays a role in processing interaural time differences (Grothe 2003; Irvine et al., 2001). Precise timing of inhibitory input is essential to enhance localization cues efficiently (e.g. Park, 1998; Oswald et al., 1999).

Crickets can segregate simultaneously played calling songs (Pollack, 1986) which suggest that song recognition and localization are inter-dependent. We suspect that song recognition happens in the brain. However, a study by Hedwig and Poulet (2004) suggests that the direction of phonotaxis is in part controlled by a short-latency pathway that leads to reactive steering to each sound pulse. Nevertheless, it has been shown that the activity of the AN1 neurons influences the direction of phonotaxis

(Schildberger and Horner, 1988). Thus, it was suggested that reactive steering movements are modulated by recognition circuits of the brain. This modulation could account for the ability of the cricket to segregate one calling song from other auditory elements present in the environment since this process must rely on brain circuits performing the identification of the calling song in order to associate this signal to a specific location.

In several organisms the temporal relationship between inhibitory and excitatory inputs influences the segregation of different auditory objects (Breebaart et al. 2001, see also Feng and Ratnam, 2000 for review). When two cricket songs are played simultaneously, ON1 encodes selectively the temporal pattern of the loudest (Pollack, 1986). In accordance with this result I showed that ON1 will encode best AM rates between 0 and 25 Hz. If two songs are heard simultaneously, the combination of the two pulse patterns will result in a stimulus with twice the number of pulses per unit of time. This stimulus with a high pulse repetition rate will not be encoded well by ON1. However, if one song is louder than the other, the stimulus will contain a slow component in its amplitude modulation. ON1 will accurately encode this slow rate, and thus represent the time course of the loudest song. These results indicate that ON1 will enhance the bilateral contrast in AN1's responses specifically for the pattern of a single song, whereas other sound elements will be associated with more diffuse localization cues. It was thus suggested that ON1 implements a "selective attention".

Ultrasound avoidance is also likely to occur in noisy environments. ON1 enhances the bilateral contrast in AN2 specifically for behaviourally relevant portions of the stimulus which elicit bursts in AN2. This allows the localization cues to be conspicuous for stimuli that the cricket needs to respond to, and more diffuse for irrelevant elements of the auditory environment. Our results suggest that ON1 enhances the localization cues selectively for behaviourally relevant sound elements and thereby improves the segregation of these signals from noise. The capacity to

segregate and attend to a signal in a noisy environment is often referred to as the "cocktail party effect". I suggest that ON1's carrier-frequency specific coding properties improve the ability of the cricket to perform this task in two different contexts, namely mate finding and predator avoidance.

In summary, this thesis demonstrated that the response properties of prothoracic interneurons are specialized to encode behaviourally relevant signals efficiently. The carrier-frequency-specific coding properties of ON1 allow its inhibition to match AN1 and AN2's response structure. This dual specificity leads to the enhancement of the localization cues selectively for behaviourally relevant stimuli. I suggest that these properties should improve the ability of the cricket to localize behaviourally relevant signals in noisy environments.

Bibliography

Alitto HJ, Weyand TG, Martin Ursey W (2005) Distinct properties of stimulus-evoked bursts in the lateral geniculate nucleus. J Neurosci 25:514-523.

Attias H, Schreiner CE (1998) Coding of naturalistic stimuli by auditory midbrain neurons. In: Advances in neural information processing systems 10. (Jordan MI, Kearns M, Solla S, eds), pp. 103–109. Cambridge, MA: MIT Press.

Atkins G, Pollack GS (1987) Correlation between structure topographic arrangement and spectral sensitivity of sound sensitivity of sound-sensitive interneurons in crickets. J Comp Neurol 266:398-412.

Atkins G, Pollack, GS (1986) Age-dependent occurrence of an ascending axon on the omega neuron of the cricket, *Teleogryllus oceanicus*. J Comp Neurol 243:527-534.

Atkins GS, Ligman F, Burghardt F, Stout FJ (1984) Changes in phonotaxis by the female cricket *Acheta domesticus* after killing identified acoustic interneurons. J Comp Physiol A 154:795–804

Baddeley R, Abbott LF, Booth MC, Sengpiel F, Freeman T (1998) Responses of neurons in primary and inferior temporal visual cortices to natural scenes. Proc R Soc London B 264:1775–1783.

Balakrishnan R, Pollack GS (1996) Recognition of courtship song in the field cricket, *Teleogryllus oceanicus*. Anim Behav 51:353-366.

Barlow HB (1995). The neuron doctrine in perception. In: The cognitive neurosciences. (Gazzaniga MS, ed), pp. 415–436, Cambridge, MA: MIT Press.

Barlow HB (1961) Possible principles underlying the transformation of sensory messages. In: Sensory communication. (Rosenblith WA, ed), pp. 217-234, Cambridge, MA: MIT press.

Batra R, Kuwada S, Stanford TR (1989) Temporal coding of envelopes and their interaural delays in the inferior colliculus of the unanesthetized rabbit. J Neurophysiol 61: 257-268.

Beckius GE, Batra R, Oliver DL (1999) Axons from anteroventral cochlear nucleus that terminate in medial superior olive of cat: observations related to delay lines. J Neurosci 19: 3146–3161.

Borst A, Theunissen FE (1999) Information theory and neural coding. Nat Neurosci 2:947-957.

Boyan GS, Fullard JH (1988) Information processing at a central synapse suggests a noise filter in the auditory pathway of the noctuid moth. J Comp Physiol A 164:251-258.

Brand A, Behrend O, Marquardt T, McAlpine D, Grothe B (2002) Precise inhibition is essential for microsecond interaural time difference coding. Nature 417:543-547.

Breebart J, van de Par S, Kohlrausch A (2001) Binaural processing model based on contralateral inhibition. I. Model structure. J Acoust Soc Am 110:1074–1088.

Brenner N, Bialek W, van Steveninck RD (2000) Adaptive rescaling maximizes information transmission. Neuron 26:695-702.

Brodfuhrer PD, Hoy RR (1990) Ultrasound sensitive neurons in the cricket brain. J comp Physiol A 166:651–662.

Brodfuehrer PD, Hoy RR (1989) Integration of ultrasound and flight inputs on descending neurons in the cricket brain. J Exp Biol 145:157-171.

Bush SL, Schul J (2006) Pulse-rate recognition in an insect: evidence of the role for oscillatory neurons. J Comp Physiol A 192:113-121.

Cariani PA (2004) Temporal codes and computations for sensory representation and scene analysis. IEEE Trans Neural Net 15:1100-1111.

Carr CE (1993) Processing of temporal information in the brain. Annu Rev Neurosci 16:223-243.

Chacron MJ, Maler L, Bastian J (2005) Feedback and feedforward control of frequency tuning to naturalistic stimuli. J Neurosci 25:5521-5532.

Chacron MJ, Longtin AE, Maler L (2004) To burst or not to burst? J Comput Neurosci 17:127-136.

Chacron MJ, Doiron B, Maler L, Longtin A, Bastian J (2003) Non-classical receptive field mediates switch in a sensory neuron's frequency tuning. Nature 423:77.

Cherry EC (1961) Two ears- but one world. In: Sensory communication. (Rosenblith WA, ed), pp:99-118, Cambridge: MIT press.

Cherry EC (1953) Some experiments on the recognition of speech, with one and two ears. J Acoust Soc Am 25: 975-979.

Clague H, Theunissen F, Miller JP (1997) Effects of adaptation on neural coding by primary sensory interneurons in the cricket cercal system. J Neurophysiol 77:207-220.

Damasio AR, Geschwind N (1984) The neural basis of language. Ann Rev Neurosci 7:127-147.

Dan Y, Atick JJ, Reid RC (1996) Efficient coding of natural scenes in the lateral geniculate nucleus: experimental test of a computational theory. J Neurosci 16:3351-3362.

Dean I, Harper, NS, McAlpine D (2005) Neural population coding of sound level adapts to stimulus statistics. Nat Neurosci 8:1684-1689.

Durlach NI (1963) Equalization and cancellation theory of binaural masking level difference. J Acoust Soc Am 35:1206-1218.

Edwards CJ, Alder TB, Rose JR (2002) Auditory midbrain neurons that count. Nature 5: 934-936.

Efron B, Tibshirani RJ (1993) An introduction to the bootstrap. New York: Chapman.

Eggermount JJ, Smith GM (1996) Burst-firing sharpens frequency-tuning in primary auditory cortex. Neuroreport 7:753-757.

Eggermont JJ (1995) Representation of a voice onset time continuum in primary auditory cortex of the cat. J Acoust Soc Am 98:911-920.

Ehret G (1987) Categorical perception of speech signals: facts and hypotheses from animal studies. In: Categorical perception: the groundwork of Cognition. (Harnad S, ed), pp 301-331, New York: Cambridge University Press.

Engler G, Zupanc GKH (2001) Differential production of chirping behaviour evoked by electrical stimulation of the weakly electric fish, *Apteronotus leptohynchus*. J Comp Physiol A 187:747-756.

Faulkes Z, Pollack GS (2001) Mechanisms of frequency-specific responses of omega neuron 1 in crickets (*Teleogryllus oceanicus*): A polysynaptic pathway for song? J Exp Biol 204:1295-1305.

Faulkes Z, Pollack GS (2000) Effects of inhibitory timing on contrast enhancement in auditory circuits in crickets (*Teleogryllus oceanicus*). J Neurophysiol 84:1247-1255.

Feng AS, Ratnam R (2000) Neural basis of hearing in real-world situations. Annu Rev Psychol 51:699-725.

Fettiplace R, Fuchs PA (1999) Mechanisms of hair cell tuning. Annu Rev Physiol 61:809-834.

Field DJ (1994) What is the goal of sensory coding? Neural Comp 6:559–601.

Filippi P (1999) Acoustics: basic physics, theory, and methods. San Diego: Academic Press.

Fortune ES, Rose GJ (2000) Short-term synaptic plasticity contributes to the temporal filtering of electrosensory information. J Neurosci 20:7122-7130.

Fortune ES, Rose GJ (1997) Passive and active membrane properties contribute to low-pass temporal filtering in *Eigenmannia*. J Neurosci 17:3815-3825.

Fricker D, Miles R (2001) Interneurons, spike timing, and perception. Neuron 32:771-774.

Frisina, RD (2001) Subcortical neural coding mechanisms for auditory temporal processing. Hear. Res 158:1:27.

Frisina DR, Frisina RD (1997) Speech recognition in noise and presbycusis: relations to possible neural sites. Hear Res 106:95-104.

Frisina RD, Karcich KJ, Tracy TC, Sullivan DM, Walton JP (1996) Preservation of amplitude modulation coding in the presence of background noise by chinchilla auditory-nerve fibers. J Acoust Soc Am 99:475-490.

Gerhardt HC (1994) The evolution of vocalization in frogs and toads. Annu Rev Ecol Syst 25:293-324.

Ghazanfar AA, Flombaum JI, Miller CT, Hauser MD (2001) The units of perception in the antiphonal calling behavior of cotton-top tamarins (*Saguinus oedipus*): Playback experiments with long calls. J Comp Physiol A 187:27-35.

Goldberg JM, Brown PB (1969) Functional organization of the dog superior olivary nucleus: an anatomical and electrophysiological study. J Neurophysiol 31:639-656.

Grothe B (2003) New roles for synaptic inhibition in sound localization. Nat Rev Neurosci 4:540-550.

Grothe B, Park TJ (1995) Time can be traded for intensity in the lower auditory system. Naturwissenschaften 82:521-523.

Grothe B (1994) Interaction of excitation and inhibition in processing of pure tone and amplitude-modulated stimuli in the medial superior olive of the mustached bat. J Neurophysiol 71:706-721.

Guido W, Lu SM, Vaughan JW, Godwin DW, Sherman SM (1995) Receiver operating characteristic (ROC) analysis of neurons in the cat's lateral geniculate nucleus during tonic and burst response mode. Vis Neurosci 12:723-741.

Haag J, Borst A (1997) Encoding of visual motion information and reliability in spiking and graded potential neurons. J Neurosci 17:4809-4819.

Hardt M, Watson AHD (1994) Distribution of synapses on two ascending interneurones carrying frequency-specific information in the auditory system of the cricket: evidence for GABAergic inputs. J Comp Neurol 345:481-495.

Hawley ML, Litovsky RY, Colburn HS (1999) Speech intelligibility and localization in complex environments. J Acoust Soc Am 105:3436–3448.

Hedwig B, Poulet JFA (2005) Mechanisms underlying phonotactic steering in the cricket *Gryllus bimaculatus* revealed with a fast trackball system. J Exp Biol 208:915:927.

Hedwig B, Poulet JFA (2004) Complex auditory behaviour emerges from simple reactive steering. Nature 430:781-785.

Heffner RS, Heffner HE (1989) Sound localization, use of binaural cues and the superior olivary complex in the pig. Brain Behav Evol 33:248-258.

Helenius P, Uutela K, Hari R (1999) Auditory stream segregation in dyslexic adults. Brain 122:907-913.

Helversen D von, Helversen O von (1995) Acoustic pattern recognition and orientation in orthopteran insects: parallel or serial processing? J Comp Physiol A 177:767-774.

Hennig RM, Franz A, Stumpner A (2004) Processing of auditory information in insects. Microsc Res Tech 63:351–374.

Hennig RM (2003) Acoustic feature extraction by cross-correlation in crickets? J Comp Physiol A 189:589–598.

Hennig RM, Weber T (1997) Filtering of temporal parameters of the calling song by cricket females of two closely related species - a behavioral analysis. J Comp Physiol A 180:621-630.

Horseman G, Huber F (1994) Sound localisation in crickets.1. Contralateral inhibition of an ascending auditory interneuron (AN1) in the cricket *Gryllus bimaculatus*. J Comp Physiol A 175:389-398.

Hoy RR (1998) Acute as a bug's ear, an informal discussion of hearing in insects. In: Comparative Hearing: insects. (Hoy RR, Popper AN, Fay RR, eds), pp. 1–17, New York: Springer.

Hoy RR (1994) Ultrasound acoustic startle in flying insects: some neuroethological and comparative aspects. In: Neural basis of behavioral adaptations. (Schildberger K, Elsner N, eds), pp. 227-241, Stuttgart, Germany: Gustav Fischer.

Hoy RR (1992) The evolution of hearing in insects as an adaptation to predation from bats. In: The evolutionary biology of hearing. (.Webster DB, Fay RR, Popper AN, eds), pp 115–129, New York: Springer-Verlag.

Hoy RR, Nolen T, Brodfuehrer P (1989) The neuroethology of acoustic startle and escape in flying insects. J Exp Biol 146, 287–306.

Imaizumi K, Pollack GS (2005) Central projections of auditory receptor neurons of crickets. J Comp Neurol 493:439-447.

Imaizumi K, Pollack GS (2001) Neural representation of sound amplitude by functionally different auditory receptors in crickets. J Acoust Soc Am 109:1247-1260.

Imaizumi K (2000) Peripheral representation of sound frequency in cricket auditory system: beyond tonotopy, (Doctoral thesis). Department of Biology, McGill University.

Imaizumi K, Pollack GS (1999) Neural coding of sound frequency by cricket auditory receptors. J Neurosci 19:1508-1516.

Irvine DRF, Park VN, McCormick L (2001) Mechanisms underlying the sensitivity of neurons in the lateral superior olive to interaural intensity differences. J Neurophysiol 86:2647-2666.

Jeffress LA (1948) A place theory of sound localization. J Comp Physiol Psychol 41:35–39.

Jones G (1999) Scaling of echolocation call parameters in bats. J Exp Biol 202:3359-3367.

Jones G, Corben C (1993) Echolocation calls from six species of Microchiropteran bats in south-eastern Queensland. Aust Mammal 16:35-38.

Joris PX, Smith PH, Yin TCT (1998) Coincidence detection in the auditory system: 50 years after Jeffress. Neuron 21:1235-1238.

Krahe R, Gabbiani F (2004) Burst firing in sensory systems. Nat Rev Neurosci 5:13-23.

Kroodsma DE, Byers BE (1991) The function of bird song. Am Zool 31:318-328.

Kulzer E, Nelson JE, McKean JL, Moehres FP (1984) Prey catching behavior and echolocation in the Australian ghost bat, *Macroderma gigas* (Microchiroptera: Megadermatidae). Aust Mammal 7:37-50.

Kuwada S, Batra R (1999) Coding of sound envelopes by inhibitory rebound in neurons of the superior olivary complex in the unanesthetized rabbit. J Neurosci 19:2273-2287.

Kvale MN, Schreiner CE (2004) Short-term adaptation of auditory receptive fields to dynamic stimuli. J Neurophysiol 91:604-612.

Langner G, Schreiner CE (1988) Periodicity coding in the inferior colliculus of the cat. I. Neuronal mechanisms. J Neurophysiol 60:1799-1822.

Laughlin SB (1981) A simple coding procedure enhances a neuron's information capacity. Z Naturforsch 36:910–912.

Lesica NA, Stanley GB (2004) Encoding of natural scene movies by tonic and burst spikes in the lateral geniculate nucleus. J Neurosci 24:10731-10740.

Lestienne R (2001) Spike timing, synchronization and information processing on the sensory side of the central nervous system. Prog Neurobiol 65:545-591.

Lewicki MS (2002) Efficient coding of natural sounds. Nat Neurosci 5:356-363.

Libersat F, Murray JA, Hoy RR (1994) Frequency as a releaser in the courtship song of two crickets, *Gryllus bimaculatus* (de Geer) and *Teleogryllus oceanicus* - a neuroethological analysis. J Comp Physiol A 174:485-494.

Lisker L, Abramson AS (1964) A cross-linguistic study of voicing in initial stops: Acoustical measurements. Word 20:384–422.

Lisman JE (1997) Bursts as a unit of neural information: making unreliable synapse reliable. Trends Neurosci 20:38-43.

Litovsky, RY, Lane, CC, Atencio, C, and Delgutte, B (2001) Physiological measures of the precedence effect and spatial release from masking in the cat inferior colliculus. In: Physiological and psychophysical bases of auditory function. (Breebaart DJ, Houtsma AJM, Kohlrausch A, Prijs VF, Schoonhoven R, eds), pp 221-228, Maastricht: Shaker.

Litovsky RY, Colburn HS, Yost WA, Guzman S (1999) The precedence effect. J Acoust Soc Am 106:1633-1654.

Machens CK, Gollish T, Kolesnikova O, Herz AVM (2005) testing the efficiency of sensory coding with optimal stimulus ensembles. Neuron 47:447-456.

Machens CK, Prinz P, Stemmler MB, Ronacher B, Herz AVM (2001) Discrimination of behaviourally relevant signals by auditory receptor neurons. Neurocomputing 38-40:263-268.

Machens CK, Stemmler MB, Prinz P, Krahe R, Ronacher B, Herz AV (2001b) Representation of acoustic communication signals by insect auditory receptor neurons. J Neurosci 21:3215-3227.

Marsat G, Pollack, GS (2006) A behavioral role for feature detection by sensory bursts. Submitted

Marsat G, Pollack GS (2005) Effect of the temporal pattern of contralateral inhibition on sound localization cues. J Neurosci 25:6137-6144.

Marsat G, Pollack GS (2004) Differential temporal coding of rhythmically diverse acoustic signals by a single interneuron. J Neurophysiol 92:939-948.

Martinez-Conde S, Macknik SL, Hubel DH (2002) The function of bursts of spikes during visual fixation in the awake primate lateral geniculate nucleus and primary visual cortex. Proc Natl Acad Sci 99:13920-13925.

May ML, Hoy RR (1991) Habituation of the ultrasound induced acoustic startle response in flying crickets. J exp Biol 159:489–499.

Metzner W, Koch C, Wessel R, Gabbiani F (1998) Feature extraction by burst-like spike patterns in multiple sensory maps. J Neurosci 18:2283-2300.

Michelsen A, Löhe G (1995) Tuned directionality in cricket ears. Nature 375: 639.

Middlebrooks JC, Green DM (1991) Sound localization by human listeners. Annu Rev Psychol 42:135-159.

Miller LA, Surlykke A (2001) How some insects detect and avoid being eaten by bats: tactics and countertactics of prey and predator. Bioscience 51:570-581.

McAlpine D, Grothe B (2003) Sound localisation and delay lines-do mammals fit the model? Trends Neurosci 26:347-350.

McAnally KI, Stein JF (1996) Auditory temporal coding in dyslexia. Proc R Soc Lond B 263:961-965.

Moiseff A, Hoy RR (1983) Sensitivity to ultrasound in an identified auditory interneuron in the cricket: a possible neural link to phonotactic behavior. J Comp Physiol A 131:113-120.

Moiseff, A, and M Konishi (1981) Neuronal and behavioral sensitivity to binaural time differences in the owl. J Neurosci 1: 40-48.

Moiseff A, Pollack GS, Hoy RR (1978) Steering responses of flying crickets to sound and ultrasound: Mate attraction and predator avoidance. Proc Natl Acad Sci USA 75:4052–4056.

Møller AR, Rees A (1986) Dynamic properties of the responses of single neurons in the inferior colliculus of the rat. Hear Res 24:203-215.

Moore DR (1987) Physiology of higher auditory system. Br Med Bull 43:856-870.

Nabatiyan A, Poulet JFA, Polavieja GG, Hedwig B (2003) Temporal pattern recognition based on instantaneous spike rate coding in a simple auditory system. J Neurophysiol 90:2484-2493.

Nagarajan SS, Cheung SW, Bedenbaugh P, Beitel RE, Schreiner CE, Merzenich MM (2002) Representation of spectral and temporal envelope of twitter vocalizations in common marmoset primary auditory cortex. J Neurophysiol 87:1723-1737.

Nelken I (2004) Processing of complex stimuli and natural scenes in the auditory cortex. Curr Op Neurobiol 14:474-480.

Nelson ME, Maciver MA (1999) Prey capture in the weakly electric fish *Apteronotus albifrons*: sensory acquisition strategies and electrosensory consequences. J Exp Biol 202:1195-1203.

Nocke H (1972) Physiological aspect of sound communication in crickets (*Gryllus campestris*). J Comp Physiol A 80:141-162.

Nolen TG, Hoy RR (1986) Phonotaxis in flying crickets. I. Attraction to the calling song and avoidance of bat-like ultrasound are discrete behaviors. J Comp Physiol A 159:423-439.

Nolen, TG, Hoy RR (1984) Initiation of behavior by single neurons: the role of behavioral context. Science 226:992-994.

Oertel D (1999) The role of timing in the brain stem auditory nuclei of vertebrates. Annu Rev Physiol 61:497-519.

Oliver DL, Huerta MF (1992) Inferior and superior colliculi. In: The mammalian auditory pathway, neuroanatomy. (Webster DP, Popper AN, Fay RR, eds), pp. 268-221, New York: Springer-Verlag.

Oswald AM, Chacron MJ, Doiron B, Bastian J, Maler L (2004) Parallel processing of sensory input by bursts and isolated spikes. J Neurosci 24:4351-4362.

Oswald JP, Klug A, Park TJ (1999) Interaural intensity difference processing in auditory midbrain neurons: effects of a transient early inhibitory input. J Neurosci 19:1149-1163.

Park TJ (1998) IID sensitivity differs between two principal centers in the interaural intensity difference pathway - the LSO and the IC. J Neurophysiol 79:2416-2431 .

Park TJ, Grothe B, Pollak GD, Schuller G, Koch U (1996) Neural delays shape selectivity to interaural intensity differences in the Lateral Superior Olive. J Neurosci 16:6554-6566.

Pollack GS (2003) Sensory cues for sound localization in the cricket *Teleogryllus oceanicus*: interaural difference in response strength versus interaural latency difference. J Comp Physiol A 189:143-151.

Pollack GS (2001) Analysis of temporal patterns of communication signals. Curr Opin Neurobiol 11:734-738.

Pollack GS (2000) Who, what, where? Recognition and localization of acoustic signals by insects. Curr Opin Neurobiol 10:763-767 .

Pollack GS, Imaizumi K (1999) Neural analysis of sound frequency in insects. Bioessays 21:295-303.

Pollack GS (1998). Neural processing of acoustic signals. In: Comparative hearing: insects. (Hoy RR, Popper AN, Fay RR, eds), pp. 139-196, New York: Springer.

Pollack GS (1994) Synaptic inputs to the omega neuron of the cricket *Teleogryllus oceanicus* - differences in EPSP waveforms evoked by low and high sound frequencies. J Comp Physiol A 174:83-89.

Pollack GS, El-Feghaly E (1993) Calling song recognition in the cricket *Teleogryllus oceanicus*: comparison of the effects of stimulus intensity and sound spectrum on selectivity for temporal pattern. J Comp Physiol A 171:759-765.

Pollack GS (1988) Selective attention in an insect auditory neuron. J Neurosci 8:2635-2639.

Pollack GS (1986) Discrimination of calling song models by the cricket *Teleogryllus oceanicus*: the influence of sound direction on neural encoding of the stimulus temporal pattern and on phonotactic behavior. J Comp Physiol A 158:549-562.

Pollack GS, Huber F, Weber T (1984) Frequency and temporal pattern dependent phonotaxis of *Teleogryllus oceanicus* in flight and walking paradigms. J Comp Physiol A 154:13–26.

Pollack GS, Plourde N (1982) Directionality of acoustic orientation in flying crickets. J Comp Physiol A 146:207-215.

Pollack GS, Hoy RR (1981) Phonotaxis to individual rhythmic components of a complex cricket calling song. J Comp Physiol A 144:367-373.

Pollack GS, Hoy RR (1979) Temporal pattern as a cue for species-specific calling song recognition in crickets. Science 204:429–432.

Pollak GD, Burger RM, Park TJ, Klug A, Bauer EE (2002) Roles of inhibition for transforming binaural properties in the brainstem auditory system. Hear Res 168:60–78.

Press WH, Flanney BP, Teukolsky SA, and Vetterling, WT (1992) Numerical recipes in C: the art of scientific computing. Cambridge, MA: Cambridge University Press.

Quian Quiroga R, Reddy L, Kreiman G, Koch C, Freid I (2005) Invariant visual representation by single neurons in the human brain. Nature 435:1102-1107.

Rayleigh Lord (1876) On our perception of the direction of a sound source. Nature 14:32-33.

Rieke F, Warland D, de Ruyter van Steveninck R, Bialek W (1997) Spikes: exploring the neural code. Cambridge, MA: MIT Press.

Rieke F, Bodnar DA, Bialek W (1995) Naturalistic stimuli increase the rate and efficiency of information transmission by primary auditory afferents. Proc R Soc Lond B 262:259-265.

Rheinlaender J, Mörchen A (1979) Time intensity trading in locust auditory interneurons. Nature 281:672-674.

Rhode WS, Greenberg S (1994) Encoding of amplitude modulation in the cochlear nucleus of the cat. J Neurophysiol 71:1797-1825.

Roddey JC, Girish B, Miller JP (2000) Assessing the performance of neural encoding models in the presence of noise. J Comput Neurosci 8:95-112.

Roman N, Wang DL, Brown GJ (2003) Speech segregation based on sound localization. J Acoust Soc Am 114:2236-2252.

Römer H, Hedwig B, Ott SR (2002) Contralateral inhibition as a sensory bias: the neural basis for a female preference in a synchronously calling bushcricket, *Mecopoda elongata*. Eur J Neurosci 15:1655–1662.

Samson A-H, Pollack GS (2002) Encoding of sound localization cues by an identified auditory interneuron: effects of stimulus temporal pattern. J Neurophysiol 88:2322-2328.

Selverston AI, Kleindienst HU, Huber F (1985) Synaptic connectivity between cricket auditory interneurons as studied by selective photoinactivation. J Neurosci 5:1283–1292.

Schildberger K, Hörner M (1988) The function of auditory neurons in cricket phonotaxis I. effect of hyperpolarization of indentified neurons on sound localization. J Comp Physiol A 163:621-631.

Schildberger K (1984) Temporal selectivity of identified auditory neurons in the cricket brain. J Comp Physiol A 155:171-185.

Schirmer A (2004) Timing speech: a review of lesion and neuroimaging findings. Cogn Brain Res 21:269–287.

Schnitzler HU, Kalko EKV (2001) Echolocation by insect-eating bats. Bioscience 51:557-569.

Schnitzler HU (1987) Echoes of fluttering insects: information for echolocating bats. In: Advances in the study of bats. (Fenton MB, Racey PA, Rayner JMV, eds), pp. 226–243, Cambridge: Cambridge University Press.

Selverston AI, Kleindienst HU, Hubert F (1985) Synaptic connectivity between cricket auditory interneurons as studied by photoinactivation. J Neurosci 5:1283-1292.

Sen K, Theunissen FE, Doupe AJ (2001) Feature analysis of natural sounds in the songbird auditory forebrain. J Neurophysiol 86:1445-1458.

Shannon RV, Zeng FG, Kamath V, Wygonski J, Ekelid M (1995) Speech recognition with primarily temporal cues. Science 270:303-305.

Sherman SM (2001) Tonic and burst firing: dual modes of thalamocortical relay. Trends Neurosci 24:122-126.

Simoncelli EP, Olshausen BA (2001) Natural image statistics and neural representation. Annu Rev Neurosci 24:1193-1216.

Simmons JA (2005) Big brown bats and june beetles: multiple pursuit strategies in a seasonal acoustic predator-prey system. Acoust Res Lett Onl 6:238-242.

Simmons JA (2003) Observing echolocating bats in real time at night. First conference on acoustic communication by animals.

Simmons JA (1989) A view of the world through the bat's ear: the formation of acoustic images in echolocation. Cognition 33:155-199.

Smirnakis SM, Berry MJ, Warland DK, Bialek W, Meister M (1997) Adaptation of retinal processing to image contrast and spatial scale. Nature 386:69-73.

Spirou GA, May BJ, Wright DD, Ryugo DK (1993) Frequency organization of the dorsal cochlear nucleus in cats. J Comp Neurol 329:36-52.

Srinivasan MV, Zhang SW, Lehrer M, Collett TS (1996) Honeybee navigation en route to the goal: visual flight control and odometry. J Exp Biol 199:237-244.

Stable J, Wendler G, Scharstein H (1989) Cricket phonotaxis localization depends on recognition of the calling song pattern. J Comp Physiol A 165:165-178.

Steinschneider M, Fishman YL, Arezzo JC (2003) Representation of the voice onset time (VOT) speech parameter in population responses within primary auditory cortex of the awake monkey. J Acoust Soc Am 114:307-321.

Strausfeld NJ, Seyan HS, Wholers D, Bacon JP (1983) Lucifer yellow histology. In: Functional neuroanatomy. (Strausfeld NJ, ed), pp. 132-155, Berlin:Spinger-Verlag.

Stumpner A, Helversen D von (2001) Evolution and function of auditory systems in insects. Naturwissenschaften 88:159-170.

Swadlow HA, Gusev AG (2001) The impact of bursting thalamic impulses at a neocortical synapse. Nat Neurosci 4:402-408.

Swartz O, Sioncelli EP (2001) Natural signal statistics and sensory gain control. Nat Neurosci 4:819-825.

Theunissen FE, Sen K, Doupe AJ (2000) Spectro-temporal receptive fields of non-linear auditory neurons obtained using natural sounds. J Neurosci 20:2315-2331.

Theunnissen FE, Roddey JC, Stufflebeam S, Clague H, Miller JP (1996) Information theoretic analysis of dynamical encoding by four identified primary sensory interneurons in the cricket cercal system. J Neurophysiol 75:1345-1364.

Thompson AM, Schofield BR (2000) Afferent projections of the superior olivary complex. Microsc Res Tech 51:330-354.

Vinje WE, Gallant JL (2002) Natural stimulation of the non-classical receptive field increases information transmission efficiency in V1. J Neurosci 22:2904-2915.

Wessel R, Koch C, Gabbiani F (1996) Coding of time-varying electric field amplitude modulations in a wave-type electric fish. J Neurophysiol 75:2280-2293.

Wiese K, Eilts K (1985) Evidence for matched frequency dependence of bilateral inhibition in the auditory pathway of *Gryllus bimaculatus*. Zool Jb Physiol 89:181-201.

Wimsalt WA (1970) Biology of bats. New York: Academic press.

Wohlers DW, Huber F (1982) Processing of sound signals by 6 types of neurons in the prothoracic ganglion of the cricket *Gryllus campestris*. J Comp Physiol A 146:161-174.

Wooley SMN, Gill PR, Theunissen FE (2006) Stimulus-dependent auditory tuning results in synchronous population coding of vocalizations in songbird midbrain. J Neurosci 26:2499-2512.

Wyttenbach RA, May ML, Hoy RR (1996) Categorical perception of sound frequency by crickets. Science 273:1542-1544.

Wyttenbach RA, Hoy RR (1993) Demonstration of the precedence effect in an insect. J Acoust Soc Am 94:777-784.

Yager DD (1999) Structure, development, and evolution of insect auditory systems. Microsc Res Tech 47:380-400.

Yu AC, Margoliash D (1996) Temporal hierarchical control of singing in birds. Science 273:1871-1875.

Zar JH (1999) Biostatistical analysis. Upper Saddle River, NJ: Prentice-Hall.

Zatorre RJ, Belin P (2001) Spectral and temporal processing in human auditory cortex. Cereb Cortex 11:945-953.

Zeng FG, Oba S, Garde S, Sininger AS (1999) Temporal and speech processing deficits in auditory neuropathy. Neuroreport 10:3429-3435.